

Controls of greenhouse gases production and  
soil nutrients dynamics in the Lena River Delta,  
Northeastern Siberia

Dissertation

with the aim of achieving a doctoral degree

at the Faculty of Mathematics, Informatics and Natural Sciences

Department of Earth System Sciences

at Universität Hamburg

submitted by

**Leonardo de Aro Galera**

Hamburg, 2024

Department of Earth System Sciences

Date of Oral Defense: 10.12.2024

Reviewers:

PD Dr. habil. Christian Knoblauch

Prof. Dr. Christian Beer

Members of the examination commission:

PD Dr. habil. Christian Knoblauch

Prof. Dr. Christian Beer

Prof. Dr. Gerhard Schmiedl

Prof. Dr. Lars Kutzbach

Prof. Dr. Uwe Schneider

Chair of the Subject Doctoral Committee

Earth System Sciences: Prof. Dr. Hermann Held

Dean of Faculty MIN: Prof. Dr.-Ing. Norbert Ritter

---

## Eidesstattliche Versicherung | Declaration on Oath

Hiermit erkläre ich an Eides statt, dass ich die vorliegende  
Dissertationsschrift selbst verfasst und keine anderen als die angegebenen  
Quellen und Hilfsmittel benutzt habe.

I hereby declare upon oath that I have written the present dissertation  
independently and have not used further resources and aids than those  
stated.

Sorocaba, 13/06/2024  
Ort, den | City, date

A handwritten signature in black ink, consisting of stylized, overlapping letters and flourishes.

Unterschrift | Signature

---

“I wish it need not have happened in my time,” said Frodo.

“So do I,” said Gandalf, “and so do all who live to see such times. But that is not for them to decide. All we have to decide is what to do with the time that is given us...”

Tolkien, J. R. R. (1954). *The Fellowship of the Ring*.

---

## Contents

Journal Articles and Manuscripts .....	8
Acknowledgments .....	10
Abstract.....	11
Zusammenfassung.....	13
1 Introduction.....	15
1.1 The permafrost and the permafrost carbon-climate feedback.....	15
1.2 The Lena River Delta .....	16
1.3 Quantification of greenhouse gas fluxes in the Arctic.....	17
1.4 Nutrients dynamics in a warming Arctic.....	22
1.5 Research questions.....	25
2 Ratio of In Situ CO <sub>2</sub> to CH <sub>4</sub> Production and Its Environmental Controls in Polygonal Tundra Soils of Samoylov Island, Northeastern Siberia.....	27
2.1 Abstract .....	27
2.2 Introduction.....	28
2.3 Methods.....	30
2.3.1 Study Site .....	30
2.3.2 Soils and meteorological data .....	32
2.3.3 Chamber measurements and plant mediated CH <sub>4</sub> transport .....	33
2.3.4 Calculation of CO <sub>2</sub> :CH <sub>4</sub> ratios and uncertainty range.....	34
2.3.5 Calculation of a seasonal CO <sub>2</sub> and CH <sub>4</sub> release .....	36
2.3.6 Statistics.....	38
2.4 Results.....	40
2.4.1 CH <sub>4</sub> fluxes and plant-mediated transport .....	40

---

2.4.2	CO <sub>2</sub> :CH <sub>4</sub> ratios, their environmental controls and uncertainty range .....	43
2.4.3	Seasonal CO <sub>2</sub> and CH <sub>4</sub> release .....	45
2.5	Discussion.....	46
2.5.1	CH <sub>4</sub> emissions in comparison to other arctic sites .....	46
2.5.2	Impact of plant mediated CH <sub>4</sub> transport.....	48
2.5.3	<i>in situ</i> CO <sub>2</sub> :CH <sub>4</sub> ratios and their environmental controls.....	51
2.5.4	<i>in situ</i> CO <sub>2</sub> :CH <sub>4</sub> production ratios uncertainty range .....	53
2.5.5	Seasonal CO <sub>2</sub> and CH <sub>4</sub> release .....	55
2.6	Conclusions .....	56
2.7	Supplementary material .....	56
3	Higher temperatures do not increase P and K availabilities in incubation of soils from Kurungnakh Island, Lena River Delta, Siberia .....	65
3.1	Abstract .....	65
3.2	Introduction.....	66
3.3	Methods .....	68
3.3.1	Study site .....	68
3.3.2	Sampling .....	68
3.3.3	Incubation experiment.....	69
3.3.4	Chemical characterization.....	70
3.3.5	Nutrient turnover rate calculation .....	71
3.3.6	Statistics.....	71
3.4	Results .....	72
3.5	Discussion.....	82
3.5.1	Soil P and K turnover rates controls .....	82

---

3.5.2	Greenhouse gases rates at different temperatures and connection to nutrients dynamics .....	84
3.6	Conclusions.....	88
4	Synthesis.....	89
4.1	Will CH <sub>4</sub> fluxes in the Arctic increase with permafrost thawing, and what factors regulate the ratio between microbial CO <sub>2</sub> and CH <sub>4</sub> production from OM decomposition in the polygonal tundra? .....	89
4.2	Will P and K availability increase in a warmer Arctic? .....	91
4.3	Integrated discussion of the research questions and results.....	94
5	Conclusions.....	96
	References.....	98

---

## Journal Articles and Manuscripts

**Galera, L. A.**, Eckhardt, T., Beer, C., Pfeiffer, E.-M., & Knoblauch, C. (2023). Ratio of in situ CO<sub>2</sub> to CH<sub>4</sub> production and its environmental controls in polygonal tundra soils of Samoylov Island, Northeastern Siberia. *Journal of Geophysical Research: Biogeosciences*, 128, e2022JG006956. <https://doi.org/10.1029/2022JG006956>

Authors contributions: Leonardo de Aro Galera: Conceptualization; Methodology; Data analysis; Writing; Review and editing. Tim Eckhardt: Conceptualization; Field work; Methodology; Data analysis; Review and editing. Christian Beer: Writing; Review and editing. Eva Maria Pfeiffer: Conceptualization. Christian Knoblauch: Conceptualization; Methodology; Data analysis; Writing; Review and editing.

**Galera, L. A.**, Beer, C. & Knoblauch, C. (in preparation). Higher temperatures do not increase P and K availabilities in incubation of soils from Kurungnakh Island, Lena River Delta, Siberia. *Journal*.

Author contributions: Leonardo de Aro Galera: Conceptualization; Methodology; Data analysis; Writing; Review and editing; Laboratory work. Christian Beer: Methodology. Christian Knoblauch: Conceptualization; Methodology; Review and editing.

*Co-authorships within the CliCCS project:*

de Vrese, P., Beckebanze, L., **Galera, L. A.**, Holl, D., Kleinen, T., Kutzbach, L., Rehder, Z. & Brovkin, V. (2023). Sensitivity of Arctic CH<sub>4</sub> emissions to landscape wetness diminished by atmospheric feedbacks. *Nature Climate Change*, 13, 832–839. <https://doi.org/10.1038/s41558-023-01715-3>

Author contributions: Philipp de Vrese: Experiment design; Simulations; Analysis and validation of simulations; Paper writing and review. Lutz Beckebanze: Experiment design; Observational data analysis; Paper writing and review. Leonardo de Aro Galera: Experiment design; Observational data analysis; Paper writing and review. David Holl:

---



Experiment design; Observational data analysis; Paper writing and review. Thomas Kleinen: Experiment design; Simulations; Analysis and validation of simulations; Paper writing and review. Lars Kutzbach: Experiment design; Observational data analysis; Paper writing and review. Zoé Rehder: Experiment design; Simulations; Analysis and validation of simulations; Paper writing and review. Victor Brovkin: Experiment design; Analysis and validation of simulations; Paper writing and review.

---

## Acknowledgments

*A Deus, pela minha existência, por sustentar o meu ser e pelo amor concedido ao me criar. Pelo privilégio de existir. À mãe de Deus, por me acolher nos momentos mais aflitivos. Obrigado pela fé que me sustentou e me sustenta na vida.*

To my wife, Amanda, my love, and partner in life.

To my family, my mother, my sisters, Adilson, and those who are not here anymore, my support, and my roots.

To my advisors, Dr. Christian Knoblauch, Prof. Dr. Christian Beer, Prof. Dr. Lars Kutzbach and Prof. Dr. Eva Maria Pfeiffer for the guidance through the path of academic development.

To my panel chair, Prof. Dr. Gerhard Schmiedl, for all the support.

To my colleagues from the IfB, Elisa, Fay, Simran, Tim, David, Oli, Norman, Tanja, Claudia, Birgit, Ralf, Carolina, and Lin, and especially to Lara, Kiri, Cosima, Min, Xavier, Jamil, and Liz, *minha madrinha*, for the crucial help and friendship. And a profound and everlasting thank you to Lutz, who supported me at all times in Germany, and became a brother to me.

To the SICSS office, to all the people I met there and especially to Dr. Berit Hachfeld and Dr. Alexandra Franzke, for all the support.

To the great friends Hamburg gave me, especially Guilherme, Linda and Mona.

To CliCCS, for the financial support.

To the Universität Hamburg, for the structure and opportunity.

*Thank you!*

---

## Abstract

The permafrost stores vast amounts of organic carbon. As permafrost thaws due to global warming, previously frozen organic matter become accessible to microbial decomposition. This process releases greenhouse gases like carbon dioxide (CO<sub>2</sub>) and methane (CH<sub>4</sub>) creating a positive feedback loop, where increased greenhouse gas emissions lead to further warming and subsequent thawing, a process known as the permafrost carbon-climate feedback. In this thesis two key research gaps in the understanding of the permafrost carbon-climate feedback are addressed with studies from sites in the Lena River Delta, Northeastern Siberia, Russia. The second chapter assessed the determining factors for the ratio between *in situ* CO<sub>2</sub> to CH<sub>4</sub> production in the polygonal tundra. This is an important topic about the permafrost carbon-climate feedback, since CH<sub>4</sub> has a 28-fold higher global warming potential than CO<sub>2</sub> and it is crucial to determine the factors modulating the partitioning between CO<sub>2</sub> and CH<sub>4</sub> fluxes from organic matter decomposition in the Arctic. In this study I quantified the CO<sub>2</sub>:CH<sub>4</sub> production ratios of soil organic matter decomposition in wet and dry tundra soils in Samoylov Island, Lena River Delta, by using CO<sub>2</sub> fluxes from clipped plots and *in situ* CH<sub>4</sub> fluxes from vegetated plots. The results show that active layer depth and soil temperature were the main factors controlling these ratios, which decreased towards the end of the growing season, when the active layer was deep and warm enough for methanogenesis. CH<sub>4</sub> production was associated with subsoil (40 cm) temperature, while heterotrophic respiration was related to topsoil (5 cm) temperatures, mainly due to the mostly oxic environment of topsoil, inducing aerobic CO<sub>2</sub> production, and the anoxic environment of the subsoil, inducing CH<sub>4</sub> production.

The third chapter assessed the effect of thawing and warming on the availabilities of phosphorus (P) and potassium (K) in incubated soils of Kurunghakh Island, Lena River Delta. The fate of soil nutrients in permafrost affected soils with warming, will determine if there will be significant constraints to enhanced primary productivity in the Arctic. The tundra vegetation is currently limited in P, thus the effect of climate change on soil P availability might alleviate P limitation and increase primary productivity and C

---

sequestration, or might magnify P limitation, restricting primary productivity, and increasing the net greenhouse gas emissions of permafrost ecosystems. However, this relationship between P and the tundra C balance is further complicated by the consumption of P by microbes, which in turn might make it less straightforward. P and K nutrients were immobilized during the experiment, instead of mineralized, regardless of the temperature treatment. P and K concentrations and turnover rates had a high correlation with C turnover, and samples that emitted more CO<sub>2</sub> were also the ones that immobilized more P, which was demonstrated by the correlation found between CO<sub>2</sub> production rates and P turnover rates.

The results of this thesis suggest that more CH<sub>4</sub> is expected to be produced in permafrost ecosystems stemming from deeper and warmer active layers. And that P limitation is likely to persist with short-term soil warming, potentially imposing significant constraints on the tundra vegetation capacity for C sequestration.

---

## Zusammenfassung

Der Permafrost speichert große Mengen an organischem Kohlenstoff. Wenn der Permafrost aufgrund der globalen Erwärmung auftaut, wird zuvor gefrorenes organisches Material für die mikrobielle Zersetzung zugänglich. Bei diesem Prozess werden Treibhausgase wie Kohlendioxid (CO<sub>2</sub>) und Methan (CH<sub>4</sub>) freigesetzt, was zu einer positiven Rückkopplung führt, bei der erhöhte Treibhausgasemissionen zu einer weiteren Erwärmung und einem anschließenden Auftauen führen - ein Prozess, der als Rückkopplung zwischen tauendem Permafrostkohlenstoff und dem Klima bekannt ist. In dieser Arbeit werden zwei wichtige Forschungslücken im Verständnis der Permafrost-Kohlenstoff-Rückkopplung durch Studien an Standorten im Lena-Flussdelta in Nordostsibirien, Russland, geschlossen. Der erste Artikel untersuchte die Faktoren, die das Verhältnis zwischen der in situ CO<sub>2</sub>- und CH<sub>4</sub>-Produktion in der polygonalen Tundra bestimmen. Dies ist ein wichtiges Thema im Zusammenhang mit der Rückkopplung zwischen tauendem Permafrostkohlenstoff und dem Klima, da CH<sub>4</sub> ein 28-fach höheres globales Erwärmungspotenzial als CO<sub>2</sub> hat und es von entscheidender Bedeutung ist, die Faktoren zu bestimmen, die das Verhältnis zwischen CO<sub>2</sub>- und CH<sub>4</sub>-Bildung während des Abbaus organischer Substanz in der Arktis beeinflussen. In dieser Studie habe ich die CO<sub>2</sub>:CH<sub>4</sub>-Produktionsverhältnisse der Zersetzung organischer Bodensubstanz in feuchten und trockenen Tundraböden auf Samoylov, einer Insel im Delta der Lena quantifiziert, indem ich CO<sub>2</sub>-Flüsse von Parzellen ohne Vegetation und in situ CH<sub>4</sub>-Flüsse von bewachsenen Parzellen verwendete. Die Ergebnisse zeigen, dass die Tiefe der aktiven Schicht und die Bodentemperatur die Hauptfaktoren für diese Verhältnisse waren, die sich gegen Ende der Vegetationsperiode 3 näherten, als die aktive Schicht tief und warm genug für die Methanogenese war. Die CH<sub>4</sub>-Produktion korrelierte mit der Temperatur des Unterbodens (40 cm), während die heterotrophe Atmung mit der Temperatur des Oberbodens (5 cm) zusammenhing, hauptsächlich aufgrund der überwiegend oxidischen Umgebung des Oberbodens, welche optimal für die CO<sub>2</sub>-Produktion ist, und der anoxischen Umgebung des Unterbodens, die die CH<sub>4</sub>-Produktion ermöglicht.

Im zweiten Artikel wurden die Auswirkungen des Auftauens und der Erwärmung auf die Verfügbarkeit von Phosphor (P) und Kalium (K) in inkubierten Böden auf der Insel

---

Kurungnakh im Lena-Flussdelta untersucht. Der Verfügbarkeit von Bodennährstoffen in Permafrostböden bei Erwärmung wird die Primärproduktion in der Arktis erheblich beeinflussen. Die Tundravegetation ist derzeit in P begrenzt, daher könnte der Effekt des Klimawandels auf die Verfügbarkeit von P im Boden die P-Begrenzung lindern und die primäre Produktivität sowie die C-Sequestrierung erhöhen, oder könnte die P-Begrenzung verstärken, die primäre Produktivität einschränken und die Nettoemissionen von Treibhausgasen der Permafrostökosysteme erhöhen. Diese Beziehung zwischen P und dem C-Gleichgewicht der Tundra wird jedoch durch den Verbrauch von P durch Mikroben weiter kompliziert, was sie weniger eindeutig machen könnte. Die Konzentration der Nährstoffe P und K nahmen während des Versuchs ab und nicht zu, unabhängig von der Inkubationstemperatur. P und K wiesen eine hohe Korrelation mit dem C-Umsatz auf, und die Proben, die mehr CO<sub>2</sub> emittierten, waren auch diejenigen, die mehr P und K immobilisierten.

Die Ergebnisse dieser Arbeit deuten darauf hin, dass eine Zunahme der Auftautiefe des Oberbodens in Permafrost-Ökosystemen zu einem Anstieg der CH<sub>4</sub>-Produktion führt. Zusätzlich wird die P-Limitierung bei kurzfristiger Bodenerwärmung tendenziell bestehen bleiben, was die Fähigkeit der Tundravegetation, durch höhere Primärproduktivität aufgrund höherer Temperaturen und CO<sub>2</sub>-Düngung mehr C zu binden, erheblich einschränken könnte.

---

# 1 Introduction

## 1.1 The permafrost and the permafrost carbon-climate feedback

The permafrost is a fundamental component of the cryosphere, and it is defined by soil or rock that remains at, or below 0 °C for at least two years (French, 2018). Although suggested by the name, permafrost is not always frozen as it includes soil, sediment, or rock that can contain water in unfrozen states due to the presence of salts, which decrease the freezing point of water (Harris et al., 1988). Permafrost occurs predominantly in the Northern Hemisphere covering extensive regions in the Arctic and alpine regions and is also present in the Antarctic. It is estimated that permafrost underlies a region of about  $22 \pm 3$  million km<sup>2</sup> worldwide (Gruber, 2012). However, a distinction must be made between "permafrost region", which refers to the broader area potentially containing permafrost, and the "permafrost area" that is actually underlain by permafrost. This discrepancy is significant due to the patchy distribution of permafrost that can cause permafrost to occur discontinuously within a permafrost region. Therefore, the permafrost area is significantly smaller, covering approximately 16 to 21 million km<sup>2</sup>, including the Antarctic and sub-sea permafrost (Gruber, 2012).

The uppermost layer of soils underlain by permafrost, thaws during the summer and is called active layer. This layer thickness can range from a few centimeters to several meters, depending on geographic location, temperature, hydrology, soil texture, vegetation, snow cover and others (Schuur et al., 2008). The dynamics of the active layer are crucial for understanding the mutual relationship between permafrost and climate change. The permafrost stores vast amounts of organic carbon, with estimates indicating that the Northern Hemisphere permafrost region soils contain approximately  $1014 \pm 184$  Pg of carbon within the 0 to 3 m depth interval (Mishra et al., 2021). As the active layer thickens due to global warming, previously frozen organic matter thaws, becoming accessible to microbial decomposition (McGuire et al., 2009). This process releases greenhouse gases like carbon dioxide (CO<sub>2</sub>) and methane (CH<sub>4</sub>) (Knoblauch et al., 2018)

---

creating a positive feedback loop, where increased greenhouse gas emissions lead to further warming and subsequent thawing, a process known as the permafrost carbon-climate feedback (Schuur et al., 2015).

The importance of the permafrost carbon-climate feedback lies in its potential to accelerate global warming. Permafrost regions in the Northern Hemisphere are experiencing rapid temperature increases, outpacing the global average, a process known as Arctic amplification (Rantanen et al., 2022; Serreze & Barry, 2011). The IPCC (2021) projects that, as global warming continues, permafrost could release 3 to 41 PgC of CO<sub>2</sub> per 1 °C of global warming by 2100. These projected emissions are significant enough to require its inclusion in the calculation of the remaining carbon budget to limit global warming between 1.5 °C to 2 °C above pre-industrial levels. The plausibility of the permafrost region to be a considerable source of CH<sub>4</sub> adds an additional layer of concern regarding the permafrost carbon-climate feedback, since CH<sub>4</sub> has a 28-fold global warming potential (GWP) of CO<sub>2</sub> over a 100-year time horizon (Myhre et al., 2013).

## 1.2 The Lena River Delta

The Lena River Delta in Northeastern Siberia (72.0 – 73.8°N, 122.0 – 129.5°E) is the largest river delta in the Arctic and one of the largest worldwide, covering an area of approximately 32000 km<sup>2</sup>. It consists of an intricate network of rivers and channels, encompassing 1500 islands of varying sizes (Feliks & Reimnitz, 2000). Geomorphologically, the delta is divided into three main river terraces and a floodplain. The first terrace was formed during the Middle Holocene, is found in the central and eastern areas of the Lena River Delta, and features active floodplains, significant thermokarst activity and ice-wedge polygonal tundra. Samoylov Island is found in the first terrace. The second terrace was formed during the Late Pleistocene and the Early Holocene, is found in the northwestern area of the delta, and features sandy sediment with reduced ice content, and the third terrace was formed in the Late Pleistocene, and features ice and organic matter-rich sandy sediments, overlain by an ice complex, displaying weak polygonal structures. Kurungnakh Island is found in the third terrace (Boike et al., 2013; Schneider et al., 2009; Schwamborn et al., 2002).

---



The climate of the Lena River Delta is arctic-continental with low temperatures and precipitation, yet considered humid due to minimal evaporation rates. (Boike et al., 2008). The continuous permafrost is a defining attribute of the Lena River Delta, with depths reaching 500 to 600 m and one of the lowest permafrost temperatures among permafrost regions, with mean annual permafrost temperature of -8.6 °C at 10.7 m depth (Boike et al., 2013; V. E. Romanovsky et al., 2010).

Samoylov Island (72°22'N, 126°28'E) is the study site of the second chapter of this thesis. This island is situated in the southern central part of the Lena River Delta and has a research station. The island of about 5 km<sup>2</sup> is divided into an active floodplain in the west and a wet ice-wedge polygonal tundra, on a Late Holocene river terrace, in the east. Building on over twenty years of prior research at Samoylov Island, that sadly ended on February 2022, this study continues to examine greenhouse gas fluxes of the island (Eckhardt et al., 2019b).

Kurungnakh Island (72.3°N, 126.2°E) is the study site of the third chapter of this thesis. The island is situated in the central part of the Lena River Delta. The island is comprised of Yedoma deposits from the Weichselian overlain by Holocene deposits. The island is dominated by thermokarst and thermoerosion lakes, including thaw slumps along the Lena River channels (Morgenstern et al., 2013).

### **1.3 Quantification of greenhouse gas fluxes in the Arctic**

The scientific interest in permafrost was historically characterized by a sense of exploration, frequently undertaken by geologists, followed by geotechnical engineers, with a focus on search for fossil fuels, military activities and consequently on the development of infrastructure, mainly in North America and the former Soviet Union (French, 2018; van Huissteden, 2020). In 1838, Karl Ernst von Baer established the basis for modern permafrost research through his comprehensive analysis of ground ice and permafrost data (Baer, 2001). In 1927, Mikhail Ivanovitch Sumgin wrote "Permafrost soils in the USSR" (free translation) synthesizing historical cryosphere studies and introducing *vechnaia merzlota* (eternally frozen earth) as a term (Smirnov, 2017). In 1943, Siemon William Muller introduced the term "permafrost" in English, translating the Russian *vechnaia merzlota* through his work with Russian literature for the U.S. government (Ray,

---

1993). By the late 20<sup>th</sup> century, research by Romanovsky and Osterkamp (1997) provided early empirical evidence of warming trends in Alaskan permafrost, highlighting its sensitivity to climate change. Following this, the unfolding of the climate change has moved the research emphasis to understanding the implications of thawing permafrost on the carbon cycle and climate system.

The responses of some ecosystems to climate change are not yet fully understood, and therefore not appropriately accounted in climate models, especially regarding the timing, magnitude, and relative roles of different greenhouse gases. Despite these significant uncertainties, this feedback poses additional risks that intensify with further warming, substantially complicating efforts to cap global temperature increases. These include CO<sub>2</sub>, CH<sub>4</sub> and N<sub>2</sub>O emissions from wetlands, wildfires, and permafrost thaw, for which the quantitative understanding is low. As a result, earth system feedbacks such as the permafrost carbon-climate feedback are often listed as the main sources of uncertainty of the remaining carbon budget to limit global warming to well below 2 °C (Lamboll et al., 2023). This is especially relevant in the case of CH<sub>4</sub> and N<sub>2</sub>O, which are gases with increased global warming potential in comparison to CO<sub>2</sub> and raise concerns regarding their role in the climate change response of permafrost environments. It is well-documented that these environments emit considerable amounts of CH<sub>4</sub> (Christensen, 2024; Kleber et al., 2023; Rößger et al., 2022; Yuan et al., 2024) and N<sub>2</sub>O (Lacroix et al., 2022; Marushchak et al., 2021; Wegner et al., 2022). Essentially more data is needed about greenhouse gas emissions and their functioning in the Arctic (IPCC, 2021).

The overarching question about the magnitude and actual impact of the permafrost carbon-climate feedback encompasses varying and complementary research lines converging to shed light on the question from different perspectives. The research effort aiming to quantify Arctic greenhouse gas emissions has been based on field measurements, with methods like chamber measurements (Eckhardt et al., 2019b; Galera et al., 2023; Juutinen et al., 2022; Wickland et al., 2020) and eddy covariance systems (Beckebanze, Rehder, et al., 2022; Beckebanze, Runkle, et al., 2022; Dengel et al., 2021; Rößger et al., 2022; Skeeter et al., 2022; Skeeter et al., 2020), laboratory experiments (Herbst et al., 2024; Knoblauch et al., 2018; Knoblauch et al., 2013) and modelling studies (Beer et al., 2023; de Vrese et al., 2023; Rehder et al., 2023).

---

The quantification and partitioning of greenhouse gas fluxes identifies the individual fluxes stemming from different ecosystem processes and elements and allows the detection of the environmental factors behind the measured fluxes with useful detailing. A fuller picture of the measured fluxes can be obtained when the analysis not only differentiates between fluxes of the same gas but also incorporates the individual fluxes of other greenhouse gases. Hence, by adopting the partitioning of greenhouse gas fluxes, Eckhardt et al. (2019b) revealed reducing autotrophic respiration with rising water table. Recent studies demonstrate the importance of spatial heterogeneity in CO<sub>2</sub> and CH<sub>4</sub> exchanges in the Arctic. In Tiksi, northeastern Siberia, the net ecosystem exchange of CO<sub>2</sub> and ecosystem gross photosynthesis were highest in graminoid-dominated habitats in contrast to barren and dwarf-shrub tundra, with fens presenting the greater summertime CO<sub>2</sub> sequestration. Nonetheless, fens were also the largest CH<sub>4</sub> source, contrarily to dry tundra that consumed CH<sub>4</sub> (Juutinen et al., 2022). Similar conclusions were drawn in Utqiagvik, Alaska, where polygon types determined greenhouse gases fluxes (Dengel et al., 2021). Regions characterized by low-centered polygons exhibited increased CO<sub>2</sub> emissions, while CH<sub>4</sub> emissions were higher from low and flat-centered polygons.

Aerobic decomposition is generally faster than anaerobic decomposition (Gao et al., 2016). Microorganisms rely on alternative electron acceptors in this case, such as nitrate, sulfate, or CO<sub>2</sub>. Alternating aerobic and anaerobic conditions, as seen in periodically flooded areas, can accelerate organic matter decomposition, the more the faster the cycle intervals (Reddy & Patrick, 1975). The rate of anaerobic respiration by soil microorganisms is influenced by several factors, including water and nutrient availability, pH, temperature, redox potential, and the quality of soil organic matter, and in spite of its slower decomposition rates, produces significant quantities of CH<sub>4</sub> to the atmosphere (Andersen & White, 2006; Herndon et al., 2015).

Heterotrophic respiration is the respiration of the soil microbial community. It is effectively measured through the root-trenching, or clipping method, in which a trench is dug to physically isolate the roots contained in the measurement plot, and the active plant biomass is removed (Bond-Lamberty et al., 2011). As expected, warming is expected to increase heterotrophic respiration in the Arctic, but also vegetation shifts are expected to

---

have an effect. The addition of litter from deciduous shrubs stimulates heterotrophic respiration compared to non-shrub vegetation (Phillips & Wurzbarger, 2019).

Significant amounts of CH<sub>4</sub> are produced in anoxic conditions in the Arctic, especially when stable CH<sub>4</sub>-producing microbial communities establish. This could be one of the reasons why active layer CH<sub>4</sub> production is often higher than permafrost samples CH<sub>4</sub> production (Treat et al., 2015). However, it is not clear if this is a prerequisite in field conditions where organic matter, nutrients and organisms can be exchanged both vertically and horizontally, since the effect of the establishment of the CH<sub>4</sub>-producing microbial communities in the CH<sub>4</sub> production was identified experimentally (Knoblauch et al., 2018). Soil moisture, temperature and vegetation are important controllers of CH<sub>4</sub> production. Organic soils in inundated areas, especially under herbaceous vegetation, show higher CH<sub>4</sub> production compared to mineral soils (Treat et al., 2015). CH<sub>4</sub> oxidation occurs when methanotrophic bacteria consume CH<sub>4</sub>, potentially offsetting part of CH<sub>4</sub> production. CH<sub>4</sub> oxidation rates is also stimulated by temperature and can sometimes exceed production, when CH<sub>4</sub> fluxes are negative and CH<sub>4</sub> uptake takes place (Berestovskaya et al., 2005; Juncher Jørgensen et al., 2015; Zheng et al., 2018). Vegetation has a crucial role on how much of the CH<sub>4</sub> produced is finally emitted to the atmosphere. Vascular plants such as sedges can channel CH<sub>4</sub> inside their aerenchyma from the anoxic region of the soil to the atmosphere, through which CH<sub>4</sub> oxidation is prevented or diminished. Additionally, root exudates provide additional substrate for methanogenesis in the rhizosphere.

It is still complex to accurately quantify CH<sub>4</sub> fluxes in the Arctic, due to the high spatial and temporal variability. Ongoing vegetation changes and more often wildfires can further complicate that due to their critical roles in altering permafrost carbon cycling dynamics and consequently, CH<sub>4</sub> production (Treat et al., 2024). A major knowledge gap in the permafrost carbon-climate feedback research has been related to long-term trends in greenhouse gas emissions and temperature in the Arctic. Some studies have addressed this gap publishing paramount data from long-term measurements or experiments. Knoblauch et al. (2018) conducted a seven-year laboratory incubation with samples from the Lena River Delta and showed that equal amounts of CO<sub>2</sub> and CH<sub>4</sub> are formed in thawing permafrost under anoxic conditions once the CH<sub>4</sub>-producing microbial

---

communities are established. Rößger et al. (2022) also highlighted the significance of CH<sub>4</sub> emissions in this region, showing that CH<sub>4</sub> emissions have increased throughout the 16 years dataset. Usually, the eddy covariance method facilitates the acquisition of long-term dataset in comparison to chamber measurements and incubation experiments, which are more labor intensive. There are several examples of longer datasets of eddy covariance greenhouse gases measurements in the Lena River Delta (Holl et al., 2019; Rößger et al., 2022) and other Arctic regions (Dengel et al., 2021; Goodrich et al., 2016). These long-term datasets provide robust evidence for projections of increasing greenhouse gas emissions and their consequent climate feedback.

Understanding the ratio of CO<sub>2</sub> to CH<sub>4</sub> produced during the decomposition of the organic matter is crucial because of the higher global warming potential of CH<sub>4</sub> (Myhre et al., 2013). Despite prior studies using laboratory incubations to assess CO<sub>2</sub> and CH<sub>4</sub> production ratios, the results vary widely due to varying incubation conditions and the complex interplay of microbial communities and environmental factors (Heslop et al., 2019; Knoblauch et al., 2018; Treat et al., 2015; Treat et al., 2014). Additionally, CH<sub>4</sub> oxidation and different CH<sub>4</sub> transport pathways further affect these ratios (Knoblauch et al., 2015). The research gap lies in the need for a comprehensive understanding of these ratios under in situ conditions, which is essential for improving models that simulate feedback between thawing permafrost and global change, as current global models often use fixed ratios for methane production or emission (Kleinen et al., 2021).

It is of critical importance that current modelling developments progresses in addressing the underrepresentation and oversimplification of permafrost carbon processes observed in previous broader climate modeling efforts (Schädel et al., 2024). Some models offer greater specificity by simulating distinct physical processes that are unfolding within Arctic landscapes, such as described in Beer et al. (2023) that focused on an impactful aspect of abrupt permafrost thaw, which still lacks detailed estimates of CO<sub>2</sub> release, the retrogressive thaw slumps. They show that although these emissions are not relevant on a global scale, they possess the potential to become a major source of CO<sub>2</sub> depending on the future evolution of permafrost thaw. Another example is the study by Rehder et al. (2023) that addresses an often overlooked component of the Arctic carbon cycle, CH<sub>4</sub> emissions from ponds, by applying a process-based model that captured a linear increase

---

in CH<sub>4</sub> emissions with warming, caused mainly by the increase in productivity of vascular plants, which provides more substrate to methanogenesis and act as an efficient CH<sub>4</sub> transport pathway to the atmosphere. In a broader modelling scale, de Vrese et al. (2023) incorporated atmospheric feedbacks to permafrost carbon processes, and surprisingly showed that both wet and dry Arctic scenarios would result into comparable CH<sub>4</sub> fluxes, since the larger wetland area in the wet scenario was compensated by the greater substrate availability, due to higher temperatures, in the dry scenario. Furthermore, the critical role of permafrost thawing in continuing global warming, even if net zero emissions is reached, have been explored by different Earth System models. Permafrost thawing would keep happening in a warmed Earth, adding additional greenhouse gases and heat to the atmosphere (MacDougall, 2021; Randers & Goluke, 2020). Important developments have been achieved in statistical modelling approaches as well, as machine learning techniques (Virkkala et al., 2021) and the application of neural network analysis (Skeeter et al., 2022). These developments results in better identification of correlations and patterns in datasets, enabling better predictions of greenhouse gas emissions, and upscaling these emissions across high-latitude terrestrial regions. This new generation of models further develop the incorporation of key processes into climate models and improve our understanding of the permafrost carbon-climate feedback.

#### **1.4 Nutrients dynamics in a warming Arctic**

Nutrient limitation occurs when the availability of nutrients fails to fulfill the demand for achieving optimal net primary productivity in case of autotrophs and optimal growth and metabolism in case of heterotrophs (Du et al., 2024). Nutrients co-limitation occurs when two independent nutrients both reach limiting levels simultaneously, affecting a single organism or a community. However, it could also be present in other ways, as when a secondary nutrient becomes limiting after a primary nutrient limitation has been alleviated. Additionally, co-limitation can also happen when the presence of one nutrient is partially compensated for the scarcity of another or when the availability of one nutrient is necessary for the uptake of another nutrient at low levels (Bannon et al., 2022; Moore et al., 2013). Overall, co-limitation exists when two or more nutrient limitations, related or not, affect biological processes simultaneously. The Arctic cold climate conditions

---

significantly slow down biogeochemical processes, resulting in low nutrients availability, which limits both microbial activities and primary productivity (Hobbie et al., 2002). Additionally, the Arctic short growing season limits plant growth and consequently the organic matter input into the soil, what together with slower decomposition rates, exacerbate nutrients scarcity (Chapin Iii et al., 1995).

The CO<sub>2</sub> fertilization effect caused by anthropogenic CO<sub>2</sub> emissions and the increase in temperatures caused by global warming may alleviate the current constraints to the Arctic vegetation primary productivity in the case the vegetation growth is not limited by nutrients availability. A potentially greener Arctic would contribute to offset part of greenhouse gas emissions through enhanced photosynthesis. The availability of soil nutrients remains a critical limiting factor. It is yet not clear what would be the effect of warming on the availability of soil nutrients. It is possible that N, P and K mineralization rates, which is primarily performed by soil microorganisms, increase with higher organic matter decomposition rates, nonetheless it is also possible that increased microbial activity promote higher immobilization rates of these nutrients, enhancing the competition between microbes and plants for nutrients (Zhang et al., 2023), and potentially offsetting the effects of the CO<sub>2</sub> fertilization and higher temperatures on primary productivity (Wieder et al., 2015a).

Plant species and microorganisms exhibit varying nutrient needs, for example, woody vegetation would require less N than grasses. These different nutrient demands of plant species and different microorganisms add an extra layer of complexity in the biogeochemistry cycles of nutrients with climate change (Kattge, 2011; Krapp & Traong, 2006). My experiment, which results can be found in chapter 3, addresses the abovementioned discussion only indirectly, since it shows the effect of temperature in the dynamics of P and K in the presence of soil microorganisms, but not of plants. However, it gives evidence of possible competition for nutrients between microorganisms and plants and the interaction between nutrients and greenhouse gases production. The general trend that nutrients concentration shows during incubation time results from both mineralization and immobilization processes. Mineralization is the process by which microorganisms decompose organic matter, converting nutrients into inorganic forms that plants can absorb, and immobilization is the conversion of inorganic nutrients into

---

organic forms, incorporating them into microbial biomass and making them temporarily unavailable for plant uptake. When mineralization rates are higher than immobilization rates, this trend is of concentration increase with time, while a negative trend would be identified when the immobilization rates are higher than mineralization. Thus, both processes are occurring concomitantly but normally one is predominating.

Beermann et al. (2017) have encountered considerable amounts of ammonium in permafrost in several sites in Siberia, and forecasted, under the RCP8.5 scenario, a potential release of N with permafrost thawing in the same magnitude of the annual atmospheric N fixation in arctic soils, which still would be a small flux in comparison with the overall ecosystem N cycling. Plant growth in the Siberian polygon tundra is often co-limited by N and P, and less by K (Beermann et al., 2015). Nevertheless, there is less potential for P mineralization since 40% of the total P is found in the biologically active fraction, compared to 5% of N (Beermann et al., 2015). This indicates a P limitation in the long-term as microbial populations continue to develop and expand in the polygonal tundra (Beermann et al., 2015). Furthermore, it is likely that the estimated global increase of nutrient mineralization rates with warming shall not be sufficient to enable increases in primary productivity (Wieder et al., 2015a). Even if N limitation constraints are removed in the future, this is most likely not occurring for P, since increasing biological P demands shall outpace exogenous P inputs and enhanced P cycling (Vitousek et al., 2010; Wieder et al., 2015a, 2015b), a trend that includes the Arctic as well (Koller & Phoenix, 2017).

Another aspect to consider is the fate of additional nutrients mineralized due to warming. Naturally, for enhanced primary productivity, these nutrients should be taken up by plants. However, as previously mentioned, a portion may be immobilized by the soil microbiota. Yet, there are evidence of other potential destinies of additional nutrients. Observational and model data show a discrepancy in the timing of maximum vegetation growth and maximum thaw depth, as a result, nutrients are wasted and incompletely used by plants (Lacroix et al., 2022). Lateral and vertical exports are important mechanisms of biogeochemical compounds removal in permafrost regions (Beckebanze, Runkle, et al., 2022), resulting in significant nutrient loss via runoff and leaching (Treat et al., 2016). There is evidence that permafrost thaw may lead to increased transport of N

---



from uphill well-drained areas to the lower lands of the landscape across the Arctic (Hansen & Elberling, 2023) and it is predicted that until 2100 the transport of C, N and P to the Kara Sea in West Siberia, could increase up to 53% (Frey et al., 2007). Therefore, new data and studies about the deposition and distribution of nutrients in Arctic ecosystems shall improve our understanding of the role of nutrients in the permafrost carbon-climate feedback.

## 1.5 Research questions

The questions addressed in this thesis are crucial research gaps for advancing the frontier of knowledge in the direction of determining whether the Arctic is currently evolving into a stronger sink or a relevant source of greenhouse gases in the atmosphere. This thesis has been undertaken with the goal of increasing our understanding of the permafrost carbon-climate feedback in the present and in the future.

### **1) Will methane (CH<sub>4</sub>) fluxes in the Arctic increase with permafrost thawing, and what factors regulate the ratio between microbial CO<sub>2</sub> and CH<sub>4</sub> production from OM decomposition in the polygonal tundra?**

These questions motivated the second chapter of this thesis. Amid the prospect of exploding CH<sub>4</sub> emissions from a warmer Arctic that would notably worsen expected climate scenarios, the scientific community has focused on this question. To determine the processes of CH<sub>4</sub> fluxes in the Arctic and what regulates whether CO<sub>2</sub> or CH<sub>4</sub> is produced during organic matter decomposition, it is essential to analyze CH<sub>4</sub> and CO<sub>2</sub> production, CH<sub>4</sub> oxidation rates, hotspots, and associated environmental factors. This analysis will help the scientific community understand the magnitude of CH<sub>4</sub> and CO<sub>2</sub> emissions in the Arctic. Additionally, it will provide insights into the region response to warming.

### **2) Will phosphorus (P) and potassium (K) availability increase in a warmer Arctic?**

This is the question that motivated the third chapter of this thesis. P limitation is pervasive in Arctic ecosystems, while K is likely not limiting. Understanding whether the primary productivity of the Arctic vegetation will increase and offset part of the region emissions with climate change hinges on how soil nutrients availability responds to these changes.

---

Comprehending whether the current nutritional limitations on vegetation growth, and consequent Arctic greening, will be alleviated, remain unchanged, or become more pronounced is crucial for predicting future Arctic carbon emissions. Assessing this question involves understanding the behavior of these nutrients in the soil under the influence of temperature and microbial activity.

---

## 2 Ratio of In Situ CO<sub>2</sub> to CH<sub>4</sub> Production and Its Environmental Controls in Polygonal Tundra Soils of Samoylov Island, Northeastern Siberia

This chapter covers data collected from Samoylov Island in 2015. The fieldwork was conducted by Tim Eckhardt. Part of the data related to the partitioning of the CO<sub>2</sub> fluxes was already published by Eckhardt et al. (2019b). I have analyzed the CH<sub>4</sub> fluxes data and part of the CO<sub>2</sub> fluxes data, and I have written as the first author of the following published paper: Galera, L. A., Eckhardt, T., Beer, C., Pfeiffer, E.-M., Knoblauch C. (2023). Ratio of in situ CO<sub>2</sub> to CH<sub>4</sub> production and its environmental controls in polygonal tundra soils of Samoylov Island, Northeastern Siberia. *Journal of Geophysical Research: Biogeosciences*, 128, 2022JG006956. <https://doi.org/10.1029/2022JG006956>

### 2.1 Abstract

Arctic warming causes permafrost thaw and accelerates microbial decomposition of soil organic matter (SOM) to CO<sub>2</sub> and CH<sub>4</sub>. The determining factors for the ratio between CO<sub>2</sub> and CH<sub>4</sub> formation are still not well understood due to scarce in situ measurements, particularly in remote Arctic regions. I quantified the CO<sub>2</sub>:CH<sub>4</sub> ratios of SOM decomposition in wet and dry tundra soils by using CO<sub>2</sub> fluxes from clipped plots and in situ CH<sub>4</sub> fluxes from vegetated plots. At the water-saturated site, CO<sub>2</sub>:CH<sub>4</sub> ratios decreased sharply from 95 at beginning of July to about 10 in August and September with a median of 12.2 (7.70–17.1; 25%–75% quartiles) over the whole vegetation period. When considering CH<sub>4</sub> oxidation, estimated to reduce in situ CH<sub>4</sub> fluxes by 10%–31%, even lower CO<sub>2</sub>:CH<sub>4</sub> ratios were calculated (median 10.9–8.41). Active layer depth and soil temperature were the main factors controlling these ratios. CH<sub>4</sub> production was associated with subsoil (40 cm) temperature, while heterotrophic respiration was related to topsoil (5 cm) temperatures. As expected, CO<sub>2</sub>:CH<sub>4</sub> ratios were substantially higher at

---

the dry site (median 373, 292–500, 25%–75% quartiles). Both tundra types lost carbon preferentially in form of CO<sub>2</sub>, and CH<sub>4</sub>-C represented only 0.27% of the dry tundra total carbon loss and 6.91% of the wet tundra total carbon loss. The current study demonstrates the dynamic of in situ CO<sub>2</sub>:CH<sub>4</sub> ratios from SOM decomposition and will help improve simulations of future CO<sub>2</sub> and CH<sub>4</sub> fluxes from thawing tundra soils.

## 2.2 Introduction

Permafrost-affected soils contain about 1000 Pg of soil organic carbon (SOC) in the uppermost 3 m (Mishra et al., 2021). The Arctic is experiencing one of the highest impacts from climate change in the world (IPCC, 2022). Record high permafrost temperatures were registered in the last two decades (Biskaborn et al., 2019), leading to permafrost thaw. The microbial decomposition of thawing permafrost organic matter (OM) releases the greenhouse gases (GHG) CO<sub>2</sub> and CH<sub>4</sub> (Lindroth et al., 2022; Miner et al., 2022; Schuur et al., 2015). CH<sub>4</sub> has an at least 28 fold global warming potential (GWP) of CO<sub>2</sub> (Myhre et al., 2013). Hence, we need to understand the relative emission of CO<sub>2</sub> to CH<sub>4</sub> when permafrost-affected soils warm and permafrost thaws.

The formation of CO<sub>2</sub> and CH<sub>4</sub> from thawing permafrost has been studied most often by laboratory incubations. Using this method, a wide range (<1 to > 1000) of ratios between CO<sub>2</sub> and CH<sub>4</sub> production in permafrost-affected soils have been reported (Heslop et al., 2019; Knoblauch et al., 2018; Treat et al., 2015; Treat et al., 2014). This wide range might be caused by differences in incubation conditions and duration, and differences in the composition of OM and microbial communities (Treat et al., 2015). Since the energy gain of methanogenesis is low in comparison to microbial processes using electron acceptors such as oxygen (O<sub>2</sub>), nitrate, iron and sulfate, CH<sub>4</sub> production is low as long as these electron acceptors are available (Bodegom & Stams, 1999). Hence, the CO<sub>2</sub>:CH<sub>4</sub> ratio in incubations is not constant and may decrease with incubation time, owing to the depletion of alternative electron acceptors but also due to the establishment of an active CH<sub>4</sub> producing community (Knoblauch et al., 2018; Philben et al., 2020). Finally, soil incubations are generally done either under anoxic or oxic conditions, while soils, even under water saturated conditions, are characterized by redox gradients, which may last from completely anoxic to fully oxic. Thus, incubation experiments give only limited

---

information on the CO<sub>2</sub> and CH<sub>4</sub> production under *in situ* conditions. One approach used to measure reliable *in situ* CO<sub>2</sub> and CH<sub>4</sub> production rates is to derive them from soil concentration depth profiles (Clymo & Bryant, 2008; Clymo et al., 1995), but attempts to deduce the CO<sub>2</sub> to CH<sub>4</sub> partitioning from gas measurements have not been done yet.

Microbial CH<sub>4</sub> oxidation in soil layers that contain oxygen, such as the rhizosphere, where oxygen is leaking from the roots, or the surface soil, is further modifying the *in situ* CO<sub>2</sub>:CH<sub>4</sub> ratio. Aerobic CH<sub>4</sub> oxidizing bacteria may oxidize up to 99% of produced CH<sub>4</sub> to CO<sub>2</sub> in water saturated permafrost soils, with a particularly high importance of CH<sub>4</sub> oxidation at sites without vascular plants (Knoblauch et al., 2015; Popp et al., 2000). The relevance of CH<sub>4</sub> oxidation strongly depend on CH<sub>4</sub> transport pathways. CH<sub>4</sub> transported by molecular diffusion through the water phase is > 10<sup>4</sup> times slower than ebullition or plant-mediated transport through the gas phase in air filled tissue. Hence CH<sub>4</sub> oxidation is most relevant when CH<sub>4</sub> moves slowly through the soil (molecular diffusion in the water phase) and lowest when rapidly transported from its production zone into the atmosphere (ebullition, plant mediated transport) (Bastviken et al., 2008; Knoblauch et al., 2015; Whalen, 2005). Hence, the release of carbon as CO<sub>2</sub> or CH<sub>4</sub> is determined by complex interactions of the factors influencing not just their production, but also their transport.

The extensive Siberian tundra is currently underrepresented in international CH<sub>4</sub> emissions databases (Saunois et al., 2020). There are large uncertainties regarding the controls of CH<sub>4</sub> production and emission in the vast Russian arctic tundra, and consequently the response of CH<sub>4</sub> emission to climate change. Permafrost acts as a barrier to drainage resulting in lakes, ponds, and wetlands, characterized by anoxic conditions and accumulation of OM. The seasonal freezing and thawing of the upper soil layer (active layer) promote the creation of pattern ground, such as polygonal structures, where the depressed centers are often water saturated while the elevated rims are drained and characterized by oxic conditions (van Huissteden, 2020). Differences in vegetation type may account for substantial variation of CH<sub>4</sub> and CO<sub>2</sub> emissions from the arctic tundra (Cannone et al., 2016; Knoblauch et al., 2015). Due to the complexity of environmental and microbial parameters affecting CH<sub>4</sub> production and turnover in permafrost soils, there are still large uncertainties on how thaw-induced changes in the soil hydrology of permafrost landscapes will impact on *in situ* CO<sub>2</sub> and CH<sub>4</sub> production from thawing

---

permafrost OM and related GHG emissions (Euskirchen et al., 2017). The quantitative understanding of the regulation of the CO<sub>2</sub>:CH<sub>4</sub> ratio is needed to improve models simulating the feedback between thawing permafrost and global change. Most global models still calculate CH<sub>4</sub> production or emission as a fixed ratio of soil organic matter (SOM) decomposition (Kleinen et al., 2021; Melton et al., 2013; Wania et al., 2010).

The objective of this study is to improve our knowledge of the regulation of the ratio between microbial CO<sub>2</sub> and CH<sub>4</sub> production from OM decomposition under *in situ* conditions of a typical polygonal tundra. For this, small-scale approaches, such as chamber measurements are more appropriate than eddy-covariance systems (Krauss et al., 2016). Therefore, I used an experimental setup based on the chamber approach and measured for a whole summer season *in situ* greenhouse gas fluxes at two soils of the Siberian polygonal tundra characterized by different hydrological regimes. CH<sub>4</sub> production was estimated using fluxes above plots vegetated by vascular plants, and CO<sub>2</sub> fluxes representing heterotrophic respiration (R<sub>h</sub>) were quantified from clipped plots of a root-trenching experiment (Eckhardt et al., 2019b). By this approach, I identified the relative contribution of CO<sub>2</sub> and CH<sub>4</sub> production during OM decomposition in permafrost-affected soils under *in situ* conditions, identified the most important environmental parameters regulating the *in situ* ratio between CO<sub>2</sub> and CH<sub>4</sub> production and estimated the contribution of plant-mediated CH<sub>4</sub> transport to total CH<sub>4</sub> emissions. Finally, I used the obtained CO<sub>2</sub> and CH<sub>4</sub> data to calculate the production of CO<sub>2</sub> and CH<sub>4</sub> in the polygonal tundra of Samoylov Island for one summer thaw season.

## 2.3 Methods

### 2.3.1 Study Site

The study was conducted on Samoylov Island in the southern central Lena River Delta, northeastern Siberia (72°22' N, 126°28' E) in the continuous permafrost zone, with permafrost depths of 300 to 500 m (Yershov, 1998) (**Figure 1**). The annual mean permafrost temperatures are -8.6 °C at about 11 m depth, while temperatures at the surface soil can vary from 20 °C to -35 °C throughout the year. The island has an arctic continental climate with an annual mean temperature of -12.5 °C and an annual mean

---

precipitation of 321 mm (Boike et al., 2013). Snowmelt starts in June and the growing season lasts from mid-June to mid-September. Polar days, which are days when the sun remains above the horizon for more than 24 hours, spans from 7 May to 8 August and polar nights, which are days when the sun remains below the horizon for more than 24 hours, spans from 15 November to 28 January. The study has been executed at the eastern part of Samoylov Island, which is covered by ice-wedge polygonal tundra on a Late Holocene river terrace, characterized by ice-rich alluvial deposits. The polygonal tundra is formed by depressed polygon centers surrounded by elevated polygon rims with an elevation difference of about 0.5 m. Water-saturated soils are often found in the polygon centers due to the underlying permafrost that prevents drainage while soils at the elevated polygon rims are well-drained. Mean carbon pools in the uppermost 1 m are higher in the polygon centers (33 kg SOC m<sup>-2</sup>) than in the polygon rims (19 kg SOC m<sup>-2</sup>) (Zubrzycki et al., 2013).

The study was conducted in a polygon (72°22'26" N, 126°29'49" E) with one sub-site in the water saturated, depressed polygon center (wet tundra) and another sub-site in its surrounding polygon rim (dry tundra). The soil at the polygon center was classified as Reductaquic Cryosol (WRB, 2015) with the water table varying from 7 cm below to 7 cm above the soil surface during the measurement period, a maximum yearly ALD of 40 cm and vegetation dominated by mosses (*Drepanocladus revolvens*, *Meesia triquetra*, *Scorpidium scorpioides*) and the hydrophilic sedge *Carex aquatilis*. Total organic carbon (TOC) concentrations in the polygon center soil ranged between 10.1% and 19.6%, with highest concentrations in the uppermost 6 cm (Supporting information, Figure S1). The soil at the polygon rim was classified as Turbic Glacic Cryosol (WRB, 2015) with the water table a few centimeter above the permafrost table, maximum ALD of 30 cm and a vegetation dominated by mosses (*Hylocomium splendens*, *Polytrichum spp.*, *Rhytidium rugosum*), some small vascular plants (*Dryas punctata* and *Astragalus frigidus*) and lichens (*Peltigera spp.*). The polygon rim soil contained 12.3% of TOC in the uppermost 15 cm depth and cryoturbated horizons below 15 cm (Supporting information, Figure S2).

---

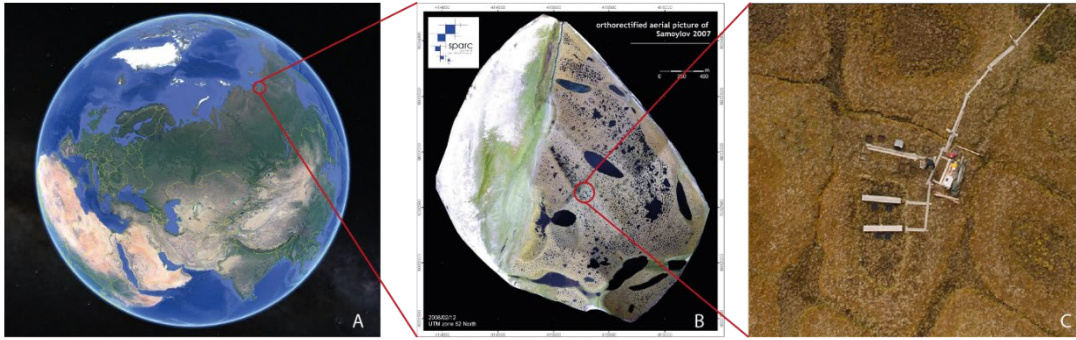


**Figure 1** - The study site on Samoylov Island, Lena River Delta, Northeastern Siberia (72°22' N, 126°28' E) from the perspective of the Eurasian continent. Panel (a): Eurasia (SIO et al.); Orthorectified aerial picture of Samoylov Island, Lena River Delta, Northeastern Siberia, Russia (Boike et al., 2012); Studied polygon in Samoylov Island (Boike et al., 2015).

### 2.3.2 Soils and meteorological data

The soil temperatures (SoilT) at 2, 5, 10, 15 and 40 cm and air temperature (AirT) at 2 m height, precipitation and incoming and outgoing components of shortwave and longwave radiation were recorded by a nearby meteorological station in the center and rim of a similar polygon about 40 m southwest of the study site (Boike et al., 2019). The surface temperature (SurfT) was estimated by the following equation:

$$SurfT = \left( \frac{L\uparrow_B}{\varepsilon\sigma} \right)^{\frac{1}{4}}, \quad (1)$$

where  $L\uparrow_B$  is the upward infrared radiation ( $W\ m^{-2}$ ),  $\varepsilon$  is the dimensionless emissivity in the value of 0.98 and  $\sigma$  is the Stefan-Boltzmann constant ( $W\ m^{-2}\ K^{-4}$ ) (Wilber et al., 1999). The SurfT was calculated in Kelvin with equation (1) and converted to degrees Celsius.

The description of the water table depth (WT) measurements in the center, the volumetric soil water content (VWC) at the rim and the ALD in both sub-sites can be found in Eckhardt et al. (2019b).



### 2.3.3 Chamber measurements and plant mediated CH<sub>4</sub> transport

At each sub-site, ten measurement plots made of PVC frames (50 x 50 cm) were established. From these, four had their original vegetation intact (hereafter called 'vegetated'), while six had the surface vegetation removed (hereafter called 'clipped'). The experiment has been described in detail by Eckhardt et al. (2019b). The frames were inserted 20 cm deep into the soil, below the main rooting zone. The opaque acrylic emission chamber was equipped with a fan for the mixing of the air. The chambers were 50 cm high and enclosed a volume between 124 and 143 L, depending on the terrain inside the chamber frames. Two holes with 3 cm of diameter were left open at the top of the chamber while placing it slowly on the frames to avoid pressure-induced gas release from the soil (Christiansen et al., 2011; Eckhardt et al., 2019b). These holes were closed before the measurement. A boardwalk was installed at the polygon to avoid disturbances. I performed a clipping experiment by using the root-trenching method in 4 frames at each sub-site on the polygon (center and rim) in 2014. In addition to the cutting of the lateral roots through the insertion of the PVC frames, all living plant biomass, including mosses, was carefully removed from within the 'clipped' frames. During the measurement period in 2015, this procedure was repeated periodically to prevent plant regrowth. Additionally, two frames were installed in 2015 and clipped at each sub-site to evaluate if CO<sub>2</sub> fluxes were biased due to the additional decomposition of residual roots, which might be a possible artefact of the root-trenching method. However, no significant difference between the CO<sub>2</sub> fluxes in the clipped plots of 2014 and those clipped in 2015 were observed (Eckhardt et al., 2019b).

The CH<sub>4</sub> concentrations in the headspace of the chambers were measured with a portable gas analyzer (UGGA 30-p; Los Gatos Research, USA) and recorded with a data logger (CR800 series; Campbell Scientific Ltd., USA). The precision of the gas analyzer for CH<sub>4</sub> is better than 0.005 ppm. Chamber closure time was 120 seconds, during which chamber headspace air was pumped in a closed loop through the analyzer at a rate of 200 mL min<sup>-1</sup>. Measurements were conducted between July 11<sup>th</sup> and September 22<sup>nd</sup>, 2015, except in the periods between 2<sup>nd</sup> and 9<sup>th</sup> of August, when a shift change between researchers took longer than expected, and 17<sup>th</sup> and 24<sup>th</sup> of August, when the measurements were

---

impossible due to a heavy storm event. During the measurement period, measurements were taken at least every third day. The  $R_h$  fluxes used in this study are from Eckhardt et al. (2019b). The  $CH_4$  fluxes were calculated using MATLAB (MATLAB, 2019) with a routine combining different regression models, such as linear, exponential and increasing polynomial degrees, and statistical analysis for model selection. Details can be found in Eckhardt and Kutzbach (2016).  $CH_4$  concentrations inside the chamber headspace increased linearly over time (Supporting information, Figure S4), thus linear regressions have been used for the flux calculation. The first 30 s of each 120 s measurement period were discarded to eliminate possible perturbations when placing the chamber on the frame. The fraction of plant mediated  $CH_4$  fluxes was calculated as the difference between the daily mean  $CH_4$  fluxes from the vegetated plots and the clipped plots (**Table 1**).

**Table 1** – Median, first (Q1) and third (Q3) quartiles  $CH_4$  fluxes during the growing season of 2015 from vegetated and clipped plots in a polygon center and a polygon rim on Samoylov Island, and contribution of plant-mediated  $CH_4$  transport.

Polygon sub-site	CH <sub>4</sub> flux (mg m <sup>-2</sup> d <sup>-1</sup> )						Plant-mediated transport (%)		
	Vegetated			Clipped					
	Q1	Median	Q3	Q1	Median	Q3	Q1	Median	Q3
Center	21.1	<b>26.4</b>	32.5	2.63	<b>4.31</b>	9.19	65.3	<b>79.3</b>	89.3
Rim	1.58	<b>1.85</b>	2.20	1.50	<b>1.67</b>	1.91	-15.7	<b>2.86</b>	20.9

### 2.3.4 Calculation of CO<sub>2</sub>:CH<sub>4</sub> ratios and uncertainty range

The CO<sub>2</sub>:CH<sub>4</sub> ratios were calculated on a molar basis, using the daily mean  $CH_4$  fluxes from the vegetated plots, and the daily mean  $R_h$  fluxes, which were measured with dark chambers in the clipped plots (see Eckhardt et al. (2019b) and Eckhardt et al. (2019a)). The  $CH_4$  fluxes above vegetated plots in the water saturated polygon center are the best estimate of *in situ*  $CH_4$  production. These fluxes might underestimate the  $CH_4$  production, since no  $CH_4$  oxidation is considered. However, we have estimated the range of  $CH_4$  oxidation that could be affecting my measured fluxes using the fraction of oxidized  $CH_4$  and plant mediated  $CH_4$  transport data from studies in sites similar to this study, as it is

described later in this section. Hence, the calculated CO<sub>2</sub>:CH<sub>4</sub> ratios of the polygon center are considered as the CO<sub>2</sub>:CH<sub>4</sub> production ratios. However, this is not the case for the polygon rim CH<sub>4</sub> fluxes due to high CH<sub>4</sub> oxidation in the unsaturated soil. This procedure resulted in one single CO<sub>2</sub>:CH<sub>4</sub> ratio per day in each sub-site on the polygon center and rim. Thus, to obtain a variation measure for these daily ratios, I propagated the standard deviation of the CH<sub>4</sub> and CO<sub>2</sub> daily fluxes using the following equation:

$$\sigma_{\text{CO}_2:\text{CH}_4} = \sqrt{\left(\frac{\sigma_{\text{CO}_2}}{f_{\text{CO}_2}}\right)^2 + \left(\frac{\sigma_{\text{CH}_4}}{f_{\text{CH}_4}}\right)^2} \times \text{CO}_2:\text{CH}_4 \quad (2)$$

Where  $\sigma_{\text{CO}_2:\text{CH}_4}$  is the estimated standard deviation of the CO<sub>2</sub>:CH<sub>4</sub> ratio; CO<sub>2</sub>:CH<sub>4</sub> is the mean CO<sub>2</sub>:CH<sub>4</sub> ratio;  $\sigma_{\text{CO}_2}$  is the standard deviation of the CO<sub>2</sub> fluxes;  $f_{\text{CO}_2}$  is the mean CO<sub>2</sub> flux;  $\sigma_{\text{CH}_4}$  is the standard deviation of the CH<sub>4</sub> fluxes and  $f_{\text{CH}_4}$  is the mean CH<sub>4</sub> flux.

My approach to estimate CH<sub>4</sub> production in the soil from CH<sub>4</sub> fluxes above vegetated plots is neglecting CH<sub>4</sub> oxidation in the soil, which cause an underestimation of *in situ* CH<sub>4</sub> production. To account for this potential error, we used published data on CH<sub>4</sub> oxidation (Knoblauch et al., 2015; Preuss et al., 2013) at water saturated polygon centers on Samoylov that were vegetated by the same vascular plant (*Carex aquatilis*) as my site (**Table 2**). The polygon center daily average CH<sub>4</sub> fluxes ( $f_{\text{CH}_4(\text{corrected})}$ ) were recalculated as follows:

$$f_{\text{CH}_4(\text{corrected})} = \left(\frac{D_{\text{CH}_4}}{1-\text{MOR}} + P_{\text{CH}_4}\right) \times f_{\text{CH}_4} \quad (3)$$

Where, MOR is the fraction of produced CH<sub>4</sub> oxidized in the soil,  $D_{\text{CH}_4}$  is the fraction of CH<sub>4</sub> transported through the soil,  $P_{\text{CH}_4}$  is the fraction of CH<sub>4</sub> transported through plants and  $f_{\text{CH}_4}$  is the mean CH<sub>4</sub> flux. The MOR values were retrieved from the literature, and the  $D_{\text{CH}_4}$  values were either the clipped plots CH<sub>4</sub> fluxes of this study or additional values retrieved from the literature. The use of these values in the definition of the upper and lower boundaries of the uncertainty range is shown in **Table 2**. The lower boundary uses the lowest CH<sub>4</sub> oxidation from Preuss et al. (2013), and the highest  $P_{\text{CH}_4}$  from Knoblauch et al. (2015). The upper boundary uses the highest CH<sub>4</sub> oxidation from Knoblauch et al. (2015) and the lowest  $P_{\text{CH}_4}$ , which was found in this study. This approach assumes that

---

only CH<sub>4</sub> diffusing slowly through the soil is affected by CH<sub>4</sub> oxidation but not that fraction of CH<sub>4</sub>, which is released rapidly by plant mediated transport. These new daily mean CH<sub>4</sub> fluxes were then used to recalculate the center CO<sub>2</sub>:CH<sub>4</sub> production ratios as described above.

**Table 2** - Fraction of CH<sub>4</sub> transported through the bulk soil ( $D_{CH_4}$ ) and of plant mediated transport ( $P_{CH_4}$ ) as well as CH<sub>4</sub> oxidized in water saturated polygon centers, vegetated by *Carex aquatilis* on Samoylov Island. Methane production and CO<sub>2</sub>:CH<sub>4</sub> production ratios are calculated for three assumptions regarding the fraction of CH<sub>4</sub> oxidized and of the different transport pathways (see Methods, eq. (3)).

Study	Fraction $P_{CH_4}$	Fraction $D_{CH_4}$	Fraction of CH <sub>4</sub> oxidized in bulk soil	Fraction of total CH <sub>4</sub> oxidized	CH <sub>4</sub> production (mg CH <sub>4</sub> m <sup>-2</sup> d <sup>-1</sup> )	CO <sub>2</sub> :CH <sub>4</sub> production ratio
Assumption 1 (no CH <sub>4</sub> oxidation)	0.79 <sup>‡</sup>	0.21 <sup>‡</sup>	0	0	26.4 (21.1 - 32.5)	12.2 (7.70 - 17.1)
Assumption 2 (lowest CH <sub>4</sub> oxidation, highest $P_{CH_4}$ )	0.86 <sup>§</sup>	0.14 <sup>§</sup>	0.45 <sup>§</sup>	0.10	29.5 (23.5 - 36.3)	10.9 (6.91 - 15.4)
Assumption 3 (highest CH <sub>4</sub> oxidation, lowest $P_{CH_4}$ )	0.79 <sup>‡</sup>	0.21 <sup>‡</sup>	0.68 <sup>§</sup>	0.31	38.2 (30.5 - 47.1)	8.41 (5.32 - 11.8)

<sup>‡</sup>this study, <sup>§</sup>Knoblauch et al 2015, <sup>§</sup>Preuss et al., 2013.

### 2.3.5 Calculation of a seasonal CO<sub>2</sub> and CH<sub>4</sub> release

The seasonal CO<sub>2</sub> and CH<sub>4</sub> release were calculated from the CO<sub>2</sub> and CH<sub>4</sub> emissions of the wet (polygon center) and dry tundra (polygon rim) in kilograms per hectare per day, during the measurement period. The daily average CO<sub>2</sub> fluxes of the clipped plots, representing the  $R_h$ , were taken from Eckhardt et al. (2019b). From 11/07/2015 to 22/09/2015 there were 47 days with CO<sub>2</sub> and CH<sub>4</sub> measurements. I filled the gaps between

measurements by linearly interpolating the daily average of CO<sub>2</sub> and CH<sub>4</sub> fluxes (Bjorkegren et al., 2015; Chen et al., 2011; Gana et al., 2018; Khokhar & Park, 2017; Kwon et al., 2017; Natchimuthu et al., 2017; Savage & Davidson, 2003; Schrier-Uijl et al., 2010; Wickland et al., 2006). For the direct comparison of CO<sub>2</sub> and CH<sub>4</sub> production (**Table 3**), the median CO<sub>2</sub> fluxes ( $R_h$ ) and the median CH<sub>4</sub> fluxes were normalized to carbon (kg CO<sub>2</sub>-C/CH<sub>4</sub>-C ha<sup>-1</sup> d<sup>-1</sup>) to consider mass differences of the two molecules. For the comparison based on the whole area of Samoylov (**Table 3**), I used the fraction of wet and dry tundra (19% and 65%, respectively) of the polygonal tundra mapped by Muster et al. (2012) on Samoylov Island, resulting in 54 ha of wet tundra and 185 ha of dry tundra. The active floodplains and open water bodies have not been included in my study. The CO<sub>2</sub>-C and CH<sub>4</sub>-C fluxes were multiplied by the area of each land cover (dry and wet tundra), resulting in daily absolute CO<sub>2</sub>-C and CH<sub>4</sub>-C production (kg CO<sub>2</sub>-C/CH<sub>4</sub>-C d<sup>-1</sup>) of each tundra type.

---

**Table 3** - CO<sub>2</sub> (R<sub>H</sub>) and CH<sub>4</sub> emissions from two sub-sites in the polygonal tundra on Samoylov Island for the growing season in 2015. The table shows the median emissions calculated after the dataset gap-filling linear interpolation (see Methods). Both emission rates were converted to carbon mass emissions to allow a direct comparison between them. Moreover, both emission rates were multiplied by the wet and dry tundra area (Muster et al., 2012) to calculate the seasonal CO<sub>2</sub> and CH<sub>4</sub> release for the whole polygonal tundra of Samoylov Island. R<sub>H</sub> data are from Eckhardt et al. (2019b). The last column shows the contribution of each GHG in total C emissions.

<b>Wet tundra</b>					
<b>GHG</b>	<i>kg ha<sup>-1</sup> d<sup>-1</sup></i>	<i>kg-C ha<sup>-1</sup> d<sup>-1</sup></i>	<i>Area</i>	<i>kg-C d<sup>-1</sup></i>	<i>% of total C emissions</i>
<b>CO<sub>2</sub> (R<sub>H</sub>)</b>	9.81	2.68	<i>x 54.1 ha</i>	145	93.1
<b>CH<sub>4</sub></b>	0.265	0.199	<i>x 54.1 ha</i>	11	6.91
<b>Total</b>		2.87		155	100
<b>Dry tundra</b>					
<b>GHG</b>	<i>kg ha<sup>-1</sup> d<sup>-1</sup></i>	<i>kg-C ha<sup>-1</sup> d<sup>-1</sup></i>	<i>Area</i>	<i>kg-C d<sup>-1</sup></i>	<i>% of total C emissions</i>
<b>CO<sub>2</sub> (R<sub>H</sub>)</b>	19.5	5.32	<i>x 185 ha</i>	984	99.7
<b>CH<sub>4</sub></b>	0.019	0.014	<i>x 185 ha</i>	3	0.27
<b>Total</b>		5.33		986	100

### 2.3.6 Statistics

The CO<sub>2</sub>:CH<sub>4</sub> ratios of the polygon center and rim were analyzed separately through linear regression models. First, I have assessed the relationship between CO<sub>2</sub>:CH<sub>4</sub> ratios and each of the daily mean environmental variables, namely soil temperatures at 2 cm, 5 cm, 10 cm, 15 cm, and 40 cm depth, SurfT, ALD, WT (for the polygon center) and VWC (for the polygon rim) and selected the best predictors. The same was made with the CH<sub>4</sub> and CO<sub>2</sub> (R<sub>H</sub>) daily mean fluxes, in order to clarify the relationships found between the

predictors and the CO<sub>2</sub>:CH<sub>4</sub> ratios. Natural logarithm transformation was applied for non-normally distributed data.

Then, a multivariate regression model relating the CO<sub>2</sub>:CH<sub>4</sub> ratios with the best predictors, chosen during the abovementioned linear regressions between CO<sub>2</sub>:CH<sub>4</sub> ratios and individual environmental parameters, was set including the possible interaction between predictors. If the interaction between predictors was not significant ( $p > 0.05$ ), the sum of their effects was considered. The possibility of logarithmic and exponential relationships between response variables and predictors were also verified throughout the previous steps.

I choose the model with the highest R<sup>2</sup>, smallest root mean squared error (RMSE), lowest p-value from the model F-test ( $\alpha = 0.05$ ) and the lowest Akaike Information Criterion (AIC) that gives the relative quality of statistical models for the same dataset. The best adjusted regressions are shown in the results section. The statistical analyses were performed in R (R, 2020).

**Table 4** – Statistical models describing the relationship between CO<sub>2</sub>:CH<sub>4</sub> ratios and environmental variables, selected according to criteria described in Methods section (see 2.6 Statistics). “Interaction” states for the interaction between predictors.

Sub-site	Center	Rim
<b>Statistical model</b>	CO <sub>2</sub> :CH <sub>4</sub> = -0.811(ALD) - 174(logSoilT40) + 4.79(ALD*logSoilT40) + 40.6	CO <sub>2</sub> :CH <sub>4</sub> = 29.9(SoilT5) - 7.84(ALD) + 446
<b>R<sup>2</sup></b>	0.88	0.63
<b>p-value</b>	<0.001	<0.001
<b>RMSE</b>	6.86	103
<b>Interaction</b>	significant ( $p < 0.001$ )	not significant ( $p = 0.459$ )

## 2.4 Results

### 2.4.1 CH<sub>4</sub> fluxes and plant-mediated transport

The CH<sub>4</sub> fluxes from the vegetated plots at the polygon center varied throughout the measurement period, showing a clear seasonality (**Figure 2**). There was a fast increase in July, at the beginning of the growing season, followed by a slower increase in the first weeks of August. The fluxes stabilized at the peak emission rates, representing six times the flux measured in the beginning of July, from mid-August until the beginning of September, when the fluxes started to decrease at the end of the growing season. The variation of CH<sub>4</sub> fluxes at the polygon rim showed no seasonality but a sudden increase on the 22<sup>nd</sup> of September, the last day of measurements.

The median CH<sub>4</sub> flux of the vegetated plots at the polygon center was 26.4 mg m<sup>-2</sup>d<sup>-1</sup> (21.1-32.5 mg m<sup>-2</sup> d<sup>-1</sup>; 25%-75% quartiles). The median CH<sub>4</sub> flux at the polygon rim was 1.85 mg m<sup>-2</sup> d<sup>-1</sup> (1.58-2.22 mg m<sup>-2</sup> d<sup>-1</sup>; 25%-75% quartiles). The daily CH<sub>4</sub> fluxes means at the center were between 3.9 to 20.2 times higher than at the rim throughout the season. The log transformed CH<sub>4</sub> fluxes from vegetated plots at the center had significant relationships with the ALD ( $R^2 = 0.73$ ;  $p < 0.001$ ), with the SoilT40 ( $R^2 = 0.68$ ;  $p < 0.001$ ) and had no relationship with the SurfT ( $p = 0.172$ ). The log transformed CH<sub>4</sub> fluxes at the rim also had a significant relationship with the ALD but with a lower  $R^2$  ( $R^2 = 0.44$ ;  $p < 0.001$ ) and with the SoilT40 ( $R^2 = 0.42$ ;  $p < 0.001$ ), but no relationship with shallower soil temperatures like the SoilT5 ( $p = 0.404$ ) and SurfT ( $p = 0.824$ ).

The mean daily CH<sub>4</sub> fluxes of the clipped plots at the polygon center were lower than those from the vegetated plots. The differences between vegetated and clipped plots are smaller at the beginning of the growing season compared to later periods. Based on the differences in CH<sub>4</sub> fluxes between clipped and vegetated plots, the median plant-mediated CH<sub>4</sub> transport at the polygon center is 79% (65% - 89%, 25%-75% quartiles). At the polygon rim there was only a small difference between clipped and vegetated plots of 3% (**Table 1**)

Based on stable isotope signatures of CH<sub>4</sub> dissolved in the water saturated soil of polygon centers on Samoylov, it has been estimated that a fraction between 0.45 and 0.68 of the

---



CH<sub>4</sub> diffusing through the bulk soil is oxidized to CO<sub>2</sub> before emitted into the atmosphere (Knoblauch et al., 2015; Preuss et al., 2013)(**Table 2**). Using this range of CH<sub>4</sub> oxidation and the fraction of plant mediated CH<sub>4</sub> transport ( $P_{CH_4}$ ) and CH<sub>4</sub> transport through the bulk soil ( $D_{CH_4}$ ) determined in this and previous studies (Knoblauch et al., 2015; Preuss et al., 2013) We calculated that a fraction between 0.10 and 0.31 of produced CH<sub>4</sub> might have been oxidized before emitted into the atmosphere (assumptions 2 and 3, **Table 2**). Using these CH<sub>4</sub> oxidation estimates would increase the median of CH<sub>4</sub> production rates from 26.4 mg m<sup>-2</sup>d<sup>-1</sup> (no oxidation assumed) to 29.5 mg m<sup>-2</sup>d<sup>-1</sup> (fraction of 0.10 oxidized) and 38.2 mg m<sup>-2</sup>d<sup>-1</sup> (fraction of 0.31 oxidized) (**Table 2**).

---

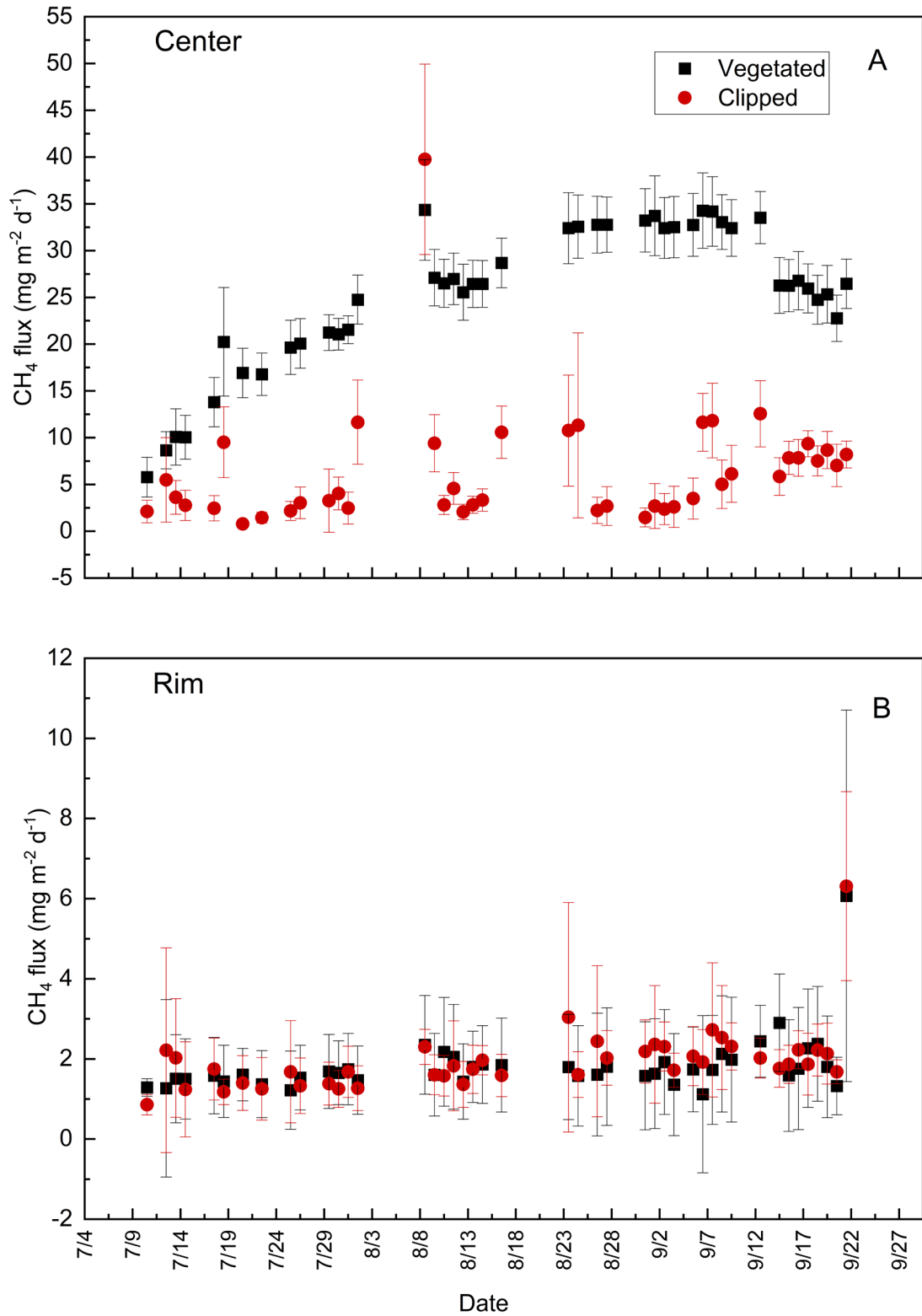


**Figure 2** - Daily mean and standard deviation of CH<sub>4</sub> fluxes (n = 8) between July and September 2015 from a polygon on Samoylov Island at vegetated and clipped plots in the polygon center (A) and polygon rim (B).

#### 2.4.2 CO<sub>2</sub>:CH<sub>4</sub> ratios, their environmental controls and uncertainty range

The CO<sub>2</sub>:CH<sub>4</sub> ratios, calculated from *in situ* CH<sub>4</sub> fluxes and heterotrophic CO<sub>2</sub> fluxes, varied between 3 and 95 at the polygon center (**Figure 3**), while it varied at the rim between 80 and 1074. The CO<sub>2</sub>:CH<sub>4</sub> ratios at the polygon center were around 95 at the beginning of July and decreased rapidly until mid-July. From 21/7 on, the ratios ranged between 7 and 15. There was a high variability of CO<sub>2</sub>:CH<sub>4</sub> ratios in the polygon rim. The amplitude of this variation and the ratios themselves are higher in July and steadily decrease over time. From 12/9 on, this downwards trend is seen more clearly. The median CO<sub>2</sub>:CH<sub>4</sub> ratio was 12.2 (7.70 - 17.1; 25%-75% quartiles) at the polygon center and 373 (292 - 500, 25%-75% quartiles) at the polygon rim.

The best predictor of the CO<sub>2</sub>:CH<sub>4</sub> ratios at the polygon center was the ALD, with a linear relationship ( $R^2 = 0.72$ ;  $p < 0.001$ ) (**Figure 3**). Both the CO<sub>2</sub>:CH<sub>4</sub> ratio and the ALD stabilize around a constant value from end of July until the 22<sup>nd</sup> of September. The second-best predictor for the CO<sub>2</sub>:CH<sub>4</sub> ratios at the polygon center was the SoilT40 with a logarithmic relationship ( $R^2 = 0.65$ ;  $p < 0.001$ ). The center CO<sub>2</sub>:CH<sub>4</sub> ratios have exponential relationships with AirT ( $R^2 = 0.36$ ;  $p < 0.001$ ) and SurfT ( $R^2 = 0.35$ ;  $p < 0.001$ ), but the inclusion of these variables into the multivariate regression model have not improved its quality.

The CO<sub>2</sub>:CH<sub>4</sub> ratios at the polygon rim had higher variability and a more gradual decreasing trend along the season than at the center. The best predictors of the CO<sub>2</sub>:CH<sub>4</sub> ratios at the polygon rim were the SoilT5 (lin;  $R^2 = 0.55$ ;  $p < 0.001$ ) and the SurfT (lin;  $R^2 = 0.45$ ;  $p < 0.001$ ). However, the inclusion of the SurfT as a predictor along with the SoilT5 into the multivariate regression model did not add explanatory power to it, which was shown by a higher AIC. For that reason, the ALD, which was the third best predictor (lin;  $R^2 = 0.30$ ;  $p < 0.001$ ), was included instead, with a significant increase in the quality of the

---

model ( $p = 0.024$ ). The statistical models that showed the best explanatory power for the  $\text{CO}_2:\text{CH}_4$  ratios at the polygon center and rim are shown in **Table 4**.

In addition to the relationships of  $R_h$  and environmental variables reported in Eckhardt et al. (2019b) I present here some additional relationships that improve our understanding of the  $\text{CO}_2:\text{CH}_4$  ratios. The  $R_h$  at the polygon center showed relationships with the SurfT (lin;  $R^2 = 0.59$ ;  $p < 0.001$ ), with the SoilT40 (log;  $R^2 = 0.24$ ;  $p < 0.001$ ) and no relationship with the ALD (lin;  $p = 0.06153$ ). The  $R_h$  at the polygon rim had a linear relationship with the SoilT5 ( $R^2 = 0.60$ ;  $p < 0.001$ ) but none with the ALD (lin;  $p = 0.07643$ ). Furthermore, there was a weak linear relationship between the SurfT and the SoilT40 at the polygon center ( $R^2 = 0.1305$ ;  $p = 0.01598$ ).

Using  $\text{CH}_4$  fluxes corrected for  $\text{CH}_4$  oxidation ( $f_{\text{CH}_4(\text{corrected})}$ ) to calculate ratios between  $\text{CO}_2$  and  $\text{CH}_4$  production results in a decrease in  $\text{CO}_2:\text{CH}_4$  ratios (**Figure 3**) with median values of 10.9 (fraction of 0.10 oxidized) and 8.41 (fraction of 0.31 oxidized) in comparison to 12.2 (no oxidation assumed) (**Table 2**).

---

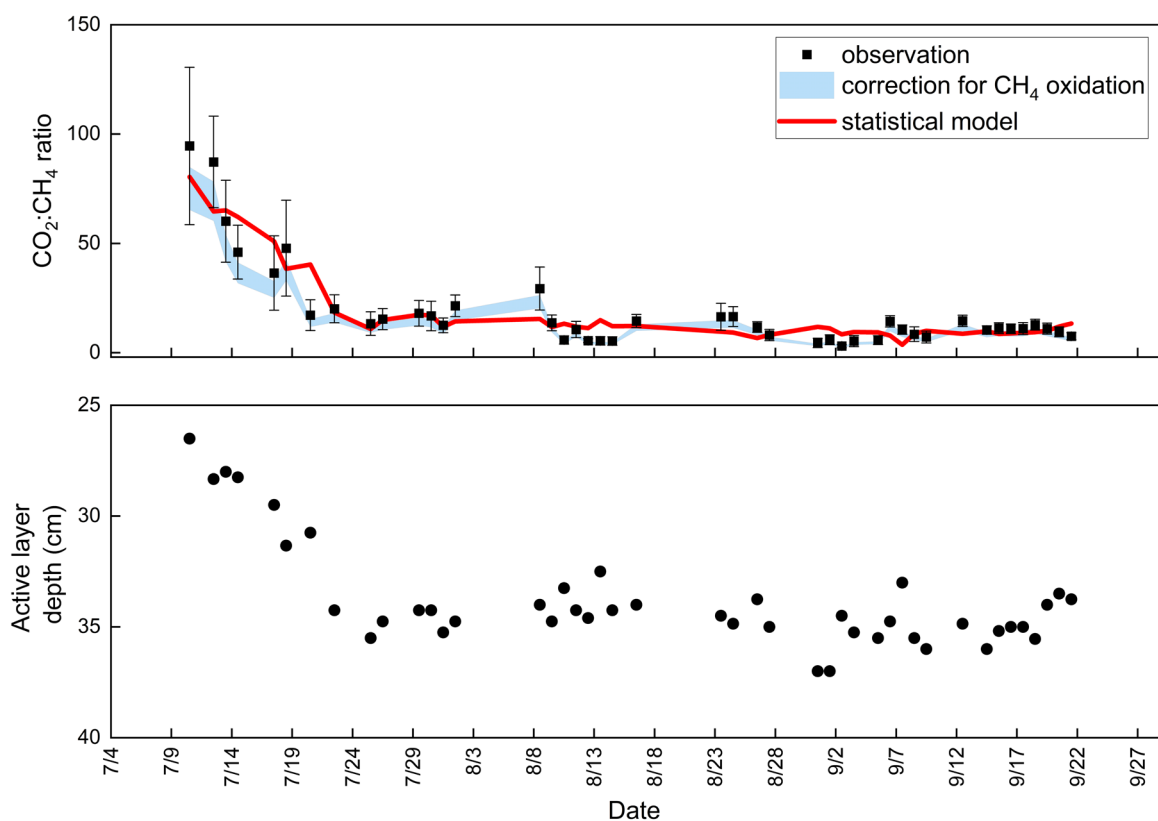


**Figure 3** - (a) Ratio of daily  $\text{CO}_2$  fluxes from heterotrophic respiration and  $\text{CH}_4$  emissions at the polygon center (black squares), range of  $\text{CO}_2:\text{CH}_4$  ratios after considering a fraction of produced  $\text{CH}_4$  oxidized between 0.10 and 0.30 (shaded area) and results from multivariate regression analysis with active layer depth (ALD) and soil temperature at 40 cm (SoilT40) as influence parameters (red line). Error bars give the estimated standard deviation. (b) Mean daily ALD at the polygon center during the growing season in 2015.

### 2.4.3 Seasonal $\text{CO}_2$ and $\text{CH}_4$ release

The median  $\text{CO}_2$  production of the wet tundra during the thaw season was lower than the one of the dry tundra, while the median  $\text{CH}_4$  production of the wet tundra was higher than of the dry tundra (Table 3). The  $\text{CO}_2$  and  $\text{CH}_4$  fluxes were converted to kg-C fluxes to allow a direct comparison between them. The wet tundra, although producing more  $\text{CH}_4$  than the dry tundra, emitted around half the total kg-C of the dry tundra. When the size of each land cover is considered, the dry tundra emits more than six times the total kg-C, as  $\text{CO}_2$  and  $\text{CH}_4$ , of the wet tundra. Due to the small area of wet tundra on Samoylov

Island and the low contribution of CH<sub>4</sub> to the dry tundra GHG fluxes, CH<sub>4</sub> emissions contributed only 1.17% (or 13.4 kg-C d<sup>-1</sup>) to the total daily release of carbon from the polygonal tundra on Samoylov (1142 kg-C d<sup>-1</sup>, **Table 3**).

## 2.5 Discussion

### 2.5.1 CH<sub>4</sub> emissions in comparison to other arctic sites

The median CH<sub>4</sub> emissions during the growing season from the polygon center in this study (26.4 mg m<sup>-2</sup> d<sup>-1</sup>) are at the lower end of CH<sub>4</sub> fluxes reported from the water saturated polygonal tundra on Samoylov vegetated by vascular plants of 28.0 – 100.0 mg m<sup>-2</sup> d<sup>-1</sup> (Knoblauch et al., 2015; Kutzbach et al., 2004; Sachs et al., 2010; Wagner et al., 2003). These differences can be related to the high spatial and temporal variability of CH<sub>4</sub> emissions in the Siberian tundra (Skeeter et al., 2020), but also to differences in data evaluation. The highest CH<sub>4</sub> emissions from water saturated polygon centers on Samoylov (77.9 – 100.0 mg m<sup>-2</sup> d<sup>-1</sup> (Sachs et al., 2010)) were calculated from an initial non-linear CH<sub>4</sub> concentration increase with an exponential model, resulting in higher fluxes than linear models. We could only observe an initial non-linear rise of CH<sub>4</sub> concentrations after inducing a pressure increase inside the chamber when placing it on the frames. Under standard measurement conditions, CH<sub>4</sub> concentrations increased linearly inside the chambers (Supporting information Figure S4). Hence, I used a simple linear fit to calculate CH<sub>4</sub> emission rates. Also, median CH<sub>4</sub> fluxes from the dry polygon rim (1.85 mg m<sup>-2</sup> d<sup>-1</sup>) were lower than from previous measurements (4.3-4.9 mg m<sup>-2</sup> d<sup>-1</sup>) (Kutzbach et al., 2004; Sachs et al., 2010; Wagner et al., 2003) but, as expected, all studies showed substantially lower fluxes from the dry rim than from the wet centers. Eddy covariance CH<sub>4</sub> measurements from a representative mix of wet and dry tundra, with some stretches of open water from Samoylov Island are a good baseline reference for my results. My median polygon center CH<sub>4</sub> emissions (26.4 mg m<sup>-2</sup> d<sup>-1</sup>) are still higher than the growing season median CH<sub>4</sub> emissions in Samoylov Island from 2014 (14.3 mg m<sup>-2</sup> d<sup>-1</sup>) (Beckebanze, Runkle, et al., 2022) and 2019 (16.7 mg m<sup>-2</sup> d<sup>-1</sup>) (Beckebanze, Rehder, et al., 2022), while my polygon rim median CH<sub>4</sub> emissions (1.85 mg m<sup>-2</sup> d<sup>-1</sup>) was still lower than the emissions of these representative areas of the polygonal tundra in the island.

---

CH<sub>4</sub> emissions from the water saturated polygon center of my study site are also at the lower end compared to other arctic tundra soils. Studies in the Arctic report CH<sub>4</sub> emissions in wet tundra environments ranging between 1.53 and 419 mg CH<sub>4</sub> m<sup>-2</sup> d<sup>-1</sup> (Andresen et al., 2017; Kwon et al., 2017; Skeeter et al., 2020; Ström et al., 2012; Vasiliev et al., 2019; Wagner et al., 2019). Most studies on arctic CH<sub>4</sub> emissions report data from organic soils, which are characterized by the highest CH<sub>4</sub> emissions (Andresen et al., 2017; Kwon et al., 2017; Ström et al., 2012), which are also supported by a dense cover of vascular plants like *Eriophorum* sp., *Carex* sp. or *Arctophila* sp. (Andresen et al., 2017; Ström et al., 2012). The CH<sub>4</sub> fluxes found in this study are high if only compared to mineral soil wetlands (Skeeter et al., 2020; Vasiliev et al., 2019; Wagner et al., 2019). The soils of both polygon center and rim in my study are mineral soils with a sandy texture (Eckhardt et al., 2019b), and lower CH<sub>4</sub> emissions from mineral soils than from organic soils have been reported in previous studies (Christiansen et al., 2015). Moreover, the Lena River Delta is one of the coldest permafrost regions on Earth (Vladimir E. Romanovsky et al., 2010) and methanogenesis is largely controlled by temperature (Yvon-Durocher et al., 2014). The temperature effect on methanogenesis is related to the temperature modulation of enzymatic processes, such as enzymes concentrations and activity inside the methanogens cells, thus, lower CH<sub>4</sub> production rates are found at lower temperatures (Westermann et al., 1989).

As expected, the CH<sub>4</sub> emissions at the drained polygon rim in my study were very low and less variable than at the wet polygon center sub-site, however it did not act as a CH<sub>4</sub> sink, as reported in other studies (Jørgensen et al., 2015; Kwon et al., 2017; Skeeter et al., 2020; St Pierre et al., 2019). The lack of water saturation and consequently oxic conditions demonstrated by the VWC, which varied from 28.1 to 31.8% within the study period, is probably the main reason for the lower CH<sub>4</sub> emissions detected at the rim compared to the center. In contrast to the polygon center, water saturation was never achieved at the polygon rim, reducing the habitat for methanogens to produce CH<sub>4</sub>, and leaving space for methanotrophs to oxidize CH<sub>4</sub>. The CH<sub>4</sub> emissions of the polygon center showed a gradual growth over the first part of the growing season until a peak and posterior decrease, while constant CH<sub>4</sub> emissions were measured at the polygon rim. These patterns were very similar to those reported by Wagner et al. (2003), although, differently

---

than here, the center CH<sub>4</sub> emissions reached the peak earlier in mid-July, when they started to decrease continuously. Wagner et al. (2003) related the seasonal fluctuations to the microbiological processes of CH<sub>4</sub> production and oxidation, with higher CH<sub>4</sub> production and lower CH<sub>4</sub> oxidation at the early summer and the opposite by the end of the season. The same seasonality trends of polygon center and rim CH<sub>4</sub> emissions can be found in other regions in Northeastern Siberia (Kwon et al., 2017), as well as in other arctic environments (Ström et al., 2012). Physical environmental parameters such as SurfT (Pickett-Heaps et al., 2011) and SoilT (Delwiche et al., 2021) have been pointed out as strong predictors of seasonal CH<sub>4</sub> variability. Seasonal vegetation patterns are also playing a crucial role in CH<sub>4</sub> seasonality. Evidences in the literature show a strong correlation between peak season CH<sub>4</sub> emissions and maximum gross ecosystem production (Nielsen, Michelsen, Strobel, et al., 2017) and between the development of the vegetation root system along the growing season and CH<sub>4</sub> emissions (Joabsson & Christensen, 2001). Yet, inter-annual CH<sub>4</sub> emissions variation can be significant, with largely different seasonal patterns found between years (Mastepanov et al., 2013).

Despite the absence of seasonality in the variation of CH<sub>4</sub> fluxes at the polygon rim, anomalously high CH<sub>4</sub> fluxes were measured there on the 22<sup>nd</sup> of September, the last day of measurements. The 22<sup>nd</sup> of September was also the only day of the campaign in which negative soil temperatures were recorded at 2 cm depth, indicating that the soil profile was becoming completely frozen, since negative temperatures were already being recorded at and below 5 cm. I hypothesize that CH<sub>4</sub> stored at soil and vegetation cavities was being squeezed out to the atmosphere during the soil freezing process. Previous studies showed similar results with a strong soil gas pressure increase (Tagesson et al., 2012) and CH<sub>4</sub> emissions increase (Mastepanov et al., 2008) as the soil started to freeze in fall.

### **2.5.2 Impact of plant mediated CH<sub>4</sub> transport**

The importance of plant mediated CH<sub>4</sub> transport in wetlands has been documented in previous studies and mainly depends on plant type and density (Knoblauch et al., 2015; Popp et al., 2000). Plants enhance CH<sub>4</sub> release by facilitating CH<sub>4</sub> transport from the soil into the atmosphere through air filled plant tissue (aerenchyma) and also support CH<sub>4</sub>

---



production by the release of root exudates, which fuel methanogenesis in the anoxic soil (Girkin et al., 2018). The seasonality of the difference between clipped and vegetated plots  $\text{CH}_4$  fluxes in my study is characterized by a smaller difference between treatments at the beginning of the growing season and a gradual increase of the difference until mid-September when the difference starts to decrease again. Notwithstanding, Noyce et al. (2014) showed, in a similar clipping experiment, that the largest difference between clipped and vegetated sites occurred during fall, when sedges were senescing. The authors hypothesized that higher water table in fall kept the rooting zone saturated, intensifying the root's influence on  $\text{CH}_4$  production and transport. This was not the case in my off-season measurements in September, as the water table depths were at the lowest level since the start of the measurements in July (Eckhardt et al., 2019b), therefore keeping a smaller volume of rooting zone saturated.

The plant-mediated  $\text{CH}_4$  transport in the polygon center (79%) is within the range of 66% to 98% reported for wet sub-arctic and Arctic tundra sites dominated by sedges and grasses (Knoblauch et al., 2015; Kutzbach et al., 2004; Morrissey & Livingston, 1992; Nielsen, Michelsen, Strobel, et al., 2017). The growth of aerenchymatous plants in arctic sedge-dominated sites is a key factor linking  $\text{CH}_4$  production with emissions. Nielsen, Michelsen, Strobel, et al. (2017) demonstrated this link by identifying a decoupling between peak dissolved  $\text{CH}_4$  in the soil solution and peak  $\text{CH}_4$  emissions, while identifying a connection between the peak gross ecosystem production and peak  $\text{CH}_4$  emissions. Therefore, demonstrating the key role of sedges connecting  $\text{CH}_4$  production by the soil to  $\text{CH}_4$  emissions.

However, it is important to notice that the contribution of plant mediated  $\text{CH}_4$  transport to total  $\text{CH}_4$  fluxes calculated from the clipping experiment is a conservative estimate. At the vegetated plots, the produced  $\text{CH}_4$  is released rapidly through the plants into the atmosphere, thereby by-passing the oxidative layer of the soil, while some produced  $\text{CH}_4$  is transported by soil diffusion. After clipping, the  $\text{CH}_4$  that was once transported via the vegetation is diffusing through the water saturated soil. It is likely that a part of the produced  $\text{CH}_4$  that would have been transported via plants at the unclipped plots is now oxidized in the soil, since now it has to slowly diffuse through the water phase. Thus, the fluxes measured at the clipped plots might not represent only the  $\text{CH}_4$  that is transported

---

via soil diffusion in the intact environment, but accounts also for a part of CH<sub>4</sub> that is transported through the vegetation under natural conditions. On the other hand, the removal of the vegetation also ends the support for CH<sub>4</sub> production by root exudates, causing a reduced CH<sub>4</sub> production. These two contrary processes, whose effects on CH<sub>4</sub> fluxes may not be quantified, introduce further uncertainties into my estimates.

I consider the difference between clipped and vegetated sites as a measure of the plant-mediated transport of CH<sub>4</sub> because there was no evidence of significant ebullitive transport at my sites. There was no abrupt increase in CH<sub>4</sub> concentrations during chamber closure times in any of my chamber measurements throughout the growing season (e.g., Supporting information, Figure S4), which would indicate ebullitive CH<sub>4</sub> fluxes. I presume that the dense root system of the vegetation at the polygon center prevented CH<sub>4</sub> to move through the water as bubbles. Although I cannot exclude the possibility of a small contribution of ebullitive CH<sub>4</sub> fluxes into the total CH<sub>4</sub> transported to the atmosphere, I consider that the linearity of CH<sub>4</sub> concentrations during chamber deployment in all my CH<sub>4</sub> chamber measurements demonstrate that the transport of CH<sub>4</sub> was overall comprised by plant-mediated and diffusive transport. Additionally, Knoblauch et al. (2015) have found negligible ebullitive fluxes in most of the studied polygon ponds on Samoylov Island, with similar soils as the one in this study.

At the polygon rim, I estimated a negligible plant-mediated transport of 3% in accordance to Wagner et al. (2003), while Kutzbach et al. (2004) detected 27%. However, the latter study also reported higher CH<sub>4</sub> fluxes at the rim and used a different approach to quantify plant-mediated transport that could be one of the causes for the distinct results: Kutzbach et al 2004 used closed chambers that enclosed single *Carex aquatilis* culms, excluding CH<sub>4</sub> being transported by the soil. Ebullitive CH<sub>4</sub> fluxes were not observed at the polygon rim due to non-water-saturated conditions. The soil at the polygon rim in my study contained a deep oxic, unsaturated layer and released less CH<sub>4</sub> regardless of the removal of the vegetation. Presumably both low CH<sub>4</sub> production and high CH<sub>4</sub> oxidation (Liebner & Wagner, 2007) affected the CH<sub>4</sub> release at the polygon rim simultaneously (Vaughn et al., 2016). Moreover, the polygon rim was mostly vegetated by mosses and small vascular plants (*Dryas punctata* and *Astragalus frigidus*) that do not possess aerenchyma like sedges. Hence, well-drained soil conditions, resulting in low CH<sub>4</sub> production and the absence of

---

aerenchymatous plants are the likely reasons for only a small difference between CH<sub>4</sub> fluxes at the clipped and vegetated plots. Additionally, although it could be shown that the plant-mediated transport at the rim was irrelevant ( $\approx 3\%$ ), sedges (*C. aquatilis*) were present within the moss-dominated environment. The roots of *C. aquatilis*, might be connected with the plants from the methane-producing polygon center due to its deep root system (Albano et al., 2021). Hence, I cannot rule out that the CH<sub>4</sub> produced at the polygon center was escaping through the polygon rim via vascular plants.

### 2.5.3 *in situ* CO<sub>2</sub>:CH<sub>4</sub> ratios and their environmental controls

The rapid decrease of CO<sub>2</sub>:CH<sub>4</sub> ratios at the polygon center from 94.6 to 12.5 between 11<sup>th</sup> of July and 1<sup>st</sup> of August shows the increasing relevance of the CH<sub>4</sub> production and decreased impact of R<sub>h</sub> during the progression of the growing season. CH<sub>4</sub> fluxes increased from 5.8 to 21.5 mg m<sup>-2</sup> d<sup>-1</sup> in this period, following the deepening of the active layer. The negative relationship of the ALD with the CO<sub>2</sub>:CH<sub>4</sub> ratios has also been demonstrated in previous studies (McCalley et al., 2014; van Huissteden et al., 2005). The reason for this relationship is an increase in the soil volume that becomes water saturated and hence anoxic (Lagomarsino & Agnelli, 2020; Rößger et al., 2022) but also the growth of vegetation, a consequence of increased substrate and nutrient availability with active layer thawing (Andresen et al., 2017).

In addition to ALD, soil temperature had a strong effect on CH<sub>4</sub> emissions and CO<sub>2</sub>:CH<sub>4</sub> ratios. CH<sub>4</sub> production is, as any other microbial process, temperature dependent (Chen et al., 2022; Kelly & Chynoweth, 1981; Schädel et al., 2016; Treat et al., 2015; Zeikus & Winfrey, 1976; Zinder et al., 1984). Kolton et al. (2019) detected a negative relationship between temperature and CO<sub>2</sub>:CH<sub>4</sub> ratios, indicating a stronger increase of CH<sub>4</sub> production with rising temperatures than of CO<sub>2</sub> production. The production of CH<sub>4</sub> was directly correlated to rising soil temperatures at the depth of 40 cm, but also indirectly by promoting the deepening of the active layer. Similar results were reported by Rößger et al. (2022) in Samoylov Island, showing that polygon center soil temperature at 30 cm, thaw depth and growing degree days were the variables with highest CH<sub>4</sub> emissions predictive power. In contrast R<sub>h</sub> at the center had only a weak relationship with the soil temperature at 40 cm depth. However, Eckhardt et al. (2019b) identified air temperature

---

followed by the surface temperature as the best predictors for  $R_h$  (lin) at the polygon center. These observations indicate that  $CH_4$  emissions are affected by processes and changes happening at deeper soil layers (Wagner et al., 2003), while  $R_h$  is affected by processes in the top-soil (Ferréa et al., 2012). The deepest soil layer of my site is less affected by water table variations and maintains its anoxic conditions for longer periods, enabling the establishment and activity of a methanogenic community (Knoblauch et al., 2015; Liebner et al., 2015), while the soil surface contains highest  $O_2$  concentrations, staying frequently above the water table. An incubation experiment using samples from Samoylov Island presented evidences for the markedly higher methanogenesis potential of the bottom active layer compared to the surface (Walz et al., 2017). Therefore, the warming of the soil surface stimulates  $R_h$ , causing elevated  $CO_2:CH_4$  ratios, while the warming of deeper anoxic soil layers, stimulates methanogenesis and decreases the  $CO_2:CH_4$  ratios. It might be expected that the surface and deep soil temperatures should be highly related, but just a weak relationship between SurfT and SoilT40 at the polygon center was detected in this study. The soil at the depth of 40 cm is in constant interaction with the underlying permafrost and remained frozen during about one third of the measurement period. The thermal regime at this depth is less controlled by solar radiation and more by the underlying permafrost temperatures than at the soil surface, thus they are different and exert different influences on methanogenesis and  $R_h$ . The  $CO_2:CH_4$  ratios at the polygon rim could be governed mainly by the  $R_h$  variability since the  $CH_4$  production is low throughout the measurement period. This is also demonstrated by the relationship between  $CO_2:CH_4$  ratios at the rim and the SurfT, which was also the case for  $R_h$ .

The theoretical  $CO_2:CH_4$  production ratio during organic matter decomposition via methanogenesis is about one, when the oxidation number of the organic matter is zero (Symons & Buswell, 1933). However, under natural conditions,  $CO_2:CH_4$  ratios above one are generally reported even under anoxic conditions, since alternative electron acceptors such as nitrate, ferric iron, sulfate or even organic matter may be used for SOM decomposition (Dettling et al., 2006). Anoxic incubations show a decrease in the  $CO_2:CH_4$  ratios over the course of experiment, reaching values of about one, most likely because alternative electron acceptors get depleted and methanogenic communities become active

---

(Knoblauch et al., 2018; Philben et al., 2020). The increase of CH<sub>4</sub> production with decreasing availability of alternative electron acceptor has been observed at other arctic sites (Rissanen et al., 2017) and could have also played a role in the change of CO<sub>2</sub>:CH<sub>4</sub> ratios in the current study. A shallow ALD at the beginning of the growing season still enables oxic conditions at the soil surface and a reoxidation of alternative electron acceptors. Later on, as the active layer keeps deepening, the bottom soil can finally stay anoxic, and after the depletion of the alternative electron acceptors methanogenesis may increase. However, a ratio between CO<sub>2</sub> and CH<sub>4</sub> production above one is expected even under optimum conditions for methanogenesis in the anoxic soil at the polygon center, since CO<sub>2</sub> from heterotrophic respiration was predominantly formed in the oxic surface soil (see discussion above), where no CH<sub>4</sub> is produced.

#### **2.5.4 *in situ* CO<sub>2</sub>:CH<sub>4</sub> production ratios uncertainty range**

While several methods are established to quantify microbial CO<sub>2</sub> production from SOM decomposition ( $R_h$ ), the quantification of *in situ* CH<sub>4</sub> production is still challenging. The current study uses CO<sub>2</sub> fluxes from clipped plots to determine  $R_h$  fluxes (Eckhardt et al., 2019b). To estimate *in situ* CH<sub>4</sub> production, the CH<sub>4</sub> fluxes above intact vegetation have been used before (Cooper et al., 2017). These CH<sub>4</sub> fluxes are the sum of CH<sub>4</sub> transported by aerenchymatous plants and by molecular diffusion through the soil and ebullition. This approach is likely underestimating *in situ* CH<sub>4</sub> production since a part of the produced CH<sub>4</sub> is oxidized in the soil before being emitted.

By using the fraction of oxidized CH<sub>4</sub> values and the fraction of CH<sub>4</sub> diffusing through the soil from Knoblauch et al. (2015) and Preuss et al. (2013) We estimated that a fraction between 0.10 and 0.31 of produced CH<sub>4</sub> might have been oxidized in the soil before emitted into the atmosphere. Knoblauch et al. (2015) and Preuss et al. (2013) determined the fraction of oxidized CH<sub>4</sub> by comparing the ratio between <sup>12</sup>CH<sub>4</sub> and <sup>13</sup>CH<sub>4</sub> from rhizospheric and emitted CH<sub>4</sub>. This method is based on the fact that isotopic fractionation occurs when CH<sub>4</sub> is oxidized during transport. Methanotrophs oxidize preferentially the lighter <sup>12</sup>CH<sub>4</sub>, leaving the heavier <sup>13</sup>CH<sub>4</sub> behind. My estimated values of 0.10 and 0.31 oxidized CH<sub>4</sub> are within in the range (0.01 - 0.40) reported by previous studies carried out in similar environments, including sites dominated by sedges of *Carex sp.* (Nielsen,

---

Michelsen, Ambus, et al., 2017; Popp et al., 1999; Ström et al., 2005). This broad range is both due to differences in the methodology to determine CH<sub>4</sub> oxidation in the soil but also due to differences in soil conditions and vegetation composition.

CH<sub>4</sub> oxidation is closely related to the efficiency of oxygen transport by the plants roots, which is a species-specific characteristic (Nielsen, Michelsen, Ambus, et al., 2017), and seemingly a more important factor determining CH<sub>4</sub> oxidation than plant biomass (Ström et al., 2005). The contribution of CH<sub>4</sub> oxidation varies throughout ecosystems and vegetation composition. A study in a wetland in South Sweden identified that 20-40% of produced CH<sub>4</sub> was oxidized in a *Carex rostrata* dominated peat monolith, and of more than 90% in monoliths with *Eriophorum vaginatum* (Ström et al., 2005), while in a southern Estonian bog, no significant CH<sub>4</sub> oxidation was found in an *Eriophorum spp.* dominated site (Frenzel & Rudolph, 1998). Thus, rhizospheric CH<sub>4</sub> oxidation regulated by the efficiency of oxygen transport by the plants roots is apparently a site-specific characteristic in addition to being species-specific. Sedge species have been related to higher CH<sub>4</sub> emissions than other plant species, not because they support CH<sub>4</sub> production but since they facilitate CH<sub>4</sub> transport through their aerenchyma, bypassing the oxidative soil layer and avoiding oxidation (Green & Baird, 2012). Nielsen, Michelsen, Ambus, et al. (2017) showed in a wet tundra ecosystem in Greenland, that the radial oxygen loss of *Carex aquatilis* has a minor impact on CH<sub>4</sub> oxidation. In their study, the fraction of CH<sub>4</sub> oxidized was less than 2%, most likely because CH<sub>4</sub> diffusion is faster than it would be required for CH<sub>4</sub> oxidation and because CH<sub>4</sub> diffuses into plant roots at a lower depth than where oxidation takes place. Isotopic signatures of CH<sub>4</sub> from a bog in Stordalen Mire, Sweden, show higher fraction of oxidized CH<sub>4</sub> occurring in periodically inundated shallower soil layers instead of permanently inundated deeper soil layers (Singleton et al., 2018). This is an evidence of the latter hypothesis conceived by Nielsen, Michelsen, Ambus, et al. (2017) about the depth separation between the region where CH<sub>4</sub> diffuses into plant roots and the region where CH<sub>4</sub> oxidation takes place.

Data from Samoylov Island, from a study on a similar polygon center reports no significant differences between the  $\delta^{13}\text{C}$  signatures of dissolved CH<sub>4</sub> in the anoxic soil and of the emitted CH<sub>4</sub> from plots vegetated by *Carex aquatilis*, and hence give no evidence for rhizospheric CH<sub>4</sub> oxidation (Knoblauch et al., 2015). Since the vascular plants in my

---

studied polygon were dominated by *C. aquatilis*, which was shown to only weakly support CH<sub>4</sub> oxidation in the rhizosphere I consider that the calculated range of rhizospheric CH<sub>4</sub> oxidation (0.10–0.31) is rather at the higher end of CH<sub>4</sub> oxidation under *in situ* conditions, and that the measured CH<sub>4</sub> fluxes in the polygon center are not severely affected by CH<sub>4</sub> oxidation. Due to the lack of estimates of the fraction of CH<sub>4</sub> oxidized at the polygon rim and high uncertainties related to the emissions measured in this sub-site, I could not calculate such range of rhizospheric CH<sub>4</sub> oxidation as I did for the polygon center. Thus, I cannot consider the CO<sub>2</sub>:CH<sub>4</sub> ratios as production ratios in the polygon rim.

### 2.5.5 Seasonal CO<sub>2</sub> and CH<sub>4</sub> release

As expected, the wet tundra, which is water saturated, showed lower R<sub>h</sub> fluxes, while higher R<sub>h</sub> fluxes were found in the dry tundra, and the opposite was the case for CH<sub>4</sub>. The dry tundra dominates total carbon emissions, both due to high CO<sub>2</sub> emissions and due to the larger area. While both tundra types lost carbon preferentially in the form of CO<sub>2</sub>, CH<sub>4</sub>-C represented 0.27% of the dry tundra total carbon loss and 6.91% of the wet tundra total carbon loss. The contribution of CH<sub>4</sub> emissions to the seasonal CO<sub>2</sub> and CH<sub>4</sub> release on Samoylov might change in the future. The ALD at Samoylov Island is predicted to increase (Beermann et al., 2017), as well as at several arctic sites, related to increasing temperatures affecting the extension of the thawing period (Andresen et al., 2017; Euskirchen et al., 2006; Strand et al., 2021). This trend can be detected through the assessment of ALD records at Arctic sites in the past and today (Andresen et al., 2017; Strand et al., 2021). As shown in this study, the importance of CH<sub>4</sub> emissions increase with increasing ALD depth. My results are consistent with the study of Rößger et al. (2022) who also found a significant relationship between ALD and CH<sub>4</sub> emissions and evidence for an increasing trend of early summer CH<sub>4</sub> emissions from wet tundra linked to atmospheric warming. Moreover, to predict the future response of CH<sub>4</sub> fluxes from thawing permafrost landscapes it will be crucial to understand if the ALD increase will result in wetter soils (Krogh & Pomeroy, 2019), thereby increasing CH<sub>4</sub> fluxes (Tagesson et al., 2012) or drier soils (Jin et al., 2021; Natali et al., 2015) resulting in lower CH<sub>4</sub> fluxes (Kim, 2015).

---

## 2.6 Conclusions

CH<sub>4</sub> emissions presented here are at the lower end compared to other arctic sites, and the differences found between these emissions and the ones from other measurements in Samoylov Island shows the high temporal and spatial variability found in GHG emissions in the Siberian tundra. Understanding the mechanisms that control the CO<sub>2</sub>:CH<sub>4</sub> production ratios is especially important for improving Earth System Models. To estimate the CO<sub>2</sub>:CH<sub>4</sub> production ratios under *in situ* conditions I used the R<sub>h</sub> fluxes from clipped plots and the CH<sub>4</sub> fluxes from vegetated plots, which were corrected for potential CH<sub>4</sub> oxidation in the soil. The CO<sub>2</sub>:CH<sub>4</sub> production ratio is associated with active-layer depth (ALD) due to a direct effect of ALD on CH<sub>4</sub> production. The effect of air temperature seasonality on the CO<sub>2</sub>:CH<sub>4</sub> ratio is complicated. Top-soil warming stimulates CO<sub>2</sub> production under more oxic conditions, hence increases the CO<sub>2</sub>:CH<sub>4</sub> ratio. In contrast, warming of anoxic subsoil layers leads to enhanced CH<sub>4</sub> production, hence a lowering of the CO<sub>2</sub>:CH<sub>4</sub> ratio.

Arctic warming will lead to a warming of the active layer and its deepening. My study indicates that for wet tundra this warming and deepening can result in pronounced enhancement of CH<sub>4</sub> production. Changing vegetation pattern and functions, however, will further complicate the net response of Arctic CH<sub>4</sub> emission to global warming. Further studies are needed focusing on the complexities of *in situ* CH<sub>4</sub> and CO<sub>2</sub> production, especially in regions where there is yet scarcity of data, like the vast Siberian tundra. There is still a high uncertainty on the response of CH<sub>4</sub> production and emission to thawing permafrost and the related feedback mechanism.

## 2.7 Supplementary material

The supporting information is presented in order to give to the reader a better overview of the experiment set-up and its characteristics described in the Methods section and the variation of the CO<sub>2</sub>:CH<sub>4</sub> ratios from the polygon rim. Additionally, the heterotrophic respiration dataset is republished here from (Eckhardt et al., 2019b) because the data are used and interpreted differently in the present study.

---



Polygonal center											
Location: Samoylov Island, Lena River Delta Geographic coordinates: 72°22.442 N, 126°29.828 E Field location: center of low-center polygon					Date of profile acquisition: 10.07.2014 Thaw depth during sampling: 31 cm Water level during sampling: -2 cm Vegetation: sedge-moss tundra						
Remarks: organic-layer very weakly decomposed, no evidence of cryoturbation											
Classification: World Reference Base for Soil Resources IUSS (WRB, 2014): Reductaquic Cryosol (Hyperhumic) – abbreviation: CR-ra-jh Russian classification (Elovskaya, 1987): Permafrost tundra humic-peatish											
Horizon	Depth	TC	TIC	TOC	TOC	N	C/N	pH	Water content	Dry bulk density	Further characteristics
	cm	%	%	%	kg m <sup>-2</sup>	%			wt%	g cm <sup>-3</sup>	
Oi	0 to 6	19.8	0.2	19.6	4.2	0.60	33.1	5.18	85.4	0.36	Slightly decomposed plant material, <i>Carex</i> rhizomes
Ah1	6 to 15	13.2	0.2	13.0	6.2	0.51	25.7	5.34	75.4	0.53	Slightly humified plant material, <i>Carex</i> rhizomes, alpha-alpha-Dipyridyl positive
Ah2	15 to 23	11.7	0.2	11.5	5.8	0.57	20.6	5.22	77.1	0.62	Slightly humified organic matter, alpha-alpha-Dipyridyl positive
Ah3	23 to 31	10.1	0.2	9.9	5.1	0.60	16.9	5.56	81.2	0.64	Intermediate humified organic matter, alpha-alpha-Dipyridyl positive
Ahf	31+										frozen

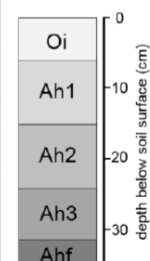


**Figure 4** - Soil characteristics and soil classification of the soil from the polygonal center.

This figure is depicted in Eckhardt (2017).

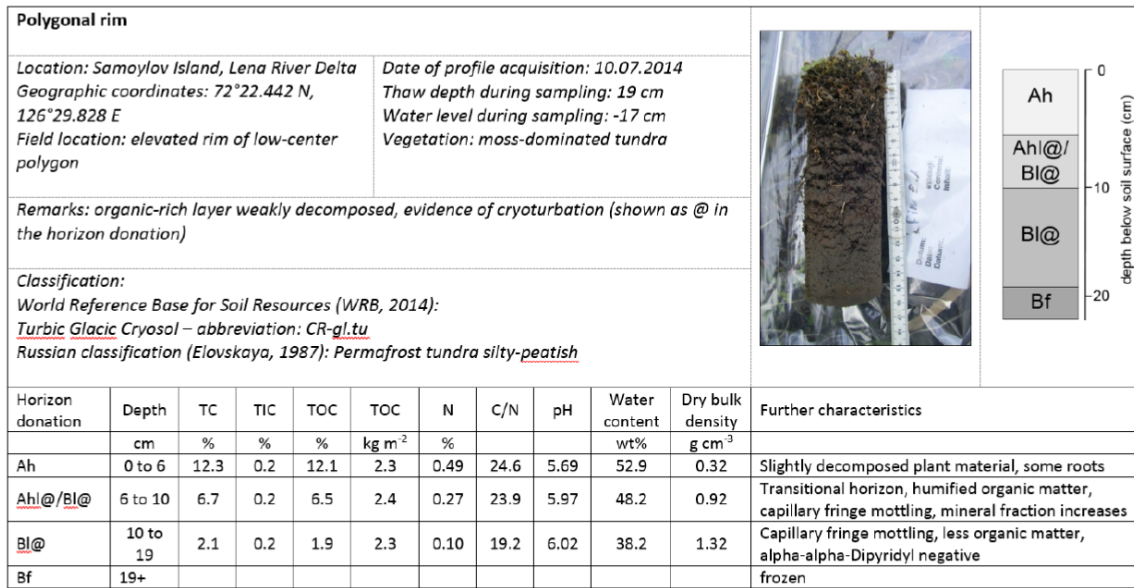


**Figure 5** - Soil characteristics and soil classification of the soil from the polygonal rim. This figure is depicted in Eckhardt (2017).

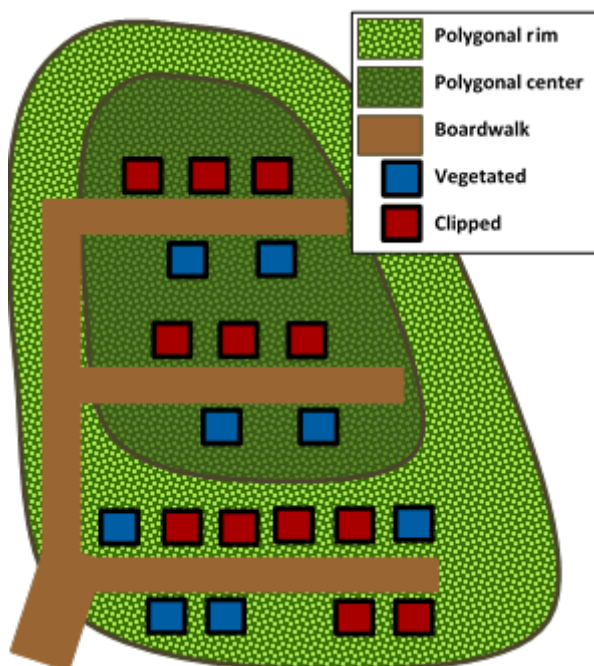


**Figure 6** - Scheme of the study site and the installed measurement plots. From the total 20 PVC collars, 10 were installed at the center and 10 at the rim. From these 10 of each polygon sub-site 6 were clipped and 4 remained with the original vegetation. This figure is depicted in Eckhardt (2017).

---

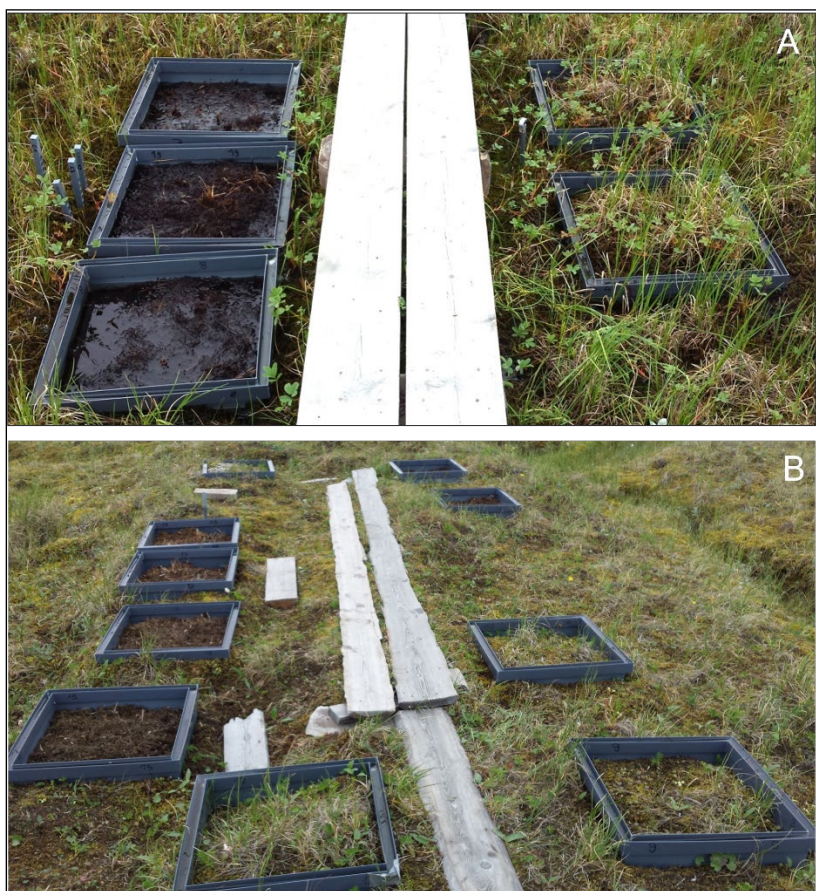


**Figure 7** - Picture of the boardwalks and measurement plots at the polygon center (A) and at the polygon rim (B). Clipped plots at the left of the boardwalks and vegetated plots at the right. This figure is adapted from Eckhardt (2017).

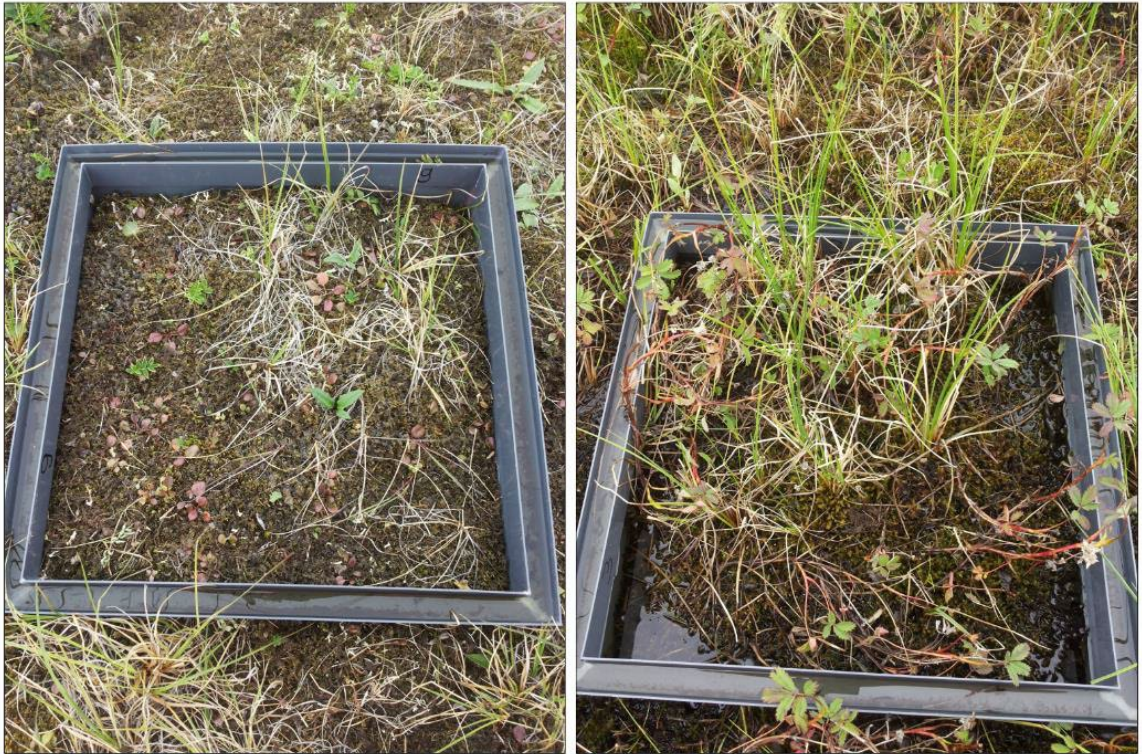


**Figure 8** – Left picture shows a vegetated plot at the polygon rim and right picture shows a vegetated plot at the polygon center. It is clear the difference between a moss-dominated environment with sparse vascular plants and a sedge-moss-dominated environment at the polygon center. This figure is depicted in Eckhardt (2017).

---

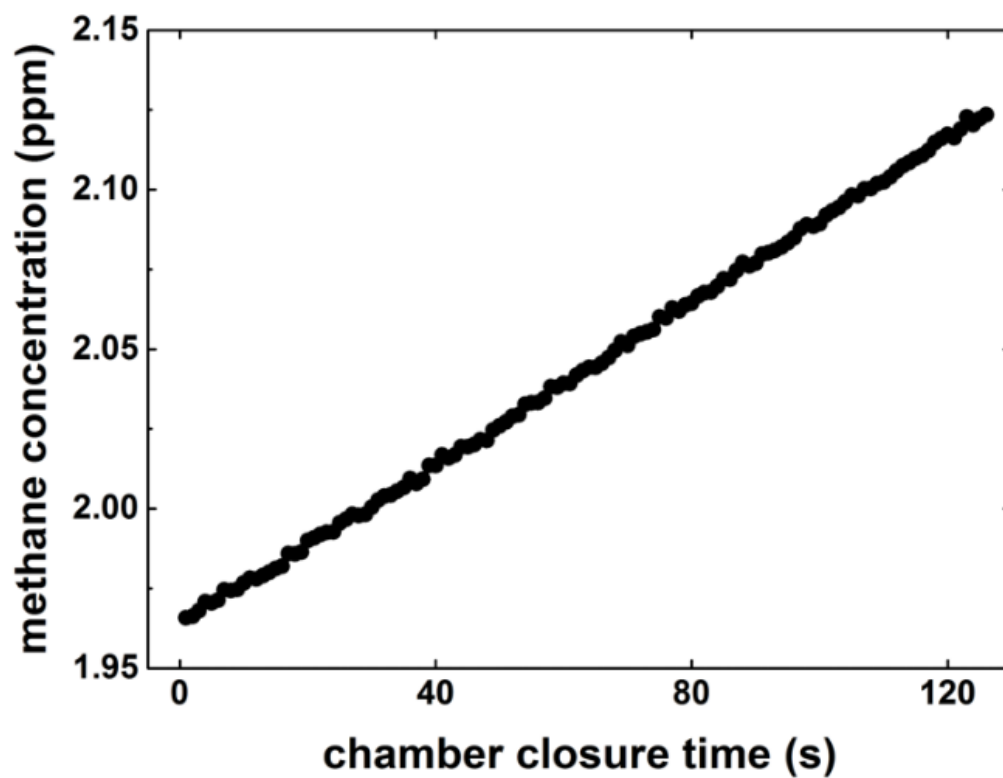


**Figure 9** - An example of the linear increase of CH<sub>4</sub> concentrations in the chamber during a single CH<sub>4</sub> flux measurement in this study. This figure is adapted from Eckhardt (2017).

---

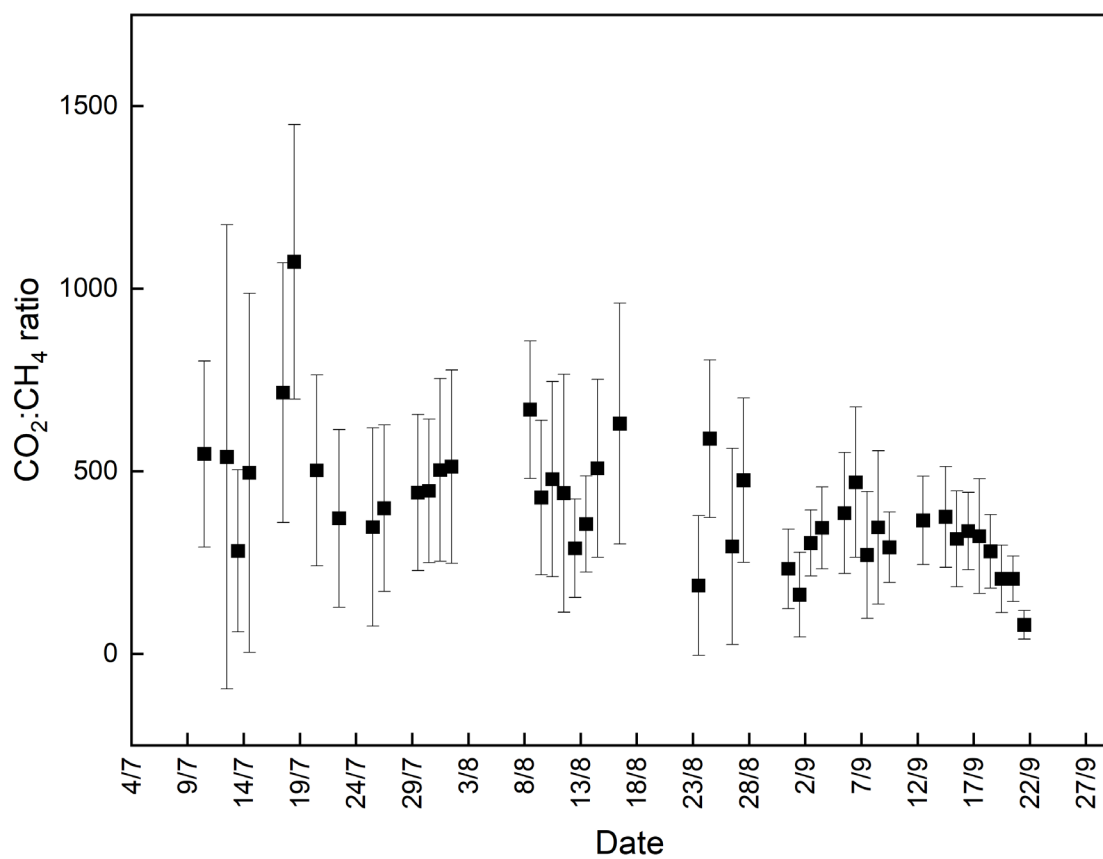


**Figure 10** - Ratio of daily CO<sub>2</sub> fluxes from heterotrophic respiration and CH<sub>4</sub> emissions at the polygon rim. Error bars give the estimated standard deviation.

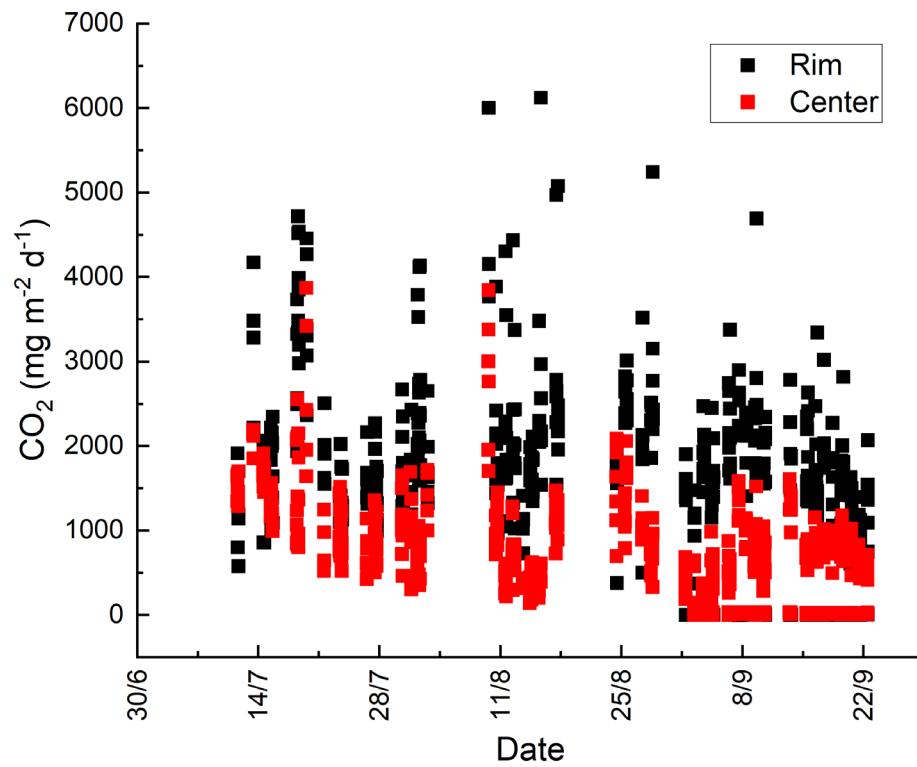


**Figure 11** - Heterotrophic respiration measurements from the two sub-sites (polygon center and rim). Heterotrophic respiration was measured in the clipped plots, using a dark chamber. This dataset is republished from Eckhardt et al. (2019a).



### **3 Higher temperatures do not increase P and K availabilities in incubation of soils from Kurungnakh Island, Lena River Delta, Siberia**

This chapter covers data from an incubation experiment designed and conducted by me in 2022 using samples from Kurungnakh Island, which were collected in 2018 and provided to me. I have analyzed the data and written the manuscript. This study is planned to be soon submitted for publication in a scientific journal.

#### **3.1 Abstract**

Global warming induces permafrost thaw and exposes organic matter, accelerating decomposition and greenhouse gas (GHG) emissions. Yet, the additional warming and increase of CO<sub>2</sub> concentrations in the atmosphere can enhance the primary productivity of the arctic vegetation. Phosphorus (P) is a scarce nutrient in the Arctic and high uncertainties remain in regard of the fate of P availability with global warming. Additionally, enhanced P availability in soils has a noted positive influence on K uptake and plant K concentrations, underscoring the interconnectedness of these nutrients. I incubated aerobically active layer samples from the Lena River Delta, Siberia, under 4 and 15 °C. This incubation aimed to assess whether the temperature increase has an impact on the P and K concentration levels and processes, such as mineralization and immobilization. Additionally, I analyzed how temperature affects aerobic GHG production, namely CO<sub>2</sub> and nitrous oxide (N<sub>2</sub>O) production or consumption throughout the experiment. I observed a general decrease in P and K concentrations with significant P and K immobilization rates, but no significant difference of the temperature treatments between them. Phosphorus turnover rates negatively correlated with soil carbon (C) and CO<sub>2</sub> production rates, implying a relationship between P dynamics and C turnover. All samples showed significant CO<sub>2</sub> production, with a trend of decreasing rates as the experiment progressed. Samples at 15°C produced substantially more CO<sub>2</sub> compared to

---

those at 4°C across all experiment stages. Nitrous oxide rates varied along the experiment, showing production or consumption depending on the sample, and no temperature effect. Contrary to expectations, warming did not enhance P and K availabilities, but P and K were immobilized during the experiment regardless of the temperature treatment. Overall, my findings imply that nutrient limitations may continue to hinder the productivity of Arctic ecosystems in a warming climate.

## 3.2 Introduction

The thawing of permafrost, induced by global warming, leads to exposure of organic matter for decomposition. The increase in the decomposition rates of soil organic matter induces greater CO<sub>2</sub> and other greenhouse gas emissions (GHG) (AminiTabrizi et al., 2020). Yet, the additional warming and increase of CO<sub>2</sub> concentrations in the atmosphere enhance the primary productivity of the arctic vegetation. Some authors argue that the higher primary productivity expected would be constrained by the low content of nutrients in arctic soils (Wieder et al., 2015), and indeed these constraints were identified experimentally in other environments with forest productivity not responding to elevated CO<sub>2</sub> due to phosphorus (P) limitation (Ellsworth et al., 2017). In this view, arctic terrestrial ecosystems would be most likely a source than a sink of carbon with global warming. However, nutrient mineralization is also a temperature sensitive process, due to the positive effect of temperature on the activity of the enzymes responsible for the extraction of nutrients from the organic matter (Souza & Billings, 2022), and it is possible that enough additional nutrients are mineralized with warming to sustain increased primary productivity (Brovkin & Goll, 2015). Whilst the effect of rising temperatures on nutrient availability in arctic soils is still poorly understood (Maslov & Maslova, 2021), especially for P (Shaw & Cleveland, 2020), it is however expected that this change in the abundance of specific elements could affect biogeochemical activities like organic matter mineralization (Stimmler et al., 2023). Phosphorus is a scarce nutrient in the Arctic, and evidence has shown that P might have stronger effects on plant growth than nitrogen (N) in permafrost ecosystems (Yang et al., 2021). A field experiment has demonstrated that higher P and N availability caused by Arctic warming is essential for increased moss productivity and increased C sequestration, while N enrichment alone may result in C

---

loss through stimulated decomposition of the soil organic matter (Street et al., 2018). High uncertainties remain in regard of the fate of P availability with global warming (Wieder et al., 2015b). The decomposition of organic matter is usually the major source of available P in Arctic soils (Chapin et al., 1978; Giblin et al., 1991; Weintraub, 2011). Thus, some authors argue that an increase in soil organic matter decomposition rates would increase nutrient mineralization rates, including P, and most likely not turn terrestrial ecosystems into a C source (Brovkin & Goll, 2015; Melillo et al., 2011). The influence of temperature on P mineralization has been shown in incubations, with both phosphatase and P availability in soil increasing with temperature (Shaw & Cleveland, 2020), but observations are still limited, with none for Siberia. Furthermore, results are often conflicting, with P concentrations both increasing or decreasing with temperature depending on the varying effects on mineralization and immobilization. Nadelhoffer et al. (1991) found decreasing P mineralization with warming in some soils and the opposite in others. P mineralization rates were overall low, likely due to high microbial demands, which can limit P availability in arctic soils. Schmidt et al. (1999) found no strong correlation between net P mineralization and temperature, because warming induced at the same time increased P mineralization and P immobilization by soil microorganisms. Thus, further research on the response of P availability to warming is required to elucidate future climate-carbon feedback (Liu et al., 2017; Shaw & Cleveland, 2020; Wieder et al., 2015). Additionally, enhanced P availability in soils has a noted positive influence on K uptake and plant K concentrations, such relationship was pointed out as being caused by the P stimulation of growth on plants (Sárdi et al., 2012). While K seems to be limiting in a variety of terrestrial ecosystems globally (Chen et al., 2023), it is possibly not a limiting factor for plant growth in the tundra (Beermann et al., 2015), and little is known about its behavior in the soil with higher temperatures. Climate, topographical conditions, and soil texture and mineralogy are determining factors controlling K content in soils (Ghiri et al., 2011; Li et al., 2021), highlighting the importance of exploring K content and dynamics in different regions, particularly in polar regions where such studies are rare. I incubated aerobically active layer samples from the Lena River Delta, Siberia, at different temperatures to assess the impact of temperature increase on P and K concentrations. Furthermore, I evaluated processes such as mineralization, where nutrients in organic compounds are made available in inorganic form through decomposition, and

---

immobilization, where nutrients in inorganic form are absorbed by organisms and incorporated into organic compounds. I also assessed how these abovementioned processes affect aerobic GHG production, namely CO<sub>2</sub> and N<sub>2</sub>O production or consumption throughout the experiment.

### 3.3 Methods

#### 3.3.1 Study site

Three sites in a transect in Kurungnakh Island (N 72.3°; E 126.2°), Lena River Delta, Siberia were selected. The transect ranged from the bottom of a thermo-erosional depression (alas) to the surface tundra plain unaffected by thermo-erosion, and for this study, only the dry sites lacking water saturation were selected. Each site was divided in two sub-sites from which soil from three different soil horizons were collected in 2019 and kept frozen until the start of this experiment in February of 2022. The first selected site was a polygon rim with an active layer of 20 cm and no standing water, and with vegetation dominated by *Carex concolor*, *Salix pulchra* and *Hylocomium splendens*. The second site was the bottom of the slope with the water table standing at the bottom of its 20 cm active layer, and with vegetation dominated by *Carex concolor*, *Arctous alpine* and *Tomentypnum nitens*. The third site was a typical surface tundra plain with a drained active layer of 35 cm and no standing water, its vegetation was dominated by *Tofieldia coccinea*, *Dryas punctate* and *Hylocomium splendens*. The identification of plant species was done by Nikolay Lashchinskiy (Central Siberian Botanical Garden, SB RAS, Novosibirsk, Russia).

#### 3.3.2 Sampling

The soil horizons sampled in each sub-site comprised: the organic-rich horizon, represented by horizon O or Ha, depending on the site. Those samples were clearly distinct from deeper samples with visible decomposed organic matter in varied stages in the case of the O horizon and containing well-humified material, with some visible roots, but overall advanced stage of humification in the case of the H horizon; the top mineral soil, represented by the A horizon in all three sites; and the bottom mineral soil, represented by the A or AB horizon, depending on the site. After thawed for one day,

---

samples from the two sub-sites were mixed to compound a composite sample representative of each site-horizon combination, resulting in nine composite samples (three sites x three horizons).

### 3.3.3 Incubation experiment

Each of the nine composite samples were further divided into 18 sub-samples of 10 g each. They were incubated under oxic conditions and in two different temperature treatments, one at 4 °C and the other at 15 °C. If the concentration of CO<sub>2</sub> inside the headspace of the vials reached 3%, the headspace was exchanged with air and there was set a new point zero for the GHG airspace concentrations measurements. The mineral sub-samples were incubated in 100 ml vials, while organic-rich sub-samples were incubated in 250 or 500 ml, because due to their higher respiration rates the limit level of CO<sub>2</sub> (3%) would be achieved too frequently. In summary, from the 162 sub-samples (9 composite samples x 18 sub-samples each), 81 were incubated in each incubator under the respective temperature treatment (either 4 or 15 °C). After 15, 30 and 120 days from the start of the experiment, three replicates from each temperature were sacrificed for P and K analyses, while nitrate and ammonium were analyzed only at 15 days. The incubation period of 120 days was chosen to represent the timespan of the growing season at the study site. Once their final incubation day was reached, samples were left two weeks in the freezer before being chemically analyzed. The ones sacrificed at around 15 days were called batch 1, the ones at around 30 days batch 2 and the ones at around 120 days batch 3. The GHG production was measured only in those samples that were incubated until the end of the incubation experiment and not in those sacrificed in between. At each GHG measurement air from the headspace was collected and analyzed with a gas chromatograph (7890 A, Agilent Technologies, Santa Clara, CA, USA). The CO<sub>2</sub> and N<sub>2</sub>O concentrations were measured twice per week until day 15 of the experiment, once per week until day 30 and biweekly until day 120, along with pressure inside the vials. The amount of CO<sub>2</sub> and N<sub>2</sub>O within the vials were determined by assessing CO<sub>2</sub> the gas concentrations in the headspace, the volume of the headspace, water content, the solubility of gases in water and HCO<sub>3</sub><sup>-</sup> and CO<sub>3</sub><sup>2-</sup> in the case of CO<sub>2</sub>, alongside the temperature and pressure, through the application of Henry's law according to the methods used in Knoblauch et al. (2018).

---

The rates at which these gases were produced were calculated by a linear regression analysis of five measurements of changing CO<sub>2</sub> and N<sub>2</sub>O quantities in the vials over time. Non-significant slopes, identified through a p-value greater than 0.05 from linear regression analysis, indicating absence of statistically significant relationship between time and gas concentration, were discarded. Three different rates were calculated per sub-sample, being representative of each experimental stage, initial, middle, and final. Initial rates were calculated based on the first five concentrations measurements of the gases from 0 to 30 days of incubation, the middle rates were calculated based on the median concentration measurement together with the two preceding and two subsequent measurements from 30 to 60 days of incubation, and the final rates were calculated based on the five last concentration measurements from 60 to 120 days of incubation. These calculations were then standardized to mg of CO<sub>2</sub>-C per g of C in the soil (mg CO<sub>2</sub>-C g C<sup>-1</sup> d<sup>-1</sup>) and µg of N<sub>2</sub>O-N per g of N in the soil (µg N<sub>2</sub>O-N g N<sup>-1</sup> d<sup>-1</sup>), per day.

### **3.3.4 Chemical characterization**

The nine composite samples representing the combination between sites and soil horizons were chemically characterized before the start of the incubation experiment. Three aliquots of 10 g and one of 5 g were retrieved from each composite sample. The 10 g aliquots were used for the determination of the total C, N, ammonium, nitrite, nitrate, P and K contents, and the 5 g aliquot was used for the determination of pH and water content. Each aliquot of 10 g of the composite samples was dried and milled and analyzed for total C and N contents by an elemental analyzer (Vario MAX, Elementar Analysis Systems GmbH). Ammonium was analyzed photometrically at 655 nm in the 10 g aliquot (Kandeler & Gerber, 1988) (DR 5000, Hach Lange GmbH, Düsseldorf, Germany) and nitrite and nitrate by high-performance liquid chromatography (HPLC) (1200 Series, Agilent Technologies, Santa Clara, CA, USA). No amount of nitrite was found in any of the samples. Due to unforeseen technical problems, the initial ammonium, nitrite, and nitrate contents and the final contents of these nutrients of some samples are not available. Moreover, in the 10 g aliquot, P was determined photometrically and K with an atomic absorption spectrometer (AAS). The soil was combined with distilled water, and the pH was determined using an integrated pH meter with a built-in combination glass electrode.

---

The gravimetric water content was determined by drying a soil aliquot of 2.5 g at 105°C for 24 hours and weighing the remaining dry soil content.

### **3.3.5 Nutrient turnover rate calculation**

The nutrient turnover rates were calculated based of the concentration values measured before the start of the experiment, and in the batch 1, 2 and 3 sub-samples, which were sacrificed for chemical analyses. A linear regression model was fitted to the nutrient data as a function of time. The turnover rate of the nutrient was computed as the slope of the regression line. Only significant slopes ( $p < 0.05$ ) were considered nutrient turnover rates. When the slope of the regression is positive, these turnover rates are called mineralization rates, when the slope is negative, these turnover rates are called immobilization rates.

### **3.3.6 Statistics**

The statistical analyses performed aimed to explore the relationships among multiple variables, both categorical and continuous. The categorical variables were site and temperature treatment, either 4 or 15 °C. Continuous variables were C, N, P, K concentrations and water content, pH, P turnover rates, K turnover rates, and initial, middle, and final CO<sub>2</sub> and N<sub>2</sub>O production or consumption rates. Ammonium and nitrate content from batch 1 (15 days, due to loss of data from initial content) were correlated with P and K turnover rates, and initial GHG rates.

Shapiro-Wilk Test was used to assess the normality of the continuous variables data and Levene's Test was used to assess the equality of variances for the distinct groups in these variables. The strength and direction of the relationship between two continuous variables were assessed through the Pearson Correlation when both variables were normal and homoscedastic and the Spearman's Rank-Order Correlation when one of the variables were not normal or homoscedastic. The relationship between a continuous and a categorical variable was assessed through an ANOVA when the continuous variable data was normal and homoscedastic, and through the Kruskal-Wallis Test when the continuous variable data was not normal or heteroscedastic. The differences between final and initial CO<sub>2</sub> production rates between soil horizons were assessed with Kruskal-Wallis

---

Test, which is suitable for small samples. All statistical analyses were performed using the SciPy library (Virtanen et al., 2020) in Python, version 3.11.3.

### **3.4 Results**

Across all sites, the transition from organic-rich to mineral soil horizons was marked by a consistent decrease in P, K, C and N contents (**Table 5**). The deeper the soil sample, the lower its nutrients content. Polygon rim soils showed the lower pH values. Water content was higher in the organic-rich samples compared to the mineral ones at the slope bottom and surface plain, but the same pattern was not identified in the polygon rim.

---



**Table 5** - Initial characterization of the study sites and soil horizons samples. Information reported here refer to the composite sample created for each site-horizon combination from the mixture of one sample from each sub-site. The average and standard deviation of three replicates is shown for available phosphorus (P) and potassium (K).

Site	Soil horizon	Soil horizon	Depth range (cm)	pH	Water content (%)	C (%)	N (%)	P (mg/kg soil)	K (mg/kg soil)
Polygon rim	organic	O	0-8	5.77	48.2	15.09	0.4	40.9 ± 4.3	416.8 ± 40.1
	top	A	7-24	5.43	55.7	8.34	0.485	2.6 ± 0.5	34 ± 6.8
	bottom	B	20-30	5.35	41.3	4.46	0.295	2.9 ± 0.4	33 ± 1.9
Slope bottom	organic	O	0-10	6.48	55.8	8.41	0.249	24.9 ± 4.4	299.3 ± 2.8
	top	A	9-17	6.32	32.3	1.96	0.11	6.1 ± 3.4	38.8 ± 4.4
	bottom	AB	16-35	5.65	27.9	1.2	0.074	2.5 ± 0.2	20.3 ± 1
Surface plain	organic	Ha	0-5	6.02	47.3	13.49	0.484	34.7 ± 0.9	459.5 ± 8.3
	top	A	5-17	6.30	37.7	5.4	0.338	6.8 ± 0.3	54.7 ± 4.3
	bottom	B	16-40	6.16	25.1	2.67	0.207	0.6 ± 0.4	20.7 ± 1.7

Throughout the experiment, I observed a general decrease in P concentrations with significant P turnover rates, but no significant difference of the temperature treatments between them ( $p > 0.05$ ) (**Figure 12**). The rate of turnover in these concentrations are then generally P immobilization rates as they are mostly negative, apart from the surface plain bottom mineral samples under the 15 °C treatment that had a P mineralization rate of 0.04

mg kg<sup>-1</sup> d<sup>-1</sup>. Not all incubated samples exhibited significant P turnover rates as is shown by the samples that do not exhibit a slope adjusted to the P concentrations in **Figure 12**. The surface plain organic-rich sample at 4 °C and 15 °C, slope bottom organic-rich sample at 4 °C, polygon rim organic-rich sample at 4 °C and 15 °, surface plain top mineral sample at 4 °C and 15 °C, slope bottom top mineral sample at 15 °C, polygon rim top mineral sample at 4 °C, slope bottom bottom mineral sample at 15 °C and polygon rim bottom mineral sample at 4 °C, showed significant P immobilization rates, while, the surface plain bottom mineral sample at 15 °C showed significant P mineralization rate and, the slope bottom organic-rich sample at 15 °C, slope bottom top mineral sample at 4 °C, polygon rim top mineral sample at 15 °C, surface plain bottom mineral sample at 4 °C, slope bottom bottom mineral sample at 4 °C and the polygon rim bottom mineral sample at 15 °C showed no significant P turnover rate ( $p > 0.05$ ). The P turnover rates of the 4 °C treatment correlated with the soil C content ( $r = -0.89$ ;  $p < 0.01$ ), soil K content ( $r = -0.79$ ;  $p < 0.05$ ) and initial CO<sub>2</sub> rates ( $r = -0.9$ ;  $p < 0.05$ ). The P turnover rates of the samples incubated at 15 °C correlated with more variables compared to the ones incubated at 4 °C. The P turnover rates at 15 °C also correlated with soil C content ( $r = -0.91$ ;  $p < 0.05$ ), soil K content ( $r = -0.94$ ;  $p < 0.01$ ) and initial CO<sub>2</sub> rates ( $r = -0.89$ ;  $p < 0.05$ ), and additionally to the middle ( $r = -0.96$ ;  $p < 0.01$ ) and final CO<sub>2</sub> ( $r = -0.91$ ;  $p < 0.05$ ) rates, P ( $r = -0.94$ ;  $p < 0.01$ ) content, and finally K turnover rates ( $r = 0.97$ ;  $p < 0.05$ ).

---

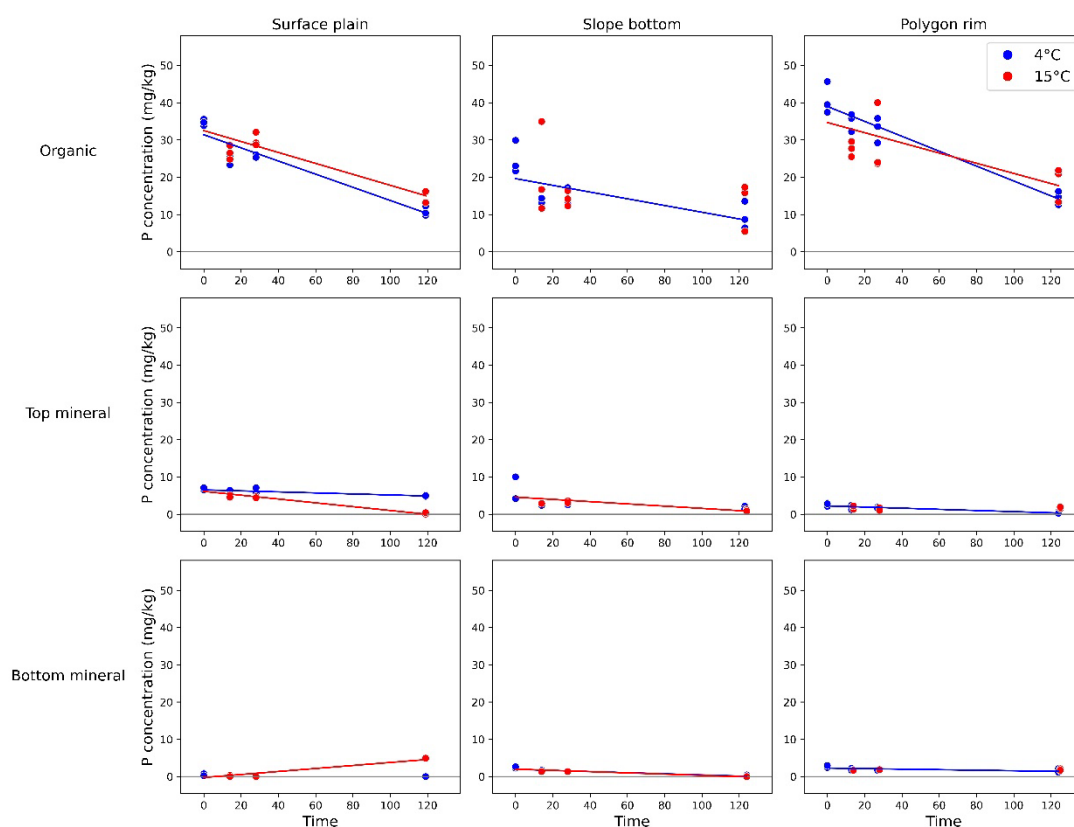


**Figure 12** – Phosphorus concentrations over the experiment time. First column plots contain data from the surface plain, second columns plots contain data from the slope bottom and third column plots contain data from the polygon rim. First row plots contain data from the organic-rich soil horizon, second row plots contain data from the top mineral soil horizon and third row plots contain data from the bottom mineral soil horizon. The blue circles identify the measured P concentrations at 4 °C and the red circles identify the measured P concentrations at 15 °C. Blue lines identify the significant slope ( $p < 0.05$ ) of the linear regression adjusted to the data, that is the P turnover rates, at 4 °C, and the red lines identify the significant slope ( $p < 0.05$ ) of the linear regression adjusted to the data, that is the P turnover rates, at 15 °C.

Organic-rich horizon samples were the ones with higher K content having on average 822% more K than top mineral samples and 1490% more K than bottom mineral samples. Potassium concentrations tended to decrease along the experiment (**Figure 13**), and all

measured K turnover rates were immobilization rates, thus negative. There was no significant difference in K turnover rates of the different temperature treatments ( $p > 0.05$ ). The surface plain top mineral sample at 15 °C, surface plain organic-rich sample at 4 °C and at 15 °C, slope bottom bottom mineral sample at 15 °C, slope bottom organic-rich sample at 4 °C and at 15 °C, polygon rim bottom mineral sample at 15 °C, polygon rim organic-rich sample at 4 °C and at 15 °C, showed significant K immobilization rates, while the surface plain top mineral sample at 4 °C, slope bottom top mineral sample at 4 and 15 °C, polygon rim top mineral sample at 4 and 15 °C, surface plain bottom mineral sample at 4 and 15 °C, slope bottom bottom mineral sample at 4 °C and polygon rim bottom mineral sample at 4 °C showed no significant K turnover rate ( $p > 0.05$ ). The K turnover rates of the 4 °C treatment did not correlate with any of the measured variables, while the K turnover rates at 15 °C correlated with the soil K ( $r = -0.89$ ;  $p < 0.05$ ), C ( $r = -0.94$ ;  $p < 0.01$ ), P ( $r = -0.94$ ;  $p < 0.01$ ), ammonium ( $r = -0.94$ ;  $p < 0.01$ ) and water ( $r = -0.83$ ;  $p < 0.05$ ) contents, and with the P turnover rates ( $r = 0.97$ ;  $p < 0.05$ ).

---

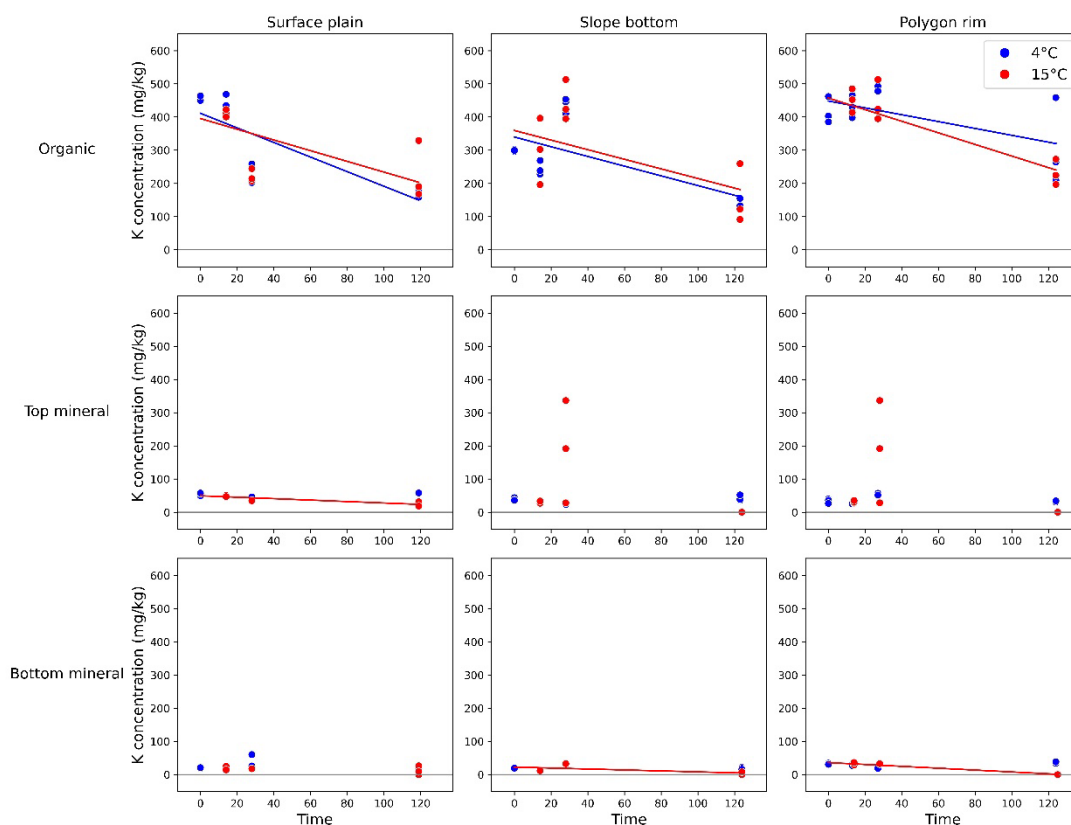


**Figure 13** - Potassium concentrations over the experiment time. First column plots contain data from the surface plain, second column plots contain data from the slope bottom and third column plots contain data from the polygon rim. First row plots contain data from the organic-rich soil horizon, second row plots contain data from the top mineral soil horizon and third row plots contain data from the bottom mineral soil horizon. The blue circles identify the measured K concentrations at 4 °C and the red circles identify the measured K concentrations at 15 °C. Blue lines identify the significant slope ( $p < 0.05$ ) of the linear regression adjusted to the data, that is the K turnover rates, at 4 °C, and the red lines identify the significant slope ( $p < 0.05$ ) of the linear regression adjusted to the data, that is the K turnover rates, at 15 °C.

The CO<sub>2</sub> production during the experiment was substantial with all samples presenting significant CO<sub>2</sub> production rates (**Figure 14**). Significant differences in initial and middle CO<sub>2</sub> production rates emerged among temperature treatments ( $p < 0.05$ ), but not in the

final rates ( $p>0.05$ ). Mean CO<sub>2</sub> production rates standard deviation was small in most cases with exception of the organic-rich horizon of the slope bottom at 15 °C. While all samples produced CO<sub>2</sub>, the production rates tended to decrease along the experiment. Furthermore, the samples incubated at 15 °C produced more CO<sub>2</sub> than the ones incubated at 4 °C, at all experimental stages. The average CO<sub>2</sub> production rate across all sites, soil horizons and experiment stages at 15 °C was of  $0.161 \pm 0.058$  mg CO<sub>2</sub>-C g C<sup>-1</sup> d<sup>-1</sup>, while at 4 °C was of  $0.067 \pm 0.025$  mg CO<sub>2</sub>-C g C<sup>-1</sup> d<sup>-1</sup>. Samples incubated at 15 °C produced 2.42 times more CO<sub>2</sub> than the ones incubated at 4 °C. Organic-rich samples showed higher CO<sub>2</sub> production rates than the mineral horizons samples. The organic-rich horizon samples produced 43,6% less CO<sub>2</sub> in the final stage compared to the initial stage at 4 °C and 48,8% at 15 °C, while the top mineral differences between final and initial stages were of 61,9% at 4 °C, and 52,2% at 15 °C and the bottom mineral 74,9% at 4 °C and 62,2% at 15 °C. However, there were no significant differences detected ( $p>0.05$ ). The organic-rich horizon samples at 4 °C produced 100% more CO<sub>2</sub> than the top mineral samples in the initial stage, 188% in the middle stage and 195% in the final stage, and at 15 °C, 153% in the initial, 182% in the middle and 172% in the final stage. In comparison with the bottom mineral samples, the organic-rich samples at 4 °C produced 224% more CO<sub>2</sub> in the initial stage, 531% in the middle and 631% in the final stage, and at 15 °C, 348% in the initial, 506% in the middle and 508% in the final stage.

In the 4 °C treatment, the initial CO<sub>2</sub> production rates correlated with the soil P ( $r=0.73$ ;  $p<0.05$ ) and K ( $r=0.68$ ;  $p<0.05$ ) contents, the middle CO<sub>2</sub> rates correlated with P ( $r=0.85$ ;  $p<0.01$ ) and K ( $r=0.88$ ;  $p<0.01$ ) contents, and the final CO<sub>2</sub> rates correlated with the soil water ( $r=0.67$ ;  $p<0.05$ ), P ( $r=0.85$ ;  $p<0.01$ ) and K ( $r=0.88$ ;  $p<0.01$ ) contents. In the 15 °C treatment, the initial CO<sub>2</sub> production rates correlated with the soil P ( $r=0.78$ ;  $p<0.05$ ) and K ( $r=0.75$ ;  $p<0.05$ ) contents, and P turnover rates ( $r=-0.89$ ;  $p<0.05$ ), the middle CO<sub>2</sub> rates correlated with the soil water ( $r=0.72$ ;  $p<0.05$ ), P ( $r=0.85$ ;  $p<0.01$ ) and K ( $r=0.88$ ;  $p<0.01$ ) contents and P turnover rates ( $r=-0.96$ ;  $p<0.01$ ), and the final CO<sub>2</sub> rates correlated with the soil P ( $r=0.77$ ;  $p<0.05$ ) and K ( $r=0.75$ ;  $p<0.05$ ) contents and P turnover rates ( $r=-0.91$ ;  $p<0.05$ ).

---

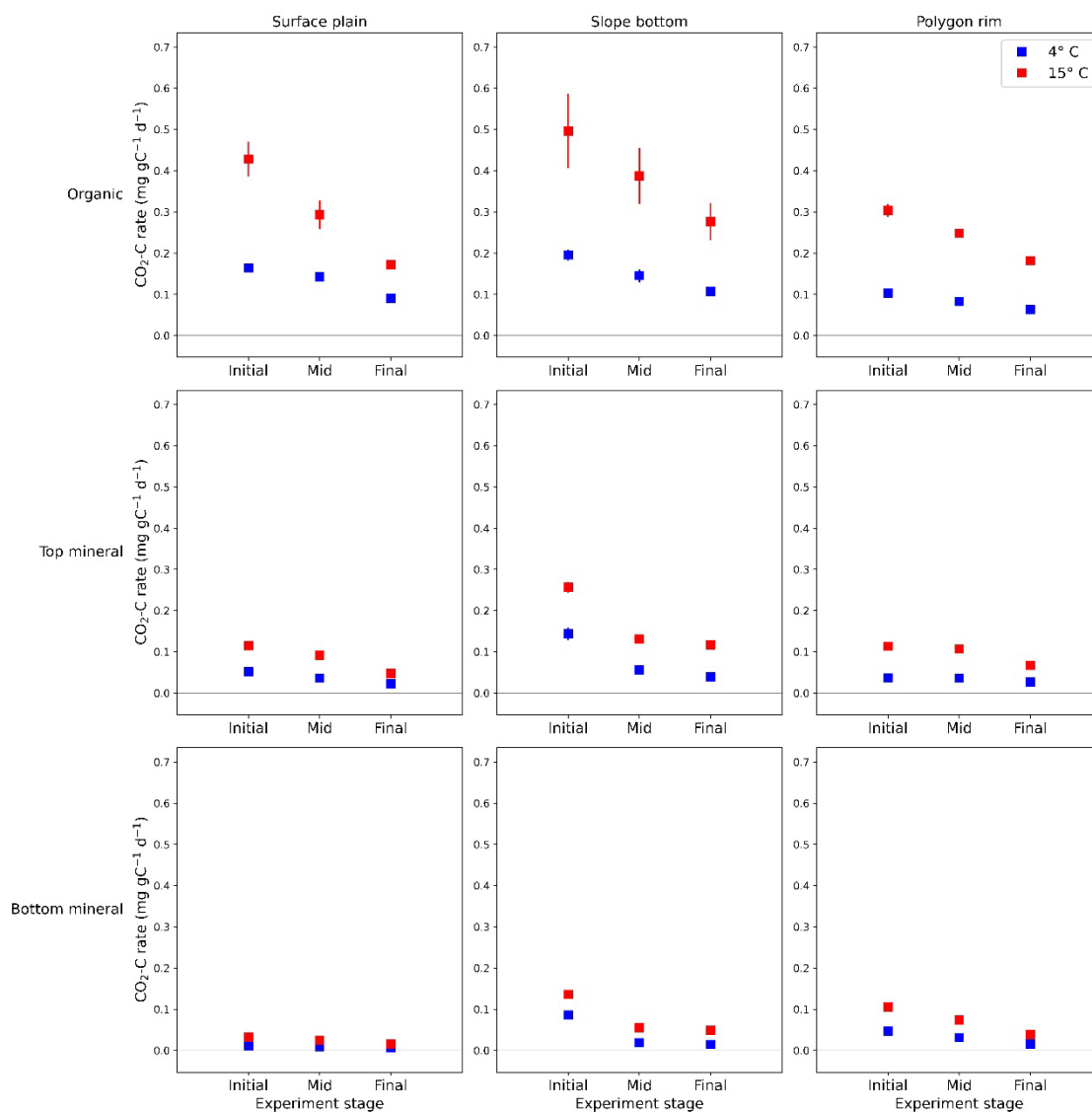


**Figure 14** – Carbon dioxide production rates in the three different experiment stage (initial, middle, and final). First column plots contain data from the surface plain, second columns plots contain data from the slope bottom and third column plots contain data from the polygon rim. First row plots contain data from the organic-rich soil horizon, second row plots contain data from the top mineral soil horizon and third row plots contain data from the bottom mineral soil horizon. The blue squares identify the calculated significant CO<sub>2</sub> production rates ( $p < 0.05$ ) at 4 °C and the red squares identify the calculated significant CO<sub>2</sub> production rates ( $p < 0.05$ ) at 15 °C. Error bars show standard deviation. Data points that have no visible error bars had negligible standard deviation.

Nitrous oxide concentrations also had diverse fates along the experiment (**Figure 15**), with no significant difference between temperature treatments ( $p>0.05$ ). The top and bottom mineral samples of the slope bottom and polygon rim consumed  $N_2O$ . These  $N_2O$  consumption rates decreased towards the end of the experiment. The organic-rich sample of the polygon rim incubated at  $15\text{ }^\circ\text{C}$  showed production of  $N_2O$ , as well as the organic-rich sample of the surface plain at  $4\text{ }^\circ\text{C}$ . The remaining samples presented some release of  $N_2O$ . Among the samples incubated at  $4\text{ }^\circ\text{C}$ , the initial  $N_2O$  rates correlated with the soil C content ( $r=0.8$ ;  $p<0.05$ ) and P turnover rates ( $r=-0.9$ ;  $p<0.05$ ). Among the ones incubated at  $15\text{ }^\circ\text{C}$ , the initial  $N_2O$  rates correlated with the soil nitrate content ( $r=0.95$ ;  $p<0.001$ ), and it was the only correlation identified.

---



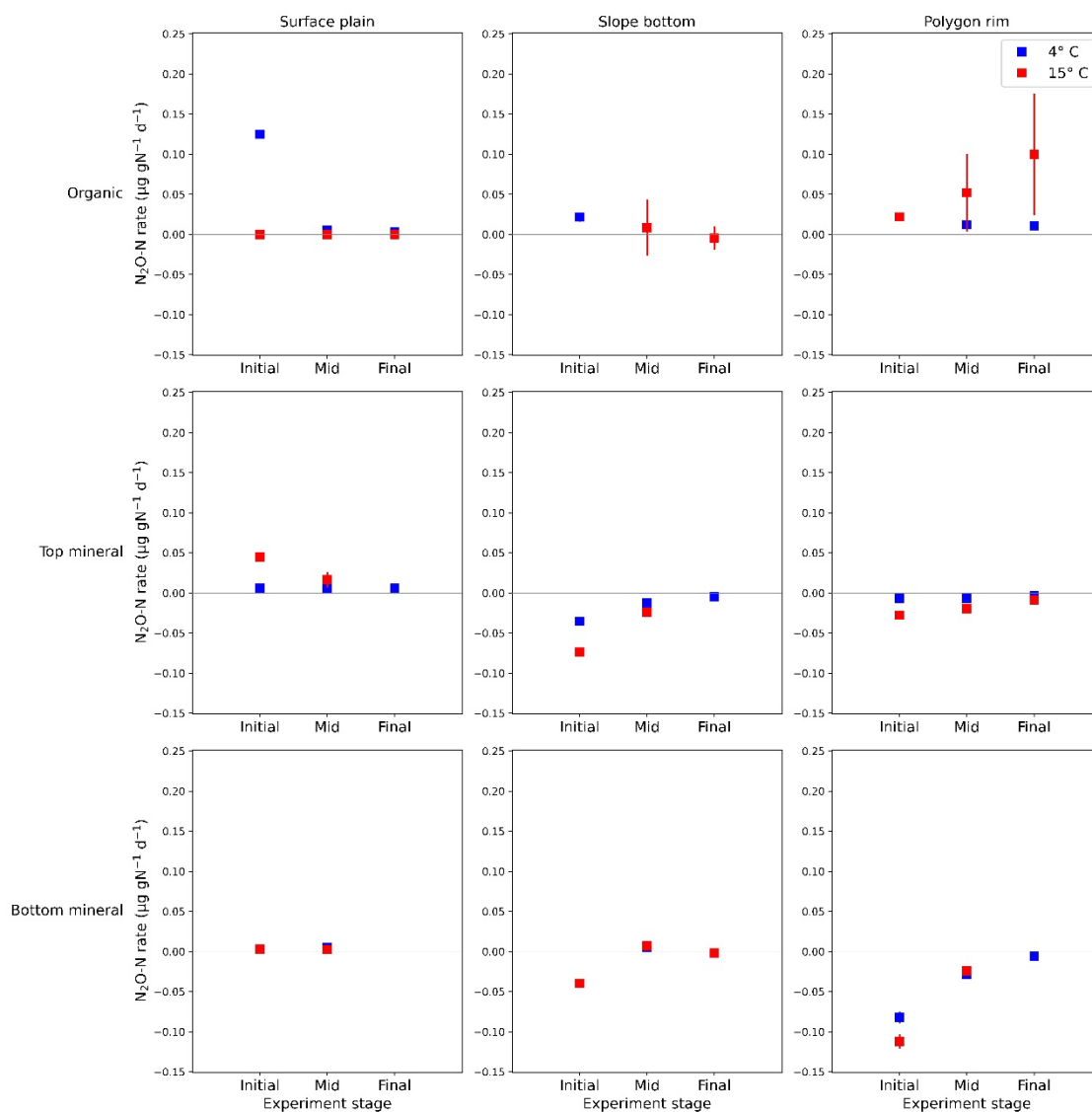


**Figure 15** – Nitrous oxide rates in the three different experiment stage (initial, middle, and final). First column plots contain data from the surface plain, second columns plots contain data from the slope bottom and third column plots contain data from the polygon rim. First row plots contain data from the organic-rich soil horizon, second row plots contain data from the top mineral soil horizon and third row plots contain data from the bottom mineral soil horizon. The blue squares identify the calculated significant N<sub>2</sub>O production rates ( $p < 0.05$ ) at 4 °C and the red squares identify the calculated significant N<sub>2</sub>O production rates ( $p < 0.05$ ) at 15 °C. Error bars show standard deviation.

## 3.5 Discussion

### 3.5.1 Soil P and K turnover rates controls

Soil P immobilization by microorganisms is seemingly higher during the growing season, resulting in intense competition between plants and the soil microbiota and less labile P left for plant uptake (Giblin et al., 1991; Weintraub, 2011). Interestingly, I have observed general P immobilization along my experiment, which was designed to emulate Siberian growing season with representative positive temperatures sustained over four months. These results contrast with the ones found in Shaw and Cleveland (2020), who identified a consistent increase in soil P availability with higher temperatures in soil incubations using samples from different environments ranging from arid shrubland to boreal forest, but did not include tundra environments. This release of P was attributed to the acceleration of P hydrolysis via extracellular phosphatase enzymes by microorganisms during the organic matter decomposition, at higher temperatures.

Data from incubated samples from tundra ecosystems in Alaska, instead, showed an increase in microbial P demands with higher temperatures (Nadelhoffer et al., 1991), resulting in a decrease in soil P concentrations. It was found that dissolved inorganic P release from organic soils was significantly greater at 3°C compared to 9°C or 15°C, suggesting that P mineralization is more active during colder periods, which could include Winter, early Spring and late Autumn (Nadelhoffer et al., 1991). My results also indicated that P immobilization dominated P dynamics along the experiment, but they have not shown a significant effect of temperature in this process. The same absence of effect of temperature in the soil P dynamics was found in Jonasson et al. (1993), who performed in situ soil incubations in Abisko, northern Swedish Lapland.

Phosphorus dynamics in my experiment were highly correlated to C turnover. The P turnover rates correlated to soil C content and initial CO<sub>2</sub> rates in both treatments (negatively because P turnover rates were mostly negative and soil C content and CO<sub>2</sub> rates were positive), and additionally to middle and final CO<sub>2</sub> rates in the 15 °C treatment. The mineral horizon samples which had less C, also produced less CO<sub>2</sub>, and immobilized less P. The availability of P can potentially limit both primary production and

---

decomposition processes in the Arctic (Stimmler et al., 2023; Weintraub, 2011). Phosphorus is a critical nutrient for plants, essential for energy transfer and the synthesis of nucleic acids and cell membranes and concurrently closely intertwined for organic matter decomposition. In the Arctic, the recharging of dissolved soil P is virtually completely achieved by organic matter decomposition, since organic P is the major source of this nutrient (Chapin Iii et al., 1995; Giblin et al., 1991; Weintraub, 2011). The significant correlation between P turnover and CO<sub>2</sub> production found in my study, indicates a close relationship between microbial activity and P availability in tundra soils. Higher CO<sub>2</sub> production is indicative of increased microbial activity in the soil, which as suggested by my results, also leads to greater P immobilization by soil microorganisms. This process identified in my experiment highlights the formation of an important soil P stock in permafrost ecosystems. As demonstrated by Chapin et al. (1978), this P source is crucial for tundra vegetation; in fact, he estimated 30% of the annual plant P uptake in a wet sedge meadow in Alaska deriving from the decline in microbial biomass during the period of snowmelt.

The P turnover rates of both treatments also had a high correlation to soil K content, and additionally to K turnover rates in the 15 °C treatment. Organic-rich horizon samples were also the ones with higher K content, thus, the correlation between P and K might be arising from the relationship of more nutrient-rich samples also being the most microbiologically active ones. Evidently, the same can be stated by the correlation between P turnover rates and soil P content also at 15 °C.

The only sample that exhibited P mineralization during the experiment was the surface plain bottom mineral samples under the 15 °C treatment. This was also the sample with third lowest C content, lowest initial, middle, and final CO<sub>2</sub> production rates, second lowest K content, no K turnover rate, lowest water, and lowest P content. Essentially, it was a mineral, nutrient poor sample with low CO<sub>2</sub> production. Mineral soils have been identified as larger sources of P, having higher P mineralization rates compared to organic soils, in Alaska (Nadelhoffer et al., 1991). Notwithstanding, Jonasson et al. (1993) presented higher P mineralization rates in the soil with higher organic matter content. While these contrasting results evidence the need of further research to clarify the relationship between type of soil and organic matter content with P dynamics in the

---

Arctic, another phenomenon could explain the observed changes in P concentrations, which is the decline in microbial population and resulting release of P after cell lysis. This is an important aspect of P availability in the Arctic as mentioned before (Chapin Iii et al., 1995; Giblin et al., 1991; Jonasson et al., 1996; Schimel et al., 1996; Schmidt et al., 2002; Weintraub, 2011). Thus, this process of microbial death could possibly have happened in this nutrient-poor sample, increasing the availability of P towards the end of the incubation.

Potassium concentrations tended to decrease along the experiment, with no significant difference between temperature treatments. Like P, K was immobilized during the experiment, but no sample showed K mineralization. A global meta-analysis discovered widespread K limitation in most of the terrestrial ecosystems analyzed. It was found that K addition significantly increases aboveground biomass production, and that K limitation is more pervasive in humid climates and weathered soils. Although K limitation was smaller than N and P limitations, it had the potential to limit ecosystems primary production (Chen et al., 2023). Potassium immobilization rates of the samples incubated at 4 °C did not correlate with any of the measured variables, while the ones incubated at 15 °C, correlated with the chemical variables demonstrating the fertility of the soil, namely K itself, C, P, ammonium, and water. Besides that, K immobilization rates showed a strong correlation with the P turnover rates. The most nutrient-rich and P consuming samples were the organic-rich horizon ones, thus similarly to P rates, it reveals that these samples contained the most active microbial community, with higher C turnover and nutrients immobilization.

### **3.5.2 Greenhouse gases rates at different temperatures and connection to nutrients dynamics**

Knoblauch et al. (2021) and Melchert et al. (2022) also performed aerobic incubations at 4 °C with samples from Kurungnakh Island, Lena River Delta. The samples from Knoblauch et al. (2021) produced between 0.186 and 0.337 mg CO<sub>2</sub>-C g C<sup>-1</sup> d<sup>-1</sup>, while the ones of my study produced between 0.006 and 0.195 mg CO<sub>2</sub>-C g C<sup>-1</sup> d<sup>-1</sup> and Melchert et al. (2022) samples produced between 0.015 and 0.093 mg CO<sub>2</sub>-C g C<sup>-1</sup> d<sup>-1</sup>. These differences can be explained by different timespans of the incubation experiments. Knoblauch et al.

---

(2021) incubated the soil for only 18 days. When those are compared with only the initial CO<sub>2</sub> production rates of my study, which were incubated for 30 days, with a mean value of 0.093 mg CO<sub>2</sub>-C g C<sup>-1</sup> d<sup>-1</sup>, Knoblauch et al. (2021) rates are still higher with a mean of 0.253 mg CO<sub>2</sub>-C g C<sup>-1</sup> d<sup>-1</sup>. Initial CO<sub>2</sub> production rates tend to be higher and decrease along the experiment as can be seen by the decaying trend in CO<sub>2</sub> production rates from initial to final experiment stages in this and previous studies (Knoblauch et al., 2013; Lee et al., 2012). Melchert et al. (2022) presented slightly lower CO<sub>2</sub> production than my study, and a longer experiment timespan until 175 days. The thawing permafrost of Kurungnakh island CO<sub>2</sub> production rates incubated at 4 °C for 200 days ranged from 0.047 to 0.054 mg CO<sub>2</sub>-C g C<sup>-1</sup> d<sup>-1</sup> in the 70 to 120 cm depth interval, comprising Holocene permafrost deposits, but reached much higher values in deeper permafrost, reaching 0.288 mg CO<sub>2</sub>-C g C<sup>-1</sup> d<sup>-1</sup> at 22.4 m from Kargin interstadial period (Knoblauch et al., 2013).

It is noticeable that the difference between organic-rich and mineral horizon CO<sub>2</sub> production generally increased towards the end of the experiment. This increasing difference with time can be better visualized by the comparison of final and initial stage CO<sub>2</sub> production rates between soil horizons, that in spite of not having a significant difference, showed clearly that the organic-rich samples sustained more of the initial CO<sub>2</sub> production rates towards the final stage of the experiment, and the mineral samples CO<sub>2</sub> rates faced a stronger reduction. Due to the lower C content, the mineral horizon samples might have experienced a faster depletion of easily decomposable C compared to the organic-rich horizon causing a faster decrease of CO<sub>2</sub> production rates. Furthermore, the probable presence of mineral-associated organic carbon in the mineral samples, might have further restrained the bioavailability of the organic matter for decomposition, leading to the measured reduction of the CO<sub>2</sub> rates along the time. Temperature affected CO<sub>2</sub> rates in my incubation as expected (Bracho et al., 2016; Galera et al., 2023; Schädel et al., 2016). Knoblauch et al. (2021) also identified soil temperature as one of the main drivers of in situ CO<sub>2</sub> emissions in sites of Kurungnakh Island. The temperature treatment significantly affected the CO<sub>2</sub> production rates in its initial and middle stages. Despite of no significant effect of temperature, 15 °C final stage CO<sub>2</sub> production rates were higher than 4 °C final stage CO<sub>2</sub> production rates in all samples.

---

Additionally, the CO<sub>2</sub> production rates in my experiment were positively correlated with the concentration of soil C, P and K, and negatively with P turnover rates. In Knoblauch et al. (2021) the amount of thawed organic carbon was one of the main factors of in situ CO<sub>2</sub> emissions in sites of Kurungnakh Island and Bracho et al. (2016) identified soil C and N contents as main factors of soil organic matter decomposition in incubated soils from Alaska as did Knoblauch et al. (2013) for Kurungnakh. Phosphorus availability in the soil tends to increase CO<sub>2</sub> rates (Zheng et al., 2022). The high correlation between CO<sub>2</sub> rates and P may emerge from the requirement of microorganisms for P to grow. Shaver et al. (1998) demonstrated in a warming and fertilization experiment in Alaska that P stimulated more CO<sub>2</sub> fluxes than N. In fact, soil CO<sub>2</sub> production measurements have been used as a method to quantify soil microbial activity and potential mineralizable N and P (Haney et al., 2008). Potassium is crucial to cell osmoregulation and protein synthesis, and has been associated to increase in soil microbial biomass (Ibrahim et al., 2023). Thus, the strong correlation between P and K with CO<sub>2</sub> rates in my study indicates microbial growth during the experiment, which occurs through the immobilization on of P and K. Overall, my results confirm the understanding that organic matter is central for nutrient storage, and from that association, nutrients turnover is intricately linked to microbial respiration. This explains the robust association linking the numerous factors pertaining to organic matter and microbial respiration.

My N<sub>2</sub>O rates results of both treatments are in the same range of Marushchak et al. (2021) that incubated soil samples from Kurungnakh aerobically at 10 °C, with few exceptions. Wegner et al. (2022) performed anaerobic incubations at 4 °C with samples from Kurungnakh and found values well above my results and those from Marushchak et al. (2021). These differences corroborate what has been shown by Marushchak et al. (2021) with the comparison of aerobic and anaerobic N<sub>2</sub>O production rates, indicating higher N<sub>2</sub>O production under the anaerobic treatment, demonstrating that denitrification is the main N<sub>2</sub>O production pathway in Kurungnakh Island.

The N<sub>2</sub>O rates detected in my study is likely a product of coupled nitrification-denitrification, a process in which nitrite or nitrate produced during nitrification is utilized by denitrifiers, which occur in soils where neighboring microhabitats provide suitable conditions for both nitrification and denitrification (Kool et al., 2011; Wrage et al.,

---

2001). Those two processes are regarded as the primary pathways for N<sub>2</sub>O production in permafrost soils (Voigt et al., 2020). N<sub>2</sub>O production might have originated in two processes. First, N<sub>2</sub>O might have been formed during the oxidation of ammonia to nitrite during nitrification, via the incomplete oxidation of the intermediary NH<sub>2</sub>OH. And secondly, N<sub>2</sub>O might have been formed through the reduction of nitrate during the denitrification process present in anoxic micropores in the soil (Wrage-Mönnig et al., 2018; Wrage et al., 2001). The N<sub>2</sub>O consumption observed in some samples could also be related to denitrification, but in this case to the complete process, that not only convert nitrate to N<sub>2</sub>O but further reduce N<sub>2</sub>O to N<sub>2</sub>, using the enzyme nitrous oxide reductase (Wrage et al., 2001).

High correlation between initial N<sub>2</sub>O rates and soil nitrate content at 15 °C has been identified in my experiment. I speculate that this correlation might be an indicative of both nitrification and denitrification processes. Of nitrification because nitrate is eventually produced following the N<sub>2</sub>O-producing process of ammonia oxidation and nitrate is reduced during the N<sub>2</sub>O-producing process of denitrification. The N<sub>2</sub>O rates evolution with time approach zero towards the final experiment stage. This can be observed for both samples producing N<sub>2</sub>O as for the ones consuming N<sub>2</sub>O. This pattern suggests a weakening of the nitrification and denitrification processes as time progressed. I hypothesize that this pattern is related to the depletion of nitrate towards the end of the experiment.

Nitrous oxide production or consumption in my experiment did not significantly differ between temperature treatments, although observations suggest that the N process in place at the 15 °C treatment was stronger than at the 4 °C. In other words, temperature tended to increase N<sub>2</sub>O production or consumption, depending on the sample. However, due to the extremely variable results among different samples, no statistical significance could be detected. Nonetheless, the N<sub>2</sub>O rates did significantly correlate to soil C content and soil P turnover rates at 4 °C. This result is in accordance to O'Neill et al. (2020) who found that P was an important factor influencing N<sub>2</sub>O emissions under C rich conditions, and also with further literature that described the influence of P on N<sub>2</sub>O rates through the relief of microorganisms from P limitation (Mehnaz & Dijkstra, 2016; Mori et al., 2010). Likely, the depletion of readily labile C sources, as evidenced by the decreasing CO<sub>2</sub> rates,

---

might have contributed to the tendency of the N<sub>2</sub>O rates to approach zero along the experiment as well (Mehnaz et al., 2019). Similarly, the immobilization of P might have suppressed the activity of bacteria involved in the N cycle, and also contributed to this tendency.

### 3.6 Conclusions

The question of whether nutrients will be more available in the Arctic to cope with increased demands from higher primary productivity caused by global warming and CO<sub>2</sub> fertilization, is not yet answered and is of utmost importance for predictions of ongoing changes in climate trajectories. Arctic soils present widespread P limitation, the impact of further warming on the fluxes of this nutrient in these soils has the potential to shape future primary productivity and soil organic matter decomposition. Data on P dynamics in the Arctic are still scarce, and data on K dynamics are even more. I have hypothesized that P and K would become more available with warming, but that was not the case since these nutrients were immobilized during the experiment regardless of the temperature treatment. Phosphorus and K had a high correlation with C turnover, and samples that emitted more CO<sub>2</sub> were also the ones that immobilized more P and K. My N<sub>2</sub>O results suggest the occurrence of coupled nitrification-denitrification in Kurungnakh soils, modulated by the amounts of nitrate, C and P in the soil. My results contradict the view in which higher soil temperatures would probably increase P and K availability to primary production in arctic terrestrial ecosystems. My findings support the perspective that climate change might increase competition between plants and soil microbes for scarce nutrients contents, instead of enhancing nutrients mineralization and subsequent availabilities. Further research is necessary to investigate in situ soil nutrients dynamics and explore the interaction between different nutrient pools, including the microbial biomass pool, and the competition between plants and the soil microbiota for nutrients.

---



## 4 Synthesis

### 4.1 Will CH<sub>4</sub> fluxes in the Arctic increase with permafrost thawing, and what factors regulate the ratio between microbial CO<sub>2</sub> and CH<sub>4</sub> production from OM decomposition in the polygonal tundra?

The understanding that tundra wetlands are a significant global source of CH<sub>4</sub> has become well-established. Eurasian permafrost regions alone have median wetland CH<sub>4</sub> fluxes of 16 to 18 g CH<sub>4</sub> m<sup>-2</sup> y<sup>-1</sup> (Treat et al., 2024). The emerging novelty is that emissions from these ecosystems are escalating in response to global warming (Parmentier et al., 2017; Röbger et al., 2022). The findings of the second chapter of this thesis shows evidence of this trend of increasing CH<sub>4</sub> fluxes. These were the active layer depth and the soil temperature at 40 cm for the wet tundra (polygon center) CH<sub>4</sub> fluxes.

It is forecasted that both the active layer depth and soil temperatures shall continue to increase in the future. de Vrese et al. (2023), showed that even in the future scenario of a drier Arctic, CH<sub>4</sub> fluxes would be similar to those of an eventual wetter Arctic, due to a greater substrate availability caused by higher temperatures. Essentially, changes in soil temperature indirectly regulate substrate availability for methanogenesis. This occurs not only through the thawing of permafrost, which exposes previously frozen ground, but also without further permafrost deterioration (Chang et al., 2019).

CH<sub>4</sub> oxidation is a counteraction to these trends and plays a significant role in determining net CH<sub>4</sub> emissions. Methanotrophs oxidize CH<sub>4</sub> into CO<sub>2</sub>, a process called low affinity CH<sub>4</sub> oxidation. The low affinity CH<sub>4</sub> oxidation essentially occurs at environments with high CH<sub>4</sub> production, such as wetlands. In contrast, high affinity CH<sub>4</sub> oxidation takes place in oxic upland soils and operates at very low concentrations of CH<sub>4</sub> (Cai et al., 2016). Voigt et al. (2023) notably demonstrated that Arctic CH<sub>4</sub> sink related to high affinity CH<sub>4</sub> oxidation might be underestimated. In the second chapter of this thesis, I found no evidence of high affinity CH<sub>4</sub> oxidation in the dry site, but rather found an

---

important influence of low affinity oxidation reducing CH<sub>4</sub> fluxes to the atmosphere. As to the wet tundra, it was considered CH<sub>4</sub> oxidation as limited due to the high prevalence of plant-mediated CH<sub>4</sub> transport, which protects CH<sub>4</sub> from oxidation. All things considered and given that CH<sub>4</sub> oxidation was not directly measured in the second chapter, an uncertainty range based on robust CH<sub>4</sub> oxidation data from prior research in Samoylov Island was calculated. The calculated rhizospheric CH<sub>4</sub> oxidation was of 10 to 31%. With this estimate is the measured CO<sub>2</sub>:CH<sub>4</sub> in situ production ratios was corrected in the second chapter of the thesis.

The ratio of CO<sub>2</sub> to CH<sub>4</sub> production is usually calculated in ex situ conditions, through incubation experiments (Knoblauch et al., 2018; Treat et al., 2015). In the second chapter of the thesis, it was proposed an in situ estimation of the CO<sub>2</sub>:CH<sub>4</sub> production ratio by measuring CH<sub>4</sub> fluxes from a wet site dominated by anaerobic conditions. This is important because measured CH<sub>4</sub> fluxes in an incubation represents the potential CH<sub>4</sub> of the incubated soil, while CH<sub>4</sub> fluxes measured in situ with the chamber technique, represent the actual CH<sub>4</sub> fluxes on site. The processes in which microbes decompose organic matter leading to carbon release to the atmosphere is of extreme importance to assess the permafrost carbon-climate feedback, since the global warming potential of CH<sub>4</sub> is 28 fold that of the CO<sub>2</sub> (Myhre et al., 2013).

Herbst et al. (2024) revealed higher CH<sub>4</sub> production in active layer samples in comparison to permafrost samples in the Lena River Delta. While one could draw the conclusion that this is evidence of a probable overestimation of the CH<sub>4</sub> emissions in the future with permafrost thaw, Knoblauch et al. (2018) show that CH<sub>4</sub> production is extremely relevant in the long term, and that microbial methanogenic communities take time to establish and produce CH<sub>4</sub>. However, above all, the results of the second chapter demonstrate that the CO<sub>2</sub>:CH<sub>4</sub> production ratios tend to 3 towards the end of the growing season, when the deeper soil layers are warm enough and present favorable redox conditions.

Moreover, one interesting finding of the second chapter was that the depth of soil temperature increases matters in the polygonal tundra. The warming of shallower soil horizons stimulates CO<sub>2</sub> production, since these horizons are more oxic, and the warming of deeper soil horizons stimulates CH<sub>4</sub> production, since these are more anoxic

---

environments. A similar result was found in the Lena Delta linking increasing soil temperatures at 20 cm depth to increasing CH<sub>4</sub> fluxes (Rößger et al., 2022). This concept should be further explored by in situ CO<sub>2</sub> and CH<sub>4</sub> fluxes measurements studies. The inclusion of the relationship of CH<sub>4</sub> production to soil temperatures at different depths to modelling efforts of permafrost affected soil processes could improve the ability to forecast future greenhouse gas emissions.

The Arctic warming is expected to lead to the deepening of the active layer. The results in of the second chapter of this thesis suggest that a notable increase in CH<sub>4</sub> production is to be expected, especially in wet tundra environments. The capacity of the Arctic greening in offsetting these emissions is still uncertain (Turetsky et al., 2020). The question of whether the Arctic CH<sub>4</sub> fluxes will increase with permafrost thawing would benefit from further research on in situ CO<sub>2</sub> and CH<sub>4</sub> production, better maps characterizing crucial hydrological, ecological and topographical disturbances of Arctic terrestrial ecosystems, year-round greenhouse gases fluxes measurements and, unifying these information, improved permafrost carbon cycle dynamics models (Schädel et al., 2024; Treat et al., 2024).

## **4.2 Will P and K availability increase in a warmer Arctic?**

While increased temperatures and CO<sub>2</sub> fertilization will likely have positive effects on primary productivity, low availability of soil nutrients may constrain these positive effects. For instance, there is ample evidence that enhanced productivity caused by increased CO<sub>2</sub> levels is constrained by soil P limitation (Ellsworth et al., 2017; Menge et al., 2023). P limitation is pervasive in arctic soils (Beermann et al., 2015; Giesler et al., 2012), where microbial activity persists at low temperatures, preventing the accumulation of organic P in the soil (Weintraub, 2011). Microbes tend to accumulate available P, becoming a significant competitor against plants (Bing et al., 2016).

The results from the third chapter of this thesis provide clear evidence the P and K are immobilized by soil microorganisms following the thawing of the soil. The experiment treatments in this incubation study were designed to mimic average temperature conditions of a typical growing season in the Lena River Delta, as well as a hypothetical warmer scenario as an effect of global warming. Consequently, the dynamics of P and K

---

in the soil leaned towards immobilization rather than mineralization. Although no significant difference was observed between the temperature treatments, both demonstrated clear immobilization.

The results revealed that P turnover rates were highly correlated with soil K content and K turnover rates at 15°C. Samples from the organic-rich horizon, which had higher K content, showed a strong correlation between P and K due to their nutrient richness and high microbial activity. Additionally, a significant correlation was found between P turnover rates and soil P content at 15°C. K was immobilized, but no samples showed K mineralization rates. K immobilization rates at 4°C did not correlate with any measured variables, whereas at 15°C, they correlated with variables indicating soil fertility, such as K, C, P, ammonium, and water. K immobilization rates also correlated strongly with P turnover rates, indicating that the most nutrient-rich samples, which were high in P and supported active microbial communities, also exhibited high nutrient immobilization and C turnover.

The high correlation between P and K immobilization rates and C turnover evidenced that the P and K were being taken up by microorganisms, and there was no other relevant abiotic process in place. Samples producing more CO<sub>2</sub> were also consuming more P and K. One could expect that while P and K would be immobilized at 4 °C, indicating a nutrient-limited microbial community, this scenario could be different at 15 °C with lower P and K immobilization rates or even the emergence of P and K mineralization rates. This result would indicate a higher capacity of the soil to provide P and K with warming, and one could draw the conclusion that this would be evidence that increasing P and K demands as a consequence from higher primary productivity in the Arctic, could be at some extent met by increasing P and K mineralization rates (Brovkin & Goll, 2015; Shaw & Cleveland, 2020).

However, that was not the case, and temperature did not increase or decrease the P and K immobilization rates in place. This result suggests a scenario in which a warmer Arctic keeps its P limitation at constant levels. This implies a limitation on the increase in primary production, and consequently, on the potential for C sequestration and partial offset of greenhouse gas emissions. Soil P was identified as the main limiting nutrient for

---

the typical arctic species *Carex aquatilis* and *Arctophila fulva* in Alaska. Moreover, the normalized difference vegetation index (NDVI) of these species was a good predictor of leaf P content in them (Andresen & Loughheed, 2021). In spite of the Arctic vegetation being often co-limited by P and N, P has a relatively lower potential for increased availability in response to warming than N (Wieder et al., 2015a, 2015b).

There is initial evidence that N recycling could meet demands from the terrestrial ecosystems in a warmer climate (Bai et al., 2013; Rustad et al., 2001; Wieder et al., 2015b), but not uniformly across different regions (Du et al., 2020) and that it might contribute to the Arctic greening (Elmendorf et al., 2012). However, there is less confidence that the same could occur with P (Menge et al., 2023). The P cycle rely substantially on the weathering of parent material, a slow and minor process of nutrient release in view of plant demands (Cleveland et al., 2013; Goll et al., 2014). Consequently, the P cycle might not quickly keep up with increased demands spurred by higher CO<sub>2</sub> levels and temperatures. This suggests a more critical role of P in the regulation of the C cycle (Reed et al., 2015).

Indisputably, there is a need that especially P processes are included in Earth System models. Since P availability regulates the exchange of CO<sub>2</sub> between land and atmosphere and exerts significant influence on carbon cycling reactions to global changes, incorporating P cycling in Earth System models would greatly enhance the ability to predict interactions between biogeochemical cycles and climate change (Reed et al., 2015). Attempts to include P processes in Earth System models have been conducted, for example for the estimation of P sorption capacity in soils (Brenner et al., 2019), of plant physiological responses to P limitation, and multinutrient models, in which, C, N and P cycles interact (Goll et al., 2012; Wang et al., 2007; Yang et al., 2014; Zhu et al., 2019). In this context, the inclusion of P processes into permafrost carbon-climate feedback models is also necessary. This necessity stems from the crucial role of P availability in influencing the permafrost carbon cycle under global warming (Zhang et al., 2023), often having a more important role than N in regulating primary productivity in these ecosystems (Yang et al., 2021). Menge et al. (2023) clarifies the need for additional data on P pools and fluxes, and a better connection of models and empirical work, mainly regarding P cycling rates constants and their dependence on temperature and moisture. Long-term experiments

---

would shed light on P dynamics, particularly on its temperature sensitivity. While P displays a limited reaction to short-term temperature changes, as showed in the third chapter of this thesis, its response to prolonged temperature changes may differ (Menge et al., 2023). It is possible that an increase in P availability induced by higher temperatures may occur more slowly than needed to support the boost in primary productivity. This is due to the known slow pace of the P cycle.

### **4.3 Integrated discussion of the research questions and results**

The second chapter shows that warming increases CO<sub>2</sub> and CH<sub>4</sub> production in the Arctic via microbial activity enhancement and increase in substrate availability through active layer thickening, and that oxic topsoil warming stimulates CO<sub>2</sub> production while anoxic deep soil warming stimulates CH<sub>4</sub> production. The third chapter shows that at least for CO<sub>2</sub>, this production comes with a great demand for P and K, since samples that produced more CO<sub>2</sub> also consumed more P and K, and C and P in the case of N<sub>2</sub>O. Furthermore, there was no indication of mineralization of additional P and K with warming, instead temperature had no effect on the immobilization rates of these nutrients.

The second chapter showed a clear tendency of higher CO<sub>2</sub> and CH<sub>4</sub> production with increasing temperatures, the second one also showed this tendency for CO<sub>2</sub>, but not for N<sub>2</sub>O. The third chapter presented results from an aerobic incubation experiment and thus represent the behavior of N<sub>2</sub>O under these settings. N<sub>2</sub>O is a powerful greenhouse gas with about 300 times the global warming potential of CO<sub>2</sub> (IPCC, 2013). Evidences show that thawing yedoma permafrost, including Kurungnakh island which was studied in the third chapter of this thesis, might be an important source of N<sub>2</sub>O that is often overlooked in accounting global N<sub>2</sub>O emissions (Marushchak et al., 2021). As the Arctic warms and permafrost thaws, N stored in Yedoma will become increasingly accessible, enabling higher N<sub>2</sub>O emissions in the future.

Hypothetical N constraints alleviation could increase primary productivity in Arctic wetlands but could also lead to increased CH<sub>4</sub> emissions (Lara et al., 2019; Lee et al., 2023; Zhu et al., 2012). This would be the case through the provision of additional substrate for methanogenesis by a larger rhizosphere, and the increase in CH<sub>4</sub> transport via plants

---

aerenchyma (Andresen et al., 2017; Joabsson & Christensen, 2001). Thus, while global warming could stimulate vegetation expansion in the Arctic, it could also increase CH<sub>4</sub> emissions that might offset the CO<sub>2</sub> sequestration capacity of these environments. The extension of the growing season caused by climate change could favor enhanced CH<sub>4</sub> production and transport to the atmosphere. This intensification in CH<sub>4</sub> emissions would be in addition to the significant emissions already observed currently year-round. In summary, climate change is leading to an extension of the most CH<sub>4</sub>-producing seasons, namely summer and fall, while shortening and warming the least CH<sub>4</sub>-producing season, winter (Rößger et al., 2022).

Nutrients released through permafrost thaw may follow different paths: a portion may be transported to waterbodies (Schuur & Mack, 2018; Vonk et al., 2015), while another may be taken up by soil microbes. The polygonal tundra is possibly not limited by K (Beermann et al., 2015), however the results of the third chapter show no additional K release from the active layer with warming. Thus, while Arctic greening is anticipated to be a consequence of warming, it is overly optimistic to assume this process has the capacity to mitigate all or most of the release of C from the vast C stocks of Arctic terrestrial ecosystems (Jeong et al., 2018; Miner et al., 2022; Pearson et al., 2013). Let alone the possibility that changes in vegetation might cause an increase in greenhouse gas emissions itself, as has been found in Lagomarsino and Agnelli (2020) that identified the shift in the tree-line of birch forests in the northern Finnish Lapland as the cause behind an increase in CO<sub>2</sub> and N<sub>2</sub>O emissions. In my view the Arctic will likely be an important source of C to the atmosphere. Nonetheless, it should also be considered that the lack of increase in the mineralization of P and K may hinder not just primary productivity but also the production of greenhouse gases, with the potential of constituting negative feedback to global climate. In the third chapter, samples with less P and K, also produced less CO<sub>2</sub> a process that might have been related to the nutritional limitation of decomposition rates (Nowinski et al., 2008).

---

## 5 Conclusions

This thesis addressed two key research gaps in the understanding of the permafrost carbon-climate feedback. The second chapter assessed in situ  $\text{CH}_4$  production and the ratio of  $\text{CO}_2$  to  $\text{CH}_4$  produced during the growing season of Samoylov Island, Lena River Delta, Northeastern Siberia. Understanding the production of not just  $\text{CO}_2$  but also  $\text{CH}_4$  and  $\text{N}_2\text{O}$  in Arctic ecosystems, under the unfolding environmental changes, would clarify the extent to which these ecosystems are and will affect global climate. Additionally, both studies in this thesis present studies from sites in Siberia, which is of vital importance for the full representation of the addressed topics in relation to the whole Arctic region and the global climate. Siberia is vast, and thus, impactful, therefore it is indispensable to concentrate efforts to acquire more data in the region. The third chapter of this thesis explores open questions in relation to soil nutrients in the region, and how those might behave under increased temperatures. It discusses the implications of these changes for future feedback mechanisms, especially the possible negative feedback of future higher primary productivity.

In the second chapter, in situ  $\text{CH}_4$  production rates could be estimated by measuring  $\text{CH}_4$  fluxes from a wet site with considerable plant-mediated  $\text{CH}_4$  transport, and also estimating the maximum range of  $\text{CH}_4$  oxidation that could be affecting the measurements there. The novel approach used in the second chapter enabled the estimation of in situ  $\text{CO}_2:\text{CH}_4$  production ratios in other sites, without the necessity of retrieving soil to the lab and performing ex situ measurements of the potential  $\text{CO}_2$  to  $\text{CH}_4$  production ratios. It had been found that these in situ  $\text{CO}_2:\text{CH}_4$  production ratios are controlled by the active layer depth. Thus, the deeper the active layer gets towards the end of the growing season, the more  $\text{CH}_4$  is produced, and closer to 1 the  $\text{CO}_2:\text{CH}_4$  production ratios approaches. Therefore, the prospects of thickening of the active layer in the future, could promote higher  $\text{CH}_4$  emissions from permafrost ecosystems. The response of the in situ  $\text{CO}_2:\text{CH}_4$  production ratios to temperature was found to be depth dependent. Topsoil warming increased  $\text{CO}_2:\text{CH}_4$  ratios, while deep soil warming decreased  $\text{CO}_2:\text{CH}_4$  ratios. This is related to the more oxic environment at the topsoil, which produces  $\text{CO}_2$ , and more anoxic environment at the deeper soil, which produces

---



CH<sub>4</sub>. In the third chapter, P and K were not additionally mineralized with warming, but were immobilized by soil microorganisms regardless of the temperature. This result shows that P and K concentrations did not increase with short-term warming. Thus, there is a potential for a cap in the increase of the primary productivity of Arctic ecosystems which is forecasted to occur with additional warming and CO<sub>2</sub> fertilization. Moreover, N<sub>2</sub>O measurements were performed in the incubation experiment and the results suggest the occurrence of coupled nitrification-denitrification in the incubated soils, influenced by nitrate, C and P.

The results and discussion presented in this thesis suggest prospects for further research on the permafrost carbon-climate feedback. Research efforts should be kept in the direction of collecting data of in situ greenhouse gases production, especially in underrepresented areas, like the Siberian Arctic, and underrepresented seasons, like the winter. A focus should be given to CH<sub>4</sub> and N<sub>2</sub>O production as well, as these are relevant greenhouse gases for which my understanding of their processes remains limited. Furthermore, the dynamics of soil nutrients and their biogeochemical cycles at present and under the influence of ongoing environmental changes should be better understood. These dynamics have a major impact on the carbon cycling responses of permafrost ecosystems under future climate scenarios. Useful information shall be retrieved from studies focusing on the interplay between different nutrient pools, the competition between the vegetation and soil microorganisms and long-term effects of warming in soil nutrients. The role of P in enabling or constraining negative feedback to the climate such as increased primary productivity in the Arctic, is yet to be investigated, with much to be ascertained about the basic understanding of the P cycle in the Arctic. The results presented in this thesis suggests that the Lena River Delta, and conceivably permafrost ecosystems overall, are gradually becoming an important source of greenhouse gases, thus having more pronounced positive feedback with the global climate. These results suggest that this process occur as a result of increased production of greenhouse gases driven by warming and permafrost thawing, and also as a result of the intensification of soil nutrients limitation to vegetation growth and consequently, C sequestration.

---

## References

- Albano, L. J., Turetsky, M. R., Mack, M. C., & Kane, E. S. (2021). Deep roots of *Carex aquatilis* have greater ammonium uptake capacity than shallow roots in peatlands following permafrost thaw. *Plant and Soil*, 465(1), 261-272. <https://doi.org/10.1007/s11104-021-04978-x>
- AminiTabrizi, R., Wilson, R. M., Fudyma, J. D., Hodgkins, S. B., Heyman, H. M., Rich, V. I., Saleska, S. R., Chanton, J. P., & Tfaily, M. M. (2020). Controls on Soil Organic Matter Degradation and Subsequent Greenhouse Gas Emissions Across a Permafrost Thaw Gradient in Northern Sweden [Original Research]. *Frontiers in Earth Science*, 8. <https://doi.org/10.3389/feart.2020.557961>
- Andersen, S. K., & White, D. M. (2006). Determining soil organic matter quality under anaerobic conditions in arctic and subarctic soils. *Cold Regions Science and Technology*, 44(2), 149-158. <https://doi.org/https://doi.org/10.1016/j.coldregions.2005.11.001>
- Andresen, C. G., Lara, M. J., Tweedie, C. E., & Lougheed, V. L. (2017). Rising plant-mediated methane emissions from arctic wetlands. *Global Change Biology*, 23(3), 1128-1139. <https://doi.org/10.1111/gcb.13469>
- Andresen, C. G., & Lougheed, V. L. (2021). Arctic aquatic graminoid tundra responses to nutrient availability. *Biogeosciences*, 18(8), 2649-2662. <https://doi.org/10.5194/bg-18-2649-2021>
- Baer, K. E. v. (2001). *Materialien zur Kenntniss des unvergänglichen Boden-Eises in Sibirien* [Berichte und Arbeiten aus der Universitätsbibliothek und dem Universitätsarchiv Giessen; 51 / 2001]. Universitätsbibliothek Giessen. <http://dx.doi.org/10.22029/jlupub-2959>
- Bai, E., Li, S., Xu, W., Li, W., Dai, W., & Jiang, P. (2013). A meta-analysis of experimental warming effects on terrestrial nitrogen pools and dynamics. *New Phytologist*, 199(2), 441-451. <https://doi.org/https://doi.org/10.1111/nph.12252>
- Bannon, C., Rapp, I., & Bertrand, E. M. (2022). Community Interaction Co-limitation: Nutrient Limitation in a Marine Microbial Community Context [Hypothesis and Theory]. *Frontiers in Microbiology*, 13. <https://doi.org/10.3389/fmicb.2022.846890>
- Bastviken, D., Cole, J. J., Pace, M. L., & Van de-Bogert, M. C. (2008). Fates of methane from different lake habitats: Connecting whole-lake budgets and CH<sub>4</sub> emissions. *Journal of Geophysical Research: Biogeosciences*, 113(2), 1-13. <https://doi.org/10.1029/2007JG000608>
- Beckebanze, L., Rehder, Z., Holl, D., Wille, C., Mirbach, C., & Kutzbach, L. (2022). Ignoring carbon emissions from thermokarst ponds results in overestimation of tundra net carbon uptake. *Biogeosciences*, 19(4), 1225-1244. <https://doi.org/10.5194/bg-19-1225-2022>
- Beckebanze, L., Runkle, B. R. K., Walz, J., Wille, C., Holl, D., Helbig, M., Boike, J., Sachs, T., & Kutzbach, L. (2022). Lateral carbon export has low impact on the net ecosystem carbon balance of a polygonal tundra catchment. *Biogeosciences*, 19(16), 3863-3876. <https://doi.org/10.5194/bg-19-3863-2022>
- Beer, C., Runge, A., Grosse, G., Hugelius, G., & Knoblauch, C. (2023). Carbon dioxide release from retrogressive thaw slumps in Siberia. *Environmental Research Letters*, 18(10), 104053. <https://doi.org/10.1088/1748-9326/acfdbb>
- Beermann, F., Langer, M., Wetterich, S., Strauss, J., Boike, J., Fiencke, C., Schirrmeister, L., Pfeiffer, E.-M., & Kutzbach, L. (2017). Permafrost Thaw and Liberation of Inorganic Nitrogen in
-

- Eastern Siberia. *Permafrost and Periglacial Processes*, 28(4), 605-618. <https://doi.org/https://doi.org/10.1002/ppp.1958>
- Beermann, F., Teltewskoi, A., Fiencke, C., Pfeiffer, E. M., & Kutzbach, L. (2015). Stoichiometric analysis of nutrient availability (N, P, K) within soils of polygonal tundra. *Biogeochemistry*, 122(2-3), 211-227. <https://doi.org/10.1007/s10533-014-0037-4>
- Berestovskaya, Y. Y., Rusanov, I. I., Vasil'eva, L. V., & Pimenov, N. V. (2005). The processes of methane production and oxidation in the soils of the Russian Arctic tundra. *Microbiology*, 74(2), 221-229. <https://doi.org/10.1007/s11021-005-0055-2>
- Bing, H., Wu, Y., Zhou, J., Sun, H., Luo, J., Wang, J., & Yu, D. (2016). Stoichiometric variation of carbon, nitrogen, and phosphorus in soils and its implication for nutrient limitation in alpine ecosystem of Eastern Tibetan Plateau. *Journal of Soils and Sediments*, 16(2), 405-416. <https://doi.org/10.1007/s11368-015-1200-9>
- Biskaborn, B. K., Smith, S. L., Noetzli, J., Matthes, H., Vieira, G., Streletskiy, D. A., Schoeneich, P., Romanovsky, V. E., Lewkowicz, A. G., Abramov, A., Allard, M., Boike, J., Cable, W. L., Christiansen, H. H., Delaloye, R., Diekmann, B., Drozdov, D., Etzelmüller, B., Grosse, G., . . . Lantuit, H. (2019). Permafrost is warming at a global scale. *Nature Communications*, 10(1), 264-264. <https://doi.org/10.1038/s41467-018-08240-4>
- Bjorkegren, A. B., Grimmond, C. S. B., Kotthaus, S., & Malamud, B. D. (2015). CO<sub>2</sub> emission estimation in the urban environment: Measurement of the CO<sub>2</sub> storage term. *Atmospheric Environment*, 122, 775-790. <https://doi.org/https://doi.org/10.1016/j.atmosenv.2015.10.012>
- Bodegom, P. M. v., & Stams, A. J. M. (1999). Effects of alternative electron acceptors and temperature on methanogenesis in rice paddy soils. *Chemosphere*, 39(2), 167-182. [https://doi.org/https://doi.org/10.1016/S0045-6535\(99\)00101-0](https://doi.org/https://doi.org/10.1016/S0045-6535(99)00101-0)
- Boike, J., Grüber, M., Langer, M., Piel, K., & Scheritz, M. (2012). *Orthomosaic of Samoylov Island, Lena Delta, Siberia* (PANGAEA). <https://doi.org/10.1594/PANGAEA.786073>
- Boike, J., Kattenstroth, B., Abramova, K., Bornemann, N., Chetverova, A., Fedorova, I., Fröb, K., Grigoriev, M., Grüber, M., Kutzbach, L., Langer, M., Minke, M., Muster, S., Piel, K., Pfeiffer, E. M., Stoof, G., Westermann, S., Wischniewski, K., Wille, C., & Hubberten, H. W. (2013). Baseline characteristics of climate, permafrost and land cover from a new permafrost observatory in the Lena River Delta, Siberia (1998-2011). *Biogeosciences*, 10(3), 2105-2128. <https://doi.org/10.5194/bg-10-2105-2013>
- Boike, J., Nitzbon, J., Anders, K., Grigoriev, M., Bolshiyarov, D., Langer, M., Lange, S., Bornemann, N., Morgenstern, A., Schreiber, P., Wille, C., Chadburn, S., Gouttevin, I., Burke, E., & Kutzbach, L. (2019). A 16-year record (2002--2017) of permafrost, active-layer, and meteorological conditions at the Samoylov Island Arctic permafrost research site, Lena River delta, northern Siberia: an opportunity to validate remote-sensing data and land surface, snow, and. *Earth System Science Data*, 11(1), 261-299. <https://doi.org/10.5194/essd-11-261-2019>
- Boike, J., Veh, G., Viitanen, L.-K., Bornemann, N., Stoof, G. n., & Muster, S. (2015). *Visible and near-infrared orthomosaic of Samoylov Island, Siberia, summer 2015 (5.3 GB)* (PANGAEA). <https://doi.org/10.1594/PANGAEA.845724>
- Boike, J., Wille, C., & Abnizova, A. (2008). Climatology and summer energy and water balance of polygonal tundra in the Lena River Delta, Siberia. *Journal of Geophysical Research: Biogeosciences*, 113(G3). <https://doi.org/10.1029/2007jg000540>
-

- Bond-Lamberty, B., Bronson, D., Bladyka, E., & Gower, S. T. (2011). A comparison of trenched plot techniques for partitioning soil respiration. *Soil Biology and Biochemistry*, 43(10), 2108-2114. <https://doi.org/https://doi.org/10.1016/j.soilbio.2011.06.011>
- Bracho, R., Natali, S., Pegoraro, E., Crummer, K., Schädel, C., Celis, G., Hale, L., Wu, L., Yin, H., Tiedje, J., Konstantinidis, K., Luo, Y., Zhou, J., & Schuur, E. (2016). Temperature sensitivity of organic matter decomposition of permafrost-region soils during laboratory incubations. *Soil Biology and Biochemistry*, 97. <https://doi.org/10.1016/j.soilbio.2016.02.008>
- Brenner, J., Porter, W., Phillips, J. R., Childs, J., Yang, X., & Mayes, M. A. (2019). Phosphorus sorption on tropical soils with relevance to Earth system model needs. *Soil Research*, 57(1), 17-27. <https://doi.org/https://doi.org/10.1071/SR18197>
- Brovkin, V., & Goll, D. (2015). Land unlikely to become large carbon source. *Nature Geoscience*, 8(12), 893-893. <https://doi.org/10.1038/ngeo2598>
- Cai, Y., Zheng, Y., Bodelier, P. L. E., Conrad, R., & Jia, Z. (2016). Conventional methanotrophs are responsible for atmospheric methane oxidation in paddy soils. *Nature Communications*, 7(1), 11728. <https://doi.org/10.1038/ncomms11728>
- Cannone, N., Augusti, A., Malfasi, F., Pallozzi, E., Calfapietra, C., & Brugnoli, E. (2016). The interaction of biotic and abiotic factors at multiple spatial scales affects the variability of CO<sub>2</sub> fluxes in polar environments. *Polar Biology*, 39(9), 1581-1596. <https://doi.org/10.1007/s00300-015-1883-9>
- Chang, K.-Y., Riley, W. J., Brodie, E. L., McCalley, C. K., Crill, P. M., & Grant, R. F. (2019). Methane Production Pathway Regulated Proximally by Substrate Availability and Distally by Temperature in a High-Latitude Mire Complex. *Journal of Geophysical Research: Biogeosciences*, 124(10), 3057-3074. <https://doi.org/https://doi.org/10.1029/2019JG005355>
- Chapin, F. S., Barsdate, R. J., & Barèl, D. (1978). Phosphorus Cycling in Alaskan Coastal Tundra: A Hypothesis for the Regulation of Nutrient Cycling. *Oikos*, 31(2), 189-199.
- Chapin Iii, F. S., Shaver, G. R., Giblin, A. E., Nadelhoffer, K. J., & Laundre, J. A. (1995). Responses of Arctic Tundra to Experimental and Observed Changes in Climate. *Ecology*, 76(3), 694-711.
- Chen, B., Fang, J., Piao, S., Ciais, P., Black, T. A., Wang, F., Niu, S., Zeng, Z., & Luo, Y. (2023). A meta-analysis highlights globally widespread potassium limitation in terrestrial ecosystems. *New Phytol.* <https://doi.org/10.1111/nph.19294>
- Chen, W., Wolf, B., Zheng, X., Yao, Z., Butterbach-Bahl, K., Brüggemann, N., Liu, C., Han, S., & Han, X. (2011). Annual methane uptake by temperate semiarid steppes as regulated by stocking rates, aboveground plant biomass and topsoil air permeability. *Global Change Biology*, 17(9), 2803-2816. <https://doi.org/https://doi.org/10.1111/j.1365-2486.2011.02444.x>
- Chen, Y., Wu, N., Liu, C., Mi, T., Li, J., He, X., Li, S., Sun, Z., & Zhen, Y. (2022). Methanogenesis pathways of methanogens and their responses to substrates and temperature in sediments from the South Yellow Sea. *Science of The Total Environment*, 815, 152645. <https://doi.org/https://doi.org/10.1016/j.scitotenv.2021.152645>
- Christensen, T. R. (2024). Wetland emissions on the rise. *Nature Climate Change*. <https://doi.org/10.1038/s41558-024-01938-y>
- Christiansen, J. R., Korhonen, J. F. J., Juszczak, R., Giebels, M., & Pihlatie, M. (2011). Assessing the effects of chamber placement, manual sampling and headspace mixing on CH<sub>4</sub> fluxes in
-

- a laboratory experiment. *Plant and Soil*, 343(1), 171-185. <https://doi.org/10.1007/s11104-010-0701-y>
- Christiansen, J. R., Romero, A. J. B., Jørgensen, N. O. G., Glaring, M. A., Jørgensen, C. J., Berg, L. K., & Elberling, B. (2015). Methane fluxes and the functional groups of methanotrophs and methanogens in a young Arctic landscape on Disko Island, West Greenland. *Biogeochemistry*, 122(1), 15-33. <https://doi.org/10.1007/s10533-014-0026-7>
- Cleveland, C. C., Houlton, B. Z., Smith, W. K., Marklein, A. R., Reed, S. C., Parton, W., Del Grosso, S. J., & Running, S. W. (2013). Patterns of new versus recycled primary production in the terrestrial biosphere. *Proceedings of the National Academy of Sciences*, 110(31), 12733-12737. <https://doi.org/doi:10.1073/pnas.1302768110>
- Clymo, R. S., & Bryant, C. L. (2008). Diffusion and mass flow of dissolved carbon dioxide, methane, and dissolved organic carbon in a 7-m deep raised peat bog. *Geochimica et Cosmochimica Acta*, 72(8), 2048-2066. <https://doi.org/https://doi.org/10.1016/j.gca.2008.01.032>
- Clymo, R. S., Pearce, D. M. E., & Conrad, R. (1995). Methane and Carbon Dioxide Production in, Transport through, and Efflux from a Peatland [and Discussion]. *Philosophical Transactions: Physical Sciences and Engineering*, 351(1696), 249-259. <http://www.jstor.org/stable/54414>
- Cooper, M. D. A., Estop-Aragónés, C., Fisher, J. P., Thierry, A., Garnett, M. H., Charman, D. J., Murton, J. B., Phoenix, G. K., Treharne, R., Kokelj, S. V., Wolfe, S. A., Lewkowicz, A. G., Williams, M., & Hartley, I. P. (2017). Limited contribution of permafrost carbon to methane release from thawing peatlands. *Nature Climate Change*, 7(7), 507-511. <https://doi.org/10.1038/nclimate3328>
- de Vrese, P., Beckebanze, L., Galera, L. d. A., Holl, D., Kleinen, T., Kutzbach, L., Rehder, Z., & Brovkin, V. (2023). Sensitivity of Arctic CH<sub>4</sub> emissions to landscape wetness diminished by atmospheric feedbacks. *Nature Climate Change*, 13(8), 832-839. <https://doi.org/10.1038/s41558-023-01715-3>
- Delwiche, K. B., Knox, S. H., Malhotra, A., Fluet-Chouinard, E., McNicol, G., Feron, S., Ouyang, Z., Papale, D., Trotta, C., Canfora, E., Cheah, Y. W., Christianson, D., Alberto, M. C. R., Alekseychik, P., Aurela, M., Baldocchi, D., Bansal, S., Billesbach, D. P., Bohrer, G., . . . Jackson, R. B. (2021). FLUXNET-CH<sub>4</sub>: a global, multi-ecosystem dataset and analysis of methane seasonality from freshwater wetlands. *Earth System Science Data*, 13(7), 3607-3689. <https://doi.org/10.5194/essd-13-3607-2021>
- Dengel, S., Billesbach, D., & Torn, M. S. (2021). Influence of Tundra Polygon Type and Climate Variability on CO<sub>2</sub> and CH<sub>4</sub> Fluxes Near Utqiagvik, Alaska. *Journal of Geophysical Research: Biogeosciences*, 126(12), e2021JG006262. <https://doi.org/https://doi.org/10.1029/2021JG006262>
- Detting, M. D., Yavitt, J. B., & Zinder, S. H. (2006). Control of organic carbon mineralization by alternative electron acceptors in four peatlands, Central New York State, USA. *Wetlands*, 26(4), 917-927. [https://doi.org/10.1672/0277-5212\(2006\)26\[917:COOCMB\]2.0.CO;2](https://doi.org/10.1672/0277-5212(2006)26[917:COOCMB]2.0.CO;2)
- Du, E., Terrer, C., McNulty, S. G., & Jackson, R. B. (2024). Chapter 4 - Nutrient limitation in global forests: current status and future trends. In S. G. McNulty (Ed.), *Future Forests* (pp. 65-74). Elsevier. <https://doi.org/https://doi.org/10.1016/B978-0-323-90430-8.00014-9>
-

- Du, E., Terrer, C., Pellegrini, A. F. A., Ahlström, A., van Lissa, C. J., Zhao, X., Xia, N., Wu, X., & Jackson, R. B. (2020). Global patterns of terrestrial nitrogen and phosphorus limitation. *Nature Geoscience*, 13(3), 221-226. <https://doi.org/10.1038/s41561-019-0530-4>
- Eckhardt, T. (2017). *Partitioning carbon fluxes in a permafrost landscape* [Dissertation, Universität Hamburg]. Universität Hamburg.
- Eckhardt, T., Knoblauch, C., Kutzbach, L., Holl, D., Simpson, G., Abakumov, E., & Pfeiffer, E.-M. (2019a). Carbon dioxide fluxes and soil, vegetation, meteorological data from a polygonal tundra in northeastern Siberia. In *Supplement to: Eckhardt, T et al. (2019): Partitioning net ecosystem exchange of CO<sub>2</sub> on the pedon scale in the Lena River Delta, Siberia. Biogeosciences*, 16(7), 1543-1562, <https://doi.org/10.5194/bg-16-1543-2019>: PANGAEA.
- Eckhardt, T., Knoblauch, C., Kutzbach, L., Holl, D., Simpson, G., Abakumov, E., & Pfeiffer, E. M. (2019b). Partitioning net ecosystem exchange of CO<sub>2</sub> on the pedon scale in the Lena River Delta, Siberia. *Biogeosciences*, 16(7), 1543-1562. <https://doi.org/10.5194/bg-16-1543-2019>
- Eckhardt, T., & Kutzbach, L. (2016). MATLAB code to calculate gas fluxes from chamber-based methods. In: PANGAEA.
- Ellsworth, D. S., Anderson, I. C., Crous, K. Y., Cooke, J., Drake, J. E., Gherlenda, A. N., Gimeno, T. E., Macdonald, C. A., Medlyn, B. E., Powell, J. R., Tjoelker, M. G., & Reich, P. B. (2017). Elevated CO<sub>2</sub> does not increase eucalypt forest productivity on a low-phosphorus soil. *Nature Climate Change*, 7(4), 279-282. <https://doi.org/10.1038/nclimate3235>
- Elmendorf, S. C., Henry, G. H. R., Hollister, R. D., Björk, R. G., Boulanger-Lapointe, N., Cooper, E. J., Cornelissen, J. H. C., Day, T. A., Dorrepaal, E., Elumeeva, T. G., Gill, M., Gould, W. A., Harte, J., Hik, D. S., Hofgaard, A., Johnson, D. R., Johnstone, J. F., Jónsdóttir, I. S., Jorgenson, J. C., . . . Wipf, S. (2012). Plot-scale evidence of tundra vegetation change and links to recent summer warming. *Nature Climate Change*, 2(6), 453-457. <https://doi.org/10.1038/nclimate1465>
- Euskirchen, E. S., Bret-Harte, M. S., Shaver, G. R., Edgar, C. W., & Romanovsky, V. E. (2017). Long-term release of carbon dioxide from arctic tundra ecosystems in Alaska. *Ecosystems*, 20(5), 960-974. <https://doi.org/10.1007/s10021-016-0085-9>
- Euskirchen, E. S., McGuire, A. D., Kicklighter, D. W., Zhuang, Q., Clein, J. S., Dargaville, R. J., Dye, D. G., Kimball, J. S., McDonald, K. C., Melillo, J. M., Romanovsky, V. E., & Smith, N. V. (2006). Importance of recent shifts in soil thermal dynamics on growing season length, productivity, and carbon sequestration in terrestrial high-latitude ecosystems. *Global Change Biology*, 12(4), 731-750. <https://doi.org/https://doi.org/10.1111/j.1365-2486.2006.01113.x>
- Feliks, A., & Reimnitz, E. (2000). An Overview of the Lena River Delta Setting: Geology, Tectonics, Geomorphology, and Hydrology. *Journal of Coastal Research*, 16(4), 1083-1093. <http://www.jstor.org/stable/4300125>
- Ferréa, C., Zenone, T., Comolli, R., & Seufert, G. (2012). Estimating heterotrophic and autotrophic soil respiration in a semi-natural forest of Lombardy, Italy. *Pedobiologia*, 55(6), 285-294. <https://doi.org/https://doi.org/10.1016/j.pedobi.2012.05.001>
- French, H. M. (2018). *The Periglacial Environment* (4th ed.). Wiley-Blackwell.
-

- Frenzel, P., & Rudolph, J. (1998). Methane emission from a wetland plant: the role of CH<sub>4</sub> oxidation in *Eriophorum*. *Plant and Soil*, 202(1), 27-32. <http://www.jstor.org/stable/42948339>
- Frey, K. E., McClelland, J. W., Holmes, R. M., & Smith, L. C. (2007). Impacts of climate warming and permafrost thaw on the riverine transport of nitrogen and phosphorus to the Kara Sea. *Journal of Geophysical Research: Biogeosciences*, 112(G4). <https://doi.org/https://doi.org/10.1029/2006JG000369>
- Galera, L. d. A., Eckhardt, T., Beer, C., Pfeiffer, E.-M., & Knoblauch, C. (2023). Ratio of In Situ CO<sub>2</sub> to CH<sub>4</sub> Production and Its Environmental Controls in Polygonal Tundra Soils of Samoylov Island, Northeastern Siberia. *Journal of Geophysical Research: Biogeosciences*, 128(4), e2022JG006956. <https://doi.org/https://doi.org/10.1029/2022JG006956>
- Gana, C., Nouvellon, Y., Marron, N., Stape, J. L., & Epron, D. (2018). Sampling and interpolation strategies derived from the analysis of continuous soil CO<sub>2</sub> flux. *Journal of Plant Nutrition and Soil Science*, 181(1), 12-20. <https://doi.org/https://doi.org/10.1002/jpln.201600133>
- Gao, H., Chen, X., Wei, J., Zhang, Y., Zhang, L., Chang, J., & Thompson, M. L. (2016). Decomposition Dynamics and Changes in Chemical Composition of Wheat Straw Residue under Anaerobic and Aerobic Conditions. *PLoS One*, 11(7), e0158172. <https://doi.org/10.1371/journal.pone.0158172>
- Ghiri, M. N., Abtahi, A., Owliaie, H., Hashemi, S. S., & Koohkan, H. (2011). Factors Affecting Potassium Pools Distribution in Calcareous Soils of Southern Iran. *Arid Land Research and Management*, 25(4), 313-327. <https://doi.org/10.1080/15324982.2011.602177>
- Giblin, A. E., Nadelhoffer, K. J., Shaver, G. R., Laundre, J. A., & McKerrow, A. J. (1991). Biogeochemical Diversity Along a Riverside Toposequence in Arctic Alaska. *Ecological Monographs*, 61(4), 415-435. <https://doi.org/https://doi.org/10.2307/2937049>
- Giesler, R., Esberg, C., Lagerström, A., & Graae, B. J. (2012). Phosphorus availability and microbial respiration across different tundra vegetation types. *Biogeochemistry*, 108(1-3), 429-445. <https://doi.org/10.1007/s10533-011-9609-8>
- Girkin, N. T., Turner, B. L., Ostle, N., Craigon, J., & Sjögersten, S. (2018). Root exudate analogues accelerate CO<sub>2</sub> and CH<sub>4</sub> production in tropical peat. *Soil Biology and Biochemistry*, 117, 48-55. <https://doi.org/https://doi.org/10.1016/j.soilbio.2017.11.008>
- Goll, D. S., Brovkin, V., Parida, B. R., Reick, C. H., Kattge, J., Reich, P. B., van Bodegom, P. M., & Niinemets, Ü. (2012). Nutrient limitation reduces land carbon uptake in simulations with a model of combined carbon, nitrogen and phosphorus cycling. *Biogeosciences*, 9(9), 3547-3569. <https://doi.org/10.5194/bg-9-3547-2012>
- Goll, D. S., Moosdorf, N., Hartmann, J., & Brovkin, V. (2014). Climate-driven changes in chemical weathering and associated phosphorus release since 1850: Implications for the land carbon balance. *Geophysical Research Letters*, 41(10), 3553-3558. <https://doi.org/https://doi.org/10.1002/2014GL059471>
- Goodrich, J. P., Oechel, W. C., Gioli, B., Moreaux, V., Murphy, P. C., Burba, G., & Zona, D. (2016). Impact of different eddy covariance sensors, site set-up, and maintenance on the annual balance of CO<sub>2</sub> and CH<sub>4</sub> in the harsh Arctic environment. *Agricultural and Forest Meteorology*, 228-229, 239-251. <https://doi.org/https://doi.org/10.1016/j.agrformet.2016.07.008>
-

- Green, S. M., & Baird, A. J. (2012). A mesocosm study of the role of the sedge *Eriophorum angustifolium* in the efflux of methane-including that due to episodic ebullition-from peatlands. *Plant and Soil*, 351(1-2), 207-218. <https://doi.org/10.1007/s11104-011-0945-1>
- Gruber, S. (2012). Derivation and analysis of a high-resolution estimate of global permafrost zonation. *The Cryosphere*, 6(1), 221-233. <https://doi.org/10.5194/tc-6-221-2012>
- Haney, R. L., Brinton, W. H., & Evans, E. (2008). Estimating Soil Carbon, Nitrogen, and Phosphorus Mineralization from Short-Term Carbon Dioxide Respiration. *Communications in Soil Science and Plant Analysis*, 39(17-18), 2706-2720. <https://doi.org/10.1080/00103620802358862>
- Hansen, H. F. E., & Elberling, B. (2023). Spatial Distribution of Bioavailable Inorganic Nitrogen From Thawing Permafrost. *Global Biogeochemical Cycles*, 37(2), e2022GB007589. <https://doi.org/https://doi.org/10.1029/2022GB007589>
- Harris, S. A., French, H. M., Heginbottom, J. A., Johnston, G. H., Ladanyi, B., Sego, D. C., & van Everdingen, R. O. (1988). *Glossary of permafrost and related ground-ice terms* (Technical Memorandum (National Research Council of Canada. Associate Committee on Geotechnical Research); no. ACGR-TM-142, Issue.
- Herbst, T., Fuchs, M., Liebner, S., & Treat, C. C. (2024). Carbon Stocks and Potential Greenhouse Gas Production of Permafrost-Affected Active Floodplains in the Lena River Delta. *Journal of Geophysical Research: Biogeosciences*, 129(1), e2023JG007590. <https://doi.org/https://doi.org/10.1029/2023JG007590>
- Herndon, E. M., Mann, B. F., Roy Chowdhury, T., Yang, Z., Wulschleger, S. D., Graham, D., Liang, L., & Gu, B. (2015). Pathways of anaerobic organic matter decomposition in tundra soils from Barrow, Alaska. *Journal of Geophysical Research: Biogeosciences*, 120(11), 2345-2359. <https://doi.org/https://doi.org/10.1002/2015JG003147>
- Heslop, J. K., Winkel, M., Walter Anthony, K. M., Spencer, R. G. M., Podgorski, D. C., Zito, P., Kholodov, A., Zhang, M., & Liebner, S. (2019). Increasing Organic Carbon Biolability With Depth in Yedoma Permafrost: Ramifications for Future Climate Change. *Journal of Geophysical Research: Biogeosciences*, 124(7), 2021-2038. <https://doi.org/https://doi.org/10.1029/2018JG004712>
- Hobbie, S. E., Nadelhoffer, K. J., & Högberg, P. (2002). A synthesis: The role of nutrients as constraints on carbon balances in boreal and arctic regions. *Plant and Soil*, 242(1), 163-170. <https://doi.org/10.1023/A:1019670731128>
- Holl, D., Wille, C., Sachs, T., Schreiber, P., Runkle, B. R. K., Beckebanze, L., Langer, M., Boike, J., Pfeiffer, E. M., Fedorova, I., Bolshianov, D. Y., Grigoriev, M. N., & Kutzbach, L. (2019). A long-term (2002 to 2017) record of closed-path and open-path eddy covariance CO<sub>2</sub> net ecosystem exchange fluxes from the Siberian Arctic. *Earth Syst. Sci. Data*, 11(1), 221-240. <https://doi.org/10.5194/essd-11-221-2019>
- Ibrahim, M. M., Li, Z., Ye, H., Chang, Z., Lin, H., Luo, X., & Hou, E. (2023). Carbon dioxide flux and microbial responses under multiple-nutrient manipulations in a subtropical forest soil. *Applied Soil Ecology*, 192, 105074. <https://doi.org/https://doi.org/10.1016/j.apsoil.2023.105074>
- IPCC. (2013). *Climate Change 2013: The Physical Science Basis. Contribution of Working Group I to the Fifth Assessment Report of the Intergovernmental Panel on Climate Change*. C. U. Press.
-



- IPCC. (2021). *Climate Change 2021: The Physical Science Basis. Contribution of Working Group I to the Sixth Assessment Report of the Intergovernmental Panel on Climate Change*. C. U. Press.
- IPCC. (2022). *Climate Change 2022: Impacts, Adaptation and Vulnerability. Contribution of Working Group II to the Sixth Assessment Report of the Intergovernmental Panel on Climate Change*. C. U. Press.
- Jeong, S.-J., Bloom, A. A., Schimel, D., Sweeney, C., Parazoo, N. C., Medvigy, D., Schaepman-Strub, G., Zheng, C., Schwalm, C. R., Huntzinger, D. N., Michalak, A. M., & Miller, C. E. (2018). Accelerating rates of Arctic carbon cycling revealed by long-term atmospheric CO<sub>2</sub> measurements. *Science Advances*, 4(7), eaa01167. <https://doi.org/doi:10.1126/sciadv.aao1167>
- Jin, X.-Y., Jin, H.-J., Iwahana, G., Marchenko, S. S., Luo, D.-L., Li, X.-Y., & Liang, S.-H. (2021). Impacts of climate-induced permafrost degradation on vegetation: A review. *Advances in Climate Change Research*, 12(1), 29-47. <https://doi.org/https://doi.org/10.1016/j.accre.2020.07.002>
- Joabsson, A., & Christensen, T. R. (2001). Methane emissions from wetlands and their relationship with vascular plants: an Arctic example. *Global Change Biology*, 7(8), 919-932. <https://doi.org/https://doi.org/10.1046/j.1354-1013.2001.00044.x>
- Jonasson, S., Havström, M., Jensen, M., & Callaghan, T. V. (1993). In situ mineralization of nitrogen and phosphorus of arctic soils after perturbations simulating climate change. *Oecologia*, 95(2), 179-186. <https://doi.org/10.1007/BF00323488>
- Jonasson, S., Michelsen, A., Schmidt, I. K., Nielsen, E. V., & Callaghan, T. V. (1996). Microbial biomass C, N and P in two arctic soils and responses to addition of NPK fertilizer and sugar: implications for plant nutrient uptake. *Oecologia*, 106(4), 507-515. <https://doi.org/10.1007/BF00329709>
- Jørgensen, C. J., Johansen, K. M. L., Westergaard-Nielsen, A., Elberling, B., Juncher Jørgensen, C., Lund Johansen, K. M., Westergaard-Nielsen, A., & Elberling, B. (2015). Net regional methane sink in High Arctic soils of northeast Greenland. *Nature Geoscience*, 8(1), 20-23. <https://doi.org/10.1038/ngeo2305>
- Juncher Jørgensen, C., Lund Johansen, K. M., Westergaard-Nielsen, A., & Elberling, B. (2015). Net regional methane sink in High Arctic soils of northeast Greenland. *Nature Geoscience*, 8(1), 20-23. <https://doi.org/10.1038/ngeo2305>
- Juutinen, S., Aurela, M., Tuovinen, J. P., Ivakhov, V., Linkosalmi, M., Räsänen, A., Virtanen, T., Mikola, J., Nyman, J., Vähä, E., Loskutova, M., Makshtas, A., & Laurila, T. (2022). Variation in CO<sub>2</sub> and CH<sub>4</sub> fluxes among land cover types in heterogeneous Arctic tundra in northeastern Siberia. *Biogeosciences*, 19(13), 3151-3167. <https://doi.org/10.5194/bg-19-3151-2022>
- Kandeler, E., & Gerber, H. (1988). Short-term assay of soil urease activity using colorimetric determination of ammonium. *Biology and Fertility of Soils*, 6(1), 68-72. <https://doi.org/10.1007/BF00257924>
- Kattge, J. D., S. Lavorel, S. Prentice, I. C. Leadley, P. Bönišch, G. Garnier, E. Westoby, M. Reich, P. B. Wright, I. J. Cornelissen, J. H. C. Violle, C. Harrison, S. P. Van Bodegom, P. M. Reichstein, M. Enquist, B. J. Soudzilovskaia, N. A. Ackerly, D. D. Anand, M. Atkin, O. Bahn, M. Baker, T. R. Baldocchi, D. Bekker, R. Blanco, C. C. Blonder, B. Bond, W. J. Bradstock, R. Bunker, D. E. Casanoves, F. Cavender-Bares, J. Chambers, J. Q. Chapin Iii,
-

- F. S. Chave, J. Coomes, D. Cornwell, W. K. Craine, J. M. Dobrin, B. H. Duarte, L. Durka, W. Elser, J. Esser, G. Estiarte, M. Fagan, W. F. Fang, J. Fernández-Méndez, F. Fidelis, A. Finegan, B. Flores, O. Ford, H. Frank, D. Freschet, G. T. Fyllas, N. M. Gallagher, R. V. Green, W. A. Gutierrez, A. G. Hickler, T. Higgins, S. I. Hodgson, J. G. Jalili, A. Jansen, S. Joly, C. A. Kerkhoff, A. J. Kirkup, D. Kitajima, K. Kleyer, M. Klotz, S. Knops, J. M. H. Kramer, K. Kühn, I. Kurokawa, H. Laughlin, D. Lee, T. D. Leishman, M. Lens, F. Lenz, T. Lewis, S. L. Lloyd, J. Llusà, J. Louault, F. Ma, S. Mahecha, M. D. Manning, P. Massad, T. Medlyn, B. E. Messier, J. Moles, A. T. Müller, S. C. Nadrowski, K. Naeem, S. Niinemets, Ü. Nöllert, S. Nüske, A. Ogaya, R. Oleksyn, J. Onipchenko, V. G. Onoda, Y. Ordoñez, J. Overbeck, G. Ozinga, W. A. Patiño, S. Paula, S. Pausas, J. G. Peñuelas, J. Phillips, O. L. Pillar, V. Poorter, H. Poorter, L. Poschlod, P. Prinzing, A. Proulx, R. Rammig, A. Reinsch, S. Reu, B. Sack, L. Salgado-Negret, B. Sardans, J. Shiodesera, S. Shipley, B. Siefert, A. Sosinski, E. Soussana, J.-F. Swaine, E. Swenson, N. Thompson, K. Thornton, P. Waldram, M. Weiher, E. White, M. White, S. Wright, S. J. Yguel, B. Zaehle, S. Zanne, A. E. Wirth, C. (2011). TRY – a global database of plant traits. *Global Change Biology*, 17(9), 2905-2935. <https://doi.org/https://doi.org/10.1111/j.1365-2486.2011.02451.x>
- Kelly, C. A., & Chynoweth, D. P. (1981). The contributions of temperature and of the input of organic matter in controlling rates of sediment methanogenesis. *Limnology and Oceanography*, 26(5), 891-897. <https://doi.org/https://doi.org/10.4319/lo.1981.26.5.0891>
- Khokhar, N. H., & Park, J.-W. (2017). A simplified sampling procedure for the estimation of methane emission in rice fields. *Environmental Monitoring and Assessment*, 189(9), 468. <https://doi.org/10.1007/s10661-017-6184-z>
- Kim, Y. (2015). Effect of thaw depth on fluxes of CO<sub>2</sub> and CH<sub>4</sub> in manipulated Arctic coastal tundra of Barrow, Alaska. *Science of The Total Environment*, 505, 385-389. <https://doi.org/https://doi.org/10.1016/j.scitotenv.2014.09.046>
- Kleber, G. E., Hodson, A. J., Magerl, L., Mannerfelt, E. S., Bradbury, H. J., Zhu, Y., Trimmer, M., & Turchyn, A. V. (2023). Groundwater springs formed during glacial retreat are a large source of methane in the high Arctic. *Nature Geoscience*, 16(7), 597-604. <https://doi.org/10.1038/s41561-023-01210-6>
- Kleinen, T., Gromov, S., Steil, B., & Brovkin, V. (2021). Atmospheric methane underestimated in future climate projections. *Environmental Research Letters*, 16(9). <https://doi.org/10.1088/1748-9326/ac1814>
- Knoblauch, C., Beer, C., Liebner, S., Grigoriev, M. N., & Pfeiffer, E. M. (2018). Methane production as key to the greenhouse gas budget of thawing permafrost. *Nature Climate Change*, 8(April), 1-4. <https://doi.org/10.1038/s41558-018-0095-z>
- Knoblauch, C., Beer, C., Schuett, A., Sauerland, L., Liebner, S., Steinhof, A., Rethemeyer, J., Grigoriev, M. N., Faguet, A., & Pfeiffer, E. M. (2021). Carbon Dioxide and Methane Release Following Abrupt Thaw of Pleistocene Permafrost Deposits in Arctic Siberia. *Journal of Geophysical Research: Biogeosciences*, 126(11). <https://doi.org/10.1029/2021jg006543>
- Knoblauch, C., Beer, C., Sosnin, A., Wagner, D., & Pfeiffer, E.-M. (2013). Predicting long-term carbon mineralization and trace gas production from thawing permafrost of Northeast Siberia. *Global Change Biology*, 19(4), 1160-1172. <https://doi.org/https://doi.org/10.1111/gcb.12116>
-

- Knoblauch, C., Spott, O., Evgrafova, S., Kutzbach, L., & Pfeiffer, E. M. (2015). Regulation of methane production, oxidation, and emission by vascular plants and bryophytes in ponds of the northeast Siberian polygonal tundra. *Journal of Geophysical Research: Biogeosciences*, 120(12), 2525-2541. <https://doi.org/10.1002/2015JG003053>
- Koller, E. K., & Phoenix, G. K. (2017). Seasonal dynamics of soil and plant nutrients at three environmentally contrasting sites along a sub-Arctic catchment sequence. *Polar Biology*, 40(9), 1821-1834. <https://doi.org/10.1007/s00300-017-2105-4>
- Kolton, M., Marks, A., Wilson, R. M., Chanton, J. P., & Kostka, J. E. (2019). Impact of warming on greenhouse gas production and microbial diversity in anoxic peat from a sphagnum-dominated bog (Grand Rapids, Minnesota, United States). *Frontiers in Microbiology*, 10, 870-870. <https://doi.org/10.3389/fmicb.2019.00870>
- Kool, D. M., Dolfing, J., Wrage, N., & Van Groenigen, J. W. (2011). Nitrifier denitrification as a distinct and significant source of nitrous oxide from soil. *Soil Biology and Biochemistry*, 43(1), 174-178. <https://doi.org/https://doi.org/10.1016/j.soilbio.2010.09.030>
- Krapp, A., & Traong, H.-N. (2006). Regulation of C/N Interaction in Model Plant Species. *Journal of Crop Improvement*, 15(2), 127-173. [https://doi.org/10.1300/J411v15n02\\_05](https://doi.org/10.1300/J411v15n02_05)
- Krauss, K. W., Holm Jr, G. O., Perez, B. C., McWhorter, D. E., Cormier, N., Moss, R. F., Johnson, D. J., Neubauer, S. C., & Raynie, R. C. (2016). Component greenhouse gas fluxes and radiative balance from two deltaic marshes in Louisiana: Pairing chamber techniques and eddy covariance. *Journal of Geophysical Research: Biogeosciences*, 121(6), 1503-1521. <https://doi.org/https://doi.org/10.1002/2015JG003224>
- Krogh, S. A., & Pomeroy, J. W. (2019). Impact of future climate and vegetation on the hydrology of an arctic headwater basin at the tundra-taiga transition. *Journal of Hydrometeorology*, 20(2), 197-215. <https://doi.org/10.1175/JHM-D-18-0187.1>
- Kutzbach, L., Wagner, D., & Pfeiffer, E. M. (2004). Effect of microrelief and vegetation on methane emission from wet polygonal tundra, Lena Delta, Northern Siberia. *Biogeochemistry*, 69(3), 341-362. <https://doi.org/10.1023/B:BIOG.0000031053.81520.db>
- Kwon, M. J., Beulig, F., Ilie, I., Wildner, M., Küsel, K., Merbold, L., Mahecha, M. D., Zimov, N., Zimov, S. A., Heimann, M., Schuur, E. A. G., Kostka, J. E., Kolle, O., Hilke, I., & Göckede, M. (2017). Plants, microorganisms, and soil temperatures contribute to a decrease in methane fluxes on a drained Arctic floodplain. *Global Change Biology*, 23, 2396-2412. <https://doi.org/10.1111/gcb.13558>
- Lacroix, F., Zaehle, S., Caldararu, S., Schaller, J., Stimmler, P., Holl, D., Kutzbach, L., & Göckede, M. (2022). Mismatch of N release from the permafrost and vegetative uptake opens pathways of increasing nitrous oxide emissions in the high Arctic. *Global Change Biology*, 28(20), 5973-5990. <https://doi.org/https://doi.org/10.1111/gcb.16345>
- Lagomarsino, A., & Agnelli, A. E. (2020). Influence of vegetation cover and soil features on CO<sub>2</sub>, CH<sub>4</sub> and N<sub>2</sub>O fluxes in northern Finnish Lapland. *Polar Science*, 24, 100531. <https://doi.org/https://doi.org/10.1016/j.polar.2020.100531>
- Lamboll, R. D., Nicholls, Z. R. J., Smith, C. J., Kikstra, J. S., Byers, E., & Rogelj, J. (2023). Assessing the size and uncertainty of remaining carbon budgets. *Nature Climate Change*, 13(12), 1360-1367. <https://doi.org/10.1038/s41558-023-01848-5>
- Lara, M. J., Lin, D. H., Andresen, C., Loughheed, V. L., & Tweedie, C. E. (2019). Nutrient Release From Permafrost Thaw Enhances CH<sub>4</sub> Emissions From Arctic Tundra Wetlands. *Journal*
-

- of *Geophysical Research: Biogeosciences*, 124(6), 1560-1573. <https://doi.org/https://doi.org/10.1029/2018JG004641>
- Lee, H., Schuur, E. A. G., Inglett, K. S., Lavoie, M., & Chanton, J. P. (2012). The rate of permafrost carbon release under aerobic and anaerobic conditions and its potential effects on climate. *Global Change Biology*, 18(2), 515-527. <https://doi.org/https://doi.org/10.1111/j.1365-2486.2011.02519.x>
- Lee, J., Yun, J., Yang, Y., Jung, J. Y., Lee, Y. K., Yuan, J., Ding, W., Freeman, C., & Kang, H. (2023). Attenuation of Methane Oxidation by Nitrogen Availability in Arctic Tundra Soils. *Environmental Science & Technology*, 57(6), 2647-2659. <https://doi.org/10.1021/acs.est.2c05228>
- Li, T., Liang, J., Chen, X., Wang, H., Zhang, S., Pu, Y., Xu, X., Li, H., Xu, J., Wu, X., & Liu, X. (2021). The interacting roles and relative importance of climate, topography, soil properties and mineralogical composition on soil potassium variations at a national scale in China. *CATENA*, 196, 104875. <https://doi.org/https://doi.org/10.1016/j.catena.2020.104875>
- Liebner, S., Ganzert, L., Kiss, A., Yang, S., Wagner, D., & Svenning, M. M. (2015). Shifts in methanogenic community composition and methane fluxes along the degradation of discontinuous permafrost. *Frontiers in Microbiology*, 6, 356-356. <https://doi.org/10.3389/fmicb.2015.00356>
- Liebner, S., & Wagner, D. (2007). Abundance, distribution and potential activity of methane oxidizing bacteria in permafrost soils from the Lena Delta, Siberia. *Environ Microbiol*, 9(1), 107-117. <https://doi.org/10.1111/j.1462-2920.2006.01120.x>
- Lindroth, A., Pirk, N., Jónsdóttir, I. S., Stiegler, C., Klemedtsson, L., & Nilsson, M. B. (2022). CO<sub>2</sub> and CH<sub>4</sub> exchanges between moist moss tundra and atmosphere on Kapp Linné, Svalbard. *Biogeosciences*, 19(16), 3921-3934. <https://doi.org/10.5194/bg-19-3921-2022>
- MacDougall, A. H. (2021). Estimated effect of the permafrost carbon feedback on the zero emissions commitment to climate change. *Biogeosciences*, 18(17), 4937-4952. <https://doi.org/10.5194/bg-18-4937-2021>
- Marushchak, M. E., Kerttula, J., Diáková, K., Faguet, A., Gil, J., Grosse, G., Knoblauch, C., Lashchinskiy, N., Martikainen, P. J., Morgenstern, A., Nykamb, M., Ronkainen, J. G., Siljanen, H. M. P., van Delden, L., Voigt, C., Zimov, N., Zimov, S., & Biasi, C. (2021). Thawing Yedoma permafrost is a neglected nitrous oxide source. *Nature Communications*, 12(1), 7107. <https://doi.org/10.1038/s41467-021-27386-2>
- Maslov, M. N., & Maslova, O. A. (2021). Nitrogen limitation of microbial activity in alpine tundra soils along an environmental gradient: Intra-seasonal variations and effect of rising temperature. *Soil Biology and Biochemistry*, 156(March), 108234-108234. <https://doi.org/10.1016/j.soilbio.2021.108234>
- Mastepanov, M., Sigsgaard, C., Dlugokencky, E. J., Houweling, S., Ström, L., Tamstorf, M. P., & Christensen, T. R. (2008). Large tundra methane burst during onset of freezing. *Nature*, 456(7222), 628-630. <https://doi.org/10.1038/nature07464>
- Mastepanov, M., Sigsgaard, C., Tagesson, T., Ström, L., Tamstorf, M. P., Lund, M., & Christensen, T. R. (2013). Revisiting factors controlling methane emissions from high-Arctic tundra. *Biogeosciences*, 10(11), 5139-5158. <https://doi.org/10.5194/bg-10-5139-2013>
- MATLAB. (2019). *R2019a*. In The MathWorks Inc.
-

- McCalley, C. K., Woodcroft, B. J., Hodgkins, S. B., Wehr, R. A., Kim, E. H., Mondav, R., Crill, P. M., Chanton, J. P., Rich, V. I., Tyson, G. W., & Saleska, S. R. (2014). Methane dynamics regulated by microbial community response to permafrost thaw. *Nature*, *514*(7253), 478-481. <https://doi.org/10.1038/nature13798>
- McGuire, A. D., Anderson, L. G., Christensen, T. R., Dallimore, S., Guo, L., Hayes, D. J., Heimann, M., Lorenson, T. D., Macdonald, R. W., & Roulet, N. (2009). Sensitivity of the carbon cycle in the Arctic to climate change. *Ecological Monographs*, *79*(4), 523-555. <https://doi.org/https://doi.org/10.1890/08-2025.1>
- Mehnaz, K. R., & Dijkstra, F. A. (2016). Denitrification and associated N<sub>2</sub>O emissions are limited by phosphorus availability in a grassland soil. *Geoderma*, *284*, 34-41. <https://doi.org/https://doi.org/10.1016/j.geoderma.2016.08.011>
- Mehnaz, K. R., Keitel, C., & Dijkstra, F. A. (2019). Phosphorus availability and plants alter soil nitrogen retention and loss. *Science of The Total Environment*, *671*, 786-794. <https://doi.org/https://doi.org/10.1016/j.scitotenv.2019.03.422>
- Melchert, J. O., Wischhöfer, P., Knoblauch, C., Eckhardt, T., Liebner, S., & Rethemeyer, J. (2022). Sources of CO<sub>2</sub> Produced in Freshly Thawed Pleistocene-Age Yedoma Permafrost. *Frontiers in Earth Science*, *9*. <https://doi.org/10.3389/feart.2021.737237>
- Melillo, J. M., Butler, S., Johnson, J., Mohan, J., Steudler, P., Lux, H., Burrows, E., Bowles, F., Smith, R., Scott, L., Vario, C., Hill, T., Burton, A., Zhou, Y.-M., & Tang, J. (2011). Soil warming, carbon-nitrogen interactions, and forest carbon budgets. *Proceedings of the National Academy of Sciences*, *108*(23), 9508-9512. <https://doi.org/10.1073/pnas.1018189108>
- Melton, J. R., Wania, R., Hodson, E. L., Poulter, B., Ringeval, B., Spahni, R., Bohn, T., Avis, C. A., Beerling, D. J., Chen, G., Eliseev, A. V., Denisov, S. N., Hopcroft, P. O., Lettenmaier, D. P., Riley, W. J., Singarayer, J. S., Subin, Z. M., Tian, H., Zürcher, S., . . . Kaplan, J. O. (2013). Present state of global wetland extent and wetland methane modelling: conclusions from a model inter-comparison project (WETCHIMP). *Biogeosciences*, *10*(2), 753-788. <https://doi.org/10.5194/bg-10-753-2013>
- Menge, D. N. L., Kou-Giesbrecht, S., Taylor, B. N., Akana, P. R., Butler, A., Pereira, K. A. C., Cooley, S. S., Lau, V. M., & Lauterbach, E. L. (2023). Terrestrial Phosphorus Cycling: Responses to Climatic Change. *Annual Review of Ecology, Evolution, and Systematics*, *54*(1), 429-449. <https://doi.org/10.1146/annurev-ecolsys-110421-102458>
- Miner, K. R., Turetsky, M. R., Malina, E., Bartsch, A., Tamminen, J., McGuire, A. D., Fix, A., Sweeney, C., Elder, C. D., & Miller, C. E. (2022). Permafrost carbon emissions in a changing Arctic. *Nature Reviews Earth & Environment*, *3*(1), 55-67. <https://doi.org/10.1038/s43017-021-00230-3>
- Mishra, U., Hugelius, G., Shelef, E., Yang, Y., Strauss, J., Lupachev, A., Harden, J. W., Jastrow, J. D., Ping, C.-L., Riley, W. J., Schuur, E. A. G., Matamala, R., Siewert, M., Nave, L. E., Koven, C. D., Fuchs, M., Palmtag, J., Kuhry, P., Treat, C. C., . . . Orr, A. (2021). Spatial heterogeneity and environmental predictors of permafrost region soil organic carbon stocks. *Science Advances*, *7*(9), eaaz5236-eaaz5236. <https://doi.org/10.1126/sciadv.aaz5236>
- Moore, C. M., Mills, M. M., Arrigo, K. R., Berman-Frank, I., Bopp, L., Boyd, P. W., Galbraith, E. D., Geider, R. J., Guieu, C., Jaccard, S. L., Jickells, T. D., La Roche, J., Lenton, T. M., Mahowald, N. M., Marañón, E., Marinov, I., Moore, J. K., Nakatsuka, T., Oschlies, A., . . . Ulloa, O. (2013). Processes and patterns of oceanic nutrient limitation. *Nature Geoscience*, *6*(9), 701-710. <https://doi.org/10.1038/ngeo1765>
-

- Morgenstern, A., Ulrich, M., Günther, F., Roessler, S., Fedorova, I. V., Rudaya, N. A., Wetterich, S., Boike, J., & Schirrmeister, L. (2013). Evolution of thermokarst in East Siberian ice-rich permafrost: A case study. *Geomorphology*, 201, 363-379. <https://doi.org/https://doi.org/10.1016/j.geomorph.2013.07.011>
- Mori, T., Ohta, S., Ishizuka, S., Konda, R., Wicaksono, A., Heriyanto, J., & Hardjono, A. (2010). Effects of phosphorus addition on N<sub>2</sub>O and NO emissions from soils of an Acacia mangium plantation. *Soil Science and Plant Nutrition*, 56(5), 782-788. <https://doi.org/10.1111/j.1747-0765.2010.00501.x>
- Morrissey, L. A., & Livingston, G. P. (1992). Methane emissions from Alaska Arctic tundra - an assessment of local spatial variability. 97. <https://doi.org/10.1029/92JD00063>
- Muster, S., Langer, M., Heim, B., Westermann, S., & Boike, J. (2012). Subpixel heterogeneity of ice-wedge polygonal tundra: a multi-scale analysis of land cover and evapotranspiration in the Lena River Delta, Siberia. *Tellus B: Chemical and Physical Meteorology*, 64(1), 17301-17301. <https://doi.org/10.3402/tellusb.v64i0.17301>
- Myhre, G., Samset, B. H., Schulz, M., Balkanski, Y., Bauer, S., Bernsten, T. K., Bian, H., Bellouin, N., Chin, M., Diehl, T., Easter, R. C., Feichter, J., Ghan, S. J., Hauglustaine, D., Iversen, T., Kinne, S., Kirkevåg, A., Lamarque, J. F., Lin, G., . . . Zhou, C. (2013). Radiative forcing of the direct aerosol effect from AeroCom Phase II simulations. *Atmospheric Chemistry and Physics*, 13(4), 1853-1877. <https://doi.org/10.5194/acp-13-1853-2013>
- Nadelhoffer, K. J., Giblin, A. E., Shaver, G. R., & Laundre, J. A. (1991). Effects of Temperature and Substrate Quality on Element Mineralization in Six Arctic Soils. *Ecology*, 72(1), 242-253. <https://doi.org/https://doi.org/10.2307/1938918>
- Natali, S. M., Schuur, E. A. G., Mauritz, M., Schade, J. D., Celis, G., Crummer, K. G., Johnston, C., Krapek, J., Pegoraro, E., Salmon, V. G., & Webb, E. E. (2015). Permafrost thaw and soil moisture driving CO<sub>2</sub> and CH<sub>4</sub> release from upland tundra. *Journal of Geophysical Research: Biogeosciences*, 120(3), 525-537. <https://doi.org/https://doi.org/10.1002/2014JG002872>
- Natchimuthu, S., Wallin, M. B., Klemetsson, L., & Bastviken, D. (2017). Spatio-temporal patterns of stream methane and carbon dioxide emissions in a hemiboreal catchment in Southwest Sweden. *Scientific Reports*, 7(1), 39729. <https://doi.org/10.1038/srep39729>
- Nielsen, C. S., Michelsen, A., Ambus, P., Deepagoda, T. K. K. C., & Elberling, B. (2017). Linking rhizospheric CH<sub>4</sub> oxidation and net CH<sub>4</sub> emissions in an arctic wetland based on <sup>13</sup>CH<sub>4</sub> labeling of mesocosms. *Plant and Soil*, 412(1-2), 201-213. <https://doi.org/10.1007/s11104-016-3061-4>
- Nielsen, C. S., Michelsen, A., Strobel, B. W., Wulff, K., Banyasz, I., & Elberling, B. (2017). Correlations between substrate availability, dissolved CH<sub>4</sub>, and CH<sub>4</sub> emissions in an arctic wetland subject to warming and plant removal. *Journal of Geophysical Research: Biogeosciences*, 122(3), 645-660. <https://doi.org/https://doi.org/10.1002/2016JG003511>
- Nowinski, N. S., Trumbore, S. E., Schuur, E. A. G., Mack, M. C., & Shaver, G. R. (2008). Nutrient Addition Prompts Rapid Destabilization of Organic Matter in an Arctic Tundra Ecosystem. *Ecosystems*, 11(1), 16-25. <https://doi.org/10.1007/s10021-007-9104-1>
- Noyce, G. L., Varner, R. K., Bubier, J. L., & Froelking, S. (2014). Effect of *Carex rostrata* on seasonal and interannual variability in peatland methane emissions. *Journal of Geophysical Research: Biogeosciences*, 119(1), 24-34. <https://doi.org/https://doi.org/10.1002/2013JG002474>
-

- O'Neill, R. M., Girkin, N. T., Krol, D. J., Wall, D. P., Brennan, F. P., Lanigan, G. J., Renou-Wilson, F., Müller, C., & Richards, K. G. (2020). The effect of carbon availability on N<sub>2</sub>O emissions is moderated by soil phosphorus. *Soil Biology and Biochemistry*, 142, 107726. <https://doi.org/10.1016/j.soilbio.2020.107726>
- Parmentier, F.-J. W., Christensen, T. R., Rysgaard, S., Bendtsen, J., Glud, R. N., Else, B., van Huissteden, J., Sachs, T., Vonk, J. E., & Sejr, M. K. (2017). A synthesis of the arctic terrestrial and marine carbon cycles under pressure from a dwindling cryosphere. *Ambio*, 46(1), 53-69. <https://doi.org/10.1007/s13280-016-0872-8>
- Pearson, R. G., Phillips, S. J., Lorant, M. M., Beck, P. S. A., Damoulas, T., Knight, S. J., & Goetz, S. J. (2013). Shifts in Arctic vegetation and associated feedbacks under climate change. *Nature Climate Change*, 3(7), 673-677. <https://doi.org/10.1038/nclimate1858>
- Philben, M., Zhang, L., Yang, Z., Taş, N., Wullschlegel, S. D., Graham, D. E., & Gu, B. (2020). Anaerobic respiration pathways and response to increased substrate availability of Arctic wetland soils. *Environmental Science: Processes & Impacts*, 22(10), 2070-2083. <https://doi.org/10.1039/D0EM00124D>
- Phillips, C. A., & Wurzbarger, N. (2019). Elevated rates of heterotrophic respiration in shrub-conditioned arctic tundra soils. *Pedobiologia*, 72, 8-15. <https://doi.org/10.1016/j.pedobi.2018.11.002>
- Pickett-Heaps, C. A., Jacob, D. J., Wecht, K. J., Kort, E. A., Wofsy, S. C., Diskin, G. S., Worthy, D. E. J., Kaplan, J. O., Bey, I., & Drevet, J. (2011). Magnitude and seasonality of wetland methane emissions from the Hudson Bay Lowlands (Canada). *Atmos. Chem. Phys.*, 11(8), 3773-3779. <https://doi.org/10.5194/acp-11-3773-2011>
- Popp, T. J., Chanton, J. P., Whiting, G. J., & Grant, N. (1999). Methane stable isotope distribution at a Carex dominated fen in north Central Alberta. *Global Biogeochemical Cycles*, 13(4), 1063-1077. <https://doi.org/10.1029/1999GB900060>
- Popp, T. J., Chanton, J. P., Whiting, G. J., & Grant, N. (2000). Evaluation of methane oxidation in the rhizosphere of a Carex dominated fen in northcentral Alberta, Canada. *Biogeochemistry*, 51(3), 259-281. <https://doi.org/10.1023/A:1006452609284>
- Preuss, I., Knoblauch, C., Gebert, J., & Pfeiffer, E. M. (2013). Improved quantification of microbial CH<sub>4</sub> oxidation efficiency in arctic wetland soils using carbon isotope fractionation. *Biogeosciences*, 10(4), 2539-2552. <https://doi.org/10.5194/bg-10-2539-2013>
- R. (2020). *R: A Language and Environment for Statistical Computing*. In R Foundation for Statistical Computing. <https://www.R-project.org/>
- Randers, J., & Goluke, U. (2020). An earth system model shows self-sustained thawing of permafrost even if all man-made GHG emissions stop in 2020. *Scientific Reports*, 10(1), 18456. <https://doi.org/10.1038/s41598-020-75481-z>
- Rantanen, M., Karpechko, A. Y., Lipponen, A., Nordling, K., Hyvärinen, O., Ruosteenoja, K., Vihma, T., & Laaksonen, A. (2022). The Arctic has warmed nearly four times faster than the globe since 1979. *Communications Earth & Environment*, 3(1), 168. <https://doi.org/10.1038/s43247-022-00498-3>
- Ray, L. L. (1993). Permafrost. In U. S. G. Survey (Ed.). Denver: U.S. Geological Survey.
- Reddy, K. R., & Patrick, W. H. (1975). Effect of alternate aerobic and anaerobic conditions on redox potential, organic matter decomposition and nitrogen loss in a flooded soil. *Soil*
-

- Biology and Biochemistry*, 7(2), 87-94. [https://doi.org/https://doi.org/10.1016/0038-0717\(75\)90004-8](https://doi.org/https://doi.org/10.1016/0038-0717(75)90004-8)
- Reed, S. C., Yang, X., & Thornton, P. E. (2015). Incorporating phosphorus cycling into global modeling efforts: a worthwhile, tractable endeavor. *New Phytologist*, 208(2), 324-329. <https://doi.org/https://doi.org/10.1111/nph.13521>
- Rehder, Z., Kleinen, T., Kutzbach, L., Stepanenko, V., Langer, M., & Brovkin, V. (2023). Simulated methane emissions from Arctic ponds are highly sensitive to warming. *Biogeosciences*, 20(14), 2837-2855. <https://doi.org/10.5194/bg-20-2837-2023>
- Rissanen, A. J., Karvinen, A., Nykänen, H., Peura, S., Tirola, M., Mäki, A., & Kankaala, P. (2017). Effects of alternative electron acceptors on the activity and community structure of methane-producing and consuming microbes in the sediments of two shallow boreal lakes. *FEMS Microbiology Ecology*, 93(7). <https://doi.org/10.1093/femsec/fix078>
- Romanovsky, V. E., Drozdov, D. S., Oberman, N. G., Malkova, G. V., Kholodov, A. L., Marchenko, S. S., Moskalenko, N. G., Sergeev, D. O., Ukraintseva, N. G., Abramov, A. A., Gilichinsky, D. A., & Vasiliev, A. A. (2010). Thermal state of permafrost in Russia. *Permafrost and Periglacial Processes*, 21(2), 136-155. <https://doi.org/https://doi.org/10.1002/ppp.683>
- Romanovsky, V. E., & Osterkamp, T. E. (1997). Thawing of the Active Layer on the Coastal Plain of the Alaskan Arctic. *Permafrost and Periglacial Processes*, 8(1), 1-22. [https://doi.org/https://doi.org/10.1002/\(SICI\)1099-1530\(199701\)8:1<1::AID-PPP243>3.0.CO;2-U](https://doi.org/https://doi.org/10.1002/(SICI)1099-1530(199701)8:1<1::AID-PPP243>3.0.CO;2-U)
- Romanovsky, V. E., Smith, S. L., & Christiansen, H. H. (2010). Permafrost thermal state in the polar Northern Hemisphere during the international polar year 2007–2009: a synthesis. *Permafrost and Periglacial Processes*, 21(2), 106-116. <https://doi.org/10.1002/ppp.689>
- Rößger, N., Sachs, T., Wille, C., Boike, J., & Kutzbach, L. (2022). Seasonal increase of methane emissions linked to warming in Siberian tundra. *Nature Climate Change*, 12(11), 1031-1036. <https://doi.org/10.1038/s41558-022-01512-4>
- Rustad, L., Campbell, J., Marion, G., Norby, R., Mitchell, M., Hartley, A., Cornelissen, J., Gurevitch, J., & Gcte, N. (2001). A meta-analysis of the response of soil respiration, net nitrogen mineralization, and aboveground plant growth to experimental ecosystem warming. *Oecologia*, 126(4), 543-562. <https://doi.org/10.1007/s004420000544>
- Sachs, T., Giebels, M., Boike, J., & Kutzbach, L. (2010). Environmental controls on CH<sub>4</sub> emission from polygonal tundra on the microsite scale in the Lena river delta, Siberia. *Global Change Biology*, 16(11), 3096-3110. <https://doi.org/10.1111/j.1365-2486.2010.02232.x>
- Sárdi, K., Balázsy, Á., & Salamon, B. (2012). Interrelations in Phosphorus and Potassium Accumulation Characteristics of Plants Grown in Different Soil Types. *Communications in Soil Science and Plant Analysis*, 43(1-2), 324-333. <https://doi.org/10.1080/00103624.2011.638603>
- Saunois, M., Stavert, A. R., Poulter, B., Bousquet, P., Canadell, J. G., Jackson, R. B., Raymond, P. A., Dlugokencky, E. J., Houweling, S., Patra, P. K., Ciais, P., Arora, V. K., Bastviken, D., Bergamaschi, P., Blake, D. R., Brailsford, G., Bruhwiler, L., Carlson, K. M., Carrol, M., . . . Zhuang, Q. (2020). The Global Methane Budget 2000–2017. *Earth System Science Data*, 12(3), 1561-1623. <https://doi.org/10.5194/essd-12-1561-2020>
-



- Savage, K. E., & Davidson, E. A. (2003). A comparison of manual and automated systems for soil CO<sub>2</sub> flux measurements: trade-offs between spatial and temporal resolution. *Journal of Experimental Botany*, 54(384), 891-899. <https://doi.org/10.1093/jxb/erg121>
- Schädel, C., Bader, M. K. F., Schuur, E. A. G., Biasi, C., Bracho, R., Čapek, P., De Baets, S., Diáková, K., Ernakovich, J., Estop-Aragones, C., Graham, D. E., Hartley, I. P., Iversen, C. M., Kane, E., Knoblauch, C., Lupascu, M., Martikainen, P. J., Natali, S. M., Norby, R. J., . . . Wickland, K. P. (2016). Potential carbon emissions dominated by carbon dioxide from thawed permafrost soils. *Nature Climate Change*, 6(10), 950-953. <https://doi.org/10.1038/nclimate3054>
- Schädel, C., Rogers, B. M., Lawrence, D. M., Koven, C. D., Brovkin, V., Burke, E. J., Genet, H., Huntzinger, D. N., Jafarov, E., McGuire, A. D., Riley, W. J., & Natali, S. M. (2024). Earth system models must include permafrost carbon processes. *Nature Climate Change*, 14(2), 114-116. <https://doi.org/10.1038/s41558-023-01909-9>
- Schimel, J. P., Kielland, K., & Chapin, F. S. (1996). Nutrient Availability and Uptake by Tundra Plants. In J. F. Reynolds & J. D. Tenhunen (Eds.), *Landscape Function and Disturbance in Arctic Tundra* (pp. 203-221). Springer Berlin Heidelberg. [https://doi.org/10.1007/978-3-662-01145-4\\_10](https://doi.org/10.1007/978-3-662-01145-4_10)
- Schmidt, I. K., Jonasson, S., & Michelsen, A. (1999). Mineralization and microbial immobilization of N and P in arctic soils in relation to season, temperature and nutrient amendment. *Applied Soil Ecology*, 11(2), 147-160. [https://doi.org/https://doi.org/10.1016/S0929-1393\(98\)00147-4](https://doi.org/https://doi.org/10.1016/S0929-1393(98)00147-4)
- Schmidt, I. K., Jonasson, S., Shaver, G. R., Michelsen, A., & Nordin, A. (2002). Mineralization and distribution of nutrients in plants and microbes in four arctic ecosystems: responses to warming. *Plant and Soil*, 242(1), 93-106. <https://doi.org/10.1023/A:1019642007929>
- Schneider, J., Grosse, G., & Wagner, D. (2009). Land cover classification of tundra environments in the Arctic Lena Delta based on Landsat 7 ETM+ data and its application for upscaling of methane emissions. *Remote Sensing of Environment*, 113(2), 380-391. <https://doi.org/10.1016/j.rse.2008.10.013>
- Schrier-Uijl, A. P., Kroon, P. S., Hensen, A., Leffelaar, P. A., Berendse, F., & Veenendaal, E. M. (2010). Comparison of chamber and eddy covariance-based CO<sub>2</sub> and CH<sub>4</sub> emission estimates in a heterogeneous grass ecosystem on peat. *Agricultural and Forest Meteorology*, 150(6), 825-831. <https://doi.org/https://doi.org/10.1016/j.agrformet.2009.11.007>
- Schuur, E. A. G., Bockheim, J., Canadell, J. G., Euskirchen, E., Field, C. B., Goryachkin, S. V., Hagemann, S., Kuhry, P., Lafleur, P. M., Lee, H., Mazhitova, G., Nelson, F. E., Rinke, A., Romanovsky, V. E., Shiklomanov, N., Tarnocai, C., Venevsky, S., Vogel, J. G., & Zimov, S. A. (2008). Vulnerability of Permafrost Carbon to Climate Change: Implications for the Global Carbon Cycle. *BioScience*, 58(8), 701-714. <https://doi.org/10.1641/b580807>
- Schuur, E. A. G., & Mack, M. C. (2018). Ecological Response to Permafrost Thaw and Consequences for Local and Global Ecosystem Services. *Annual Review of Ecology, Evolution, and Systematics*, 49(Volume 49, 2018), 279-301. <https://doi.org/https://doi.org/10.1146/annurev-ecolsys-121415-032349>
- Schuur, E. A. G., McGuire, A. D., Schädel, C., Grosse, G., Harden, J. W., Hayes, D. J., Hugelius, G., Koven, C. D., Kuhry, P., Lawrence, D. M., Natali, S. M., Olefeldt, D., Romanovsky, V. E., Schaefer, K., Turetsky, M. R., Treat, C. C., & Vonk, J. E. (2015). Climate change and the
-

- permafrost carbon feedback. *Nature*, 520(7546), 171-179. <https://doi.org/10.1038/nature14338>
- Schwamborn, G., Rachold, V., & Grigoriev, M. N. (2002). Late Quaternary sedimentation history of the Lena Delta. *Quaternary International*, 89(1), 119-134. [https://doi.org/10.1016/S1040-6182\(01\)00084-2](https://doi.org/10.1016/S1040-6182(01)00084-2)
- Serreze, M. C., & Barry, R. G. (2011). Processes and impacts of Arctic amplification: A research synthesis. *Global and Planetary Change*, 77(1), 85-96. <https://doi.org/https://doi.org/10.1016/j.gloplacha.2011.03.004>
- Shaver, G. R., Johnson, L. C., Cades, D. H., Murray, G., Laundre, J. A., Rastetter, E. B., Nadelhoffer, K. J., & Giblin, A. E. (1998). BIOMASS AND CO<sub>2</sub> FLUX IN WET SEDGE TUNDRAS: RESPONSES TO NUTRIENTS, TEMPERATURE, AND LIGHT. *Ecological Monographs*, 68(1), 75-97. [https://doi.org/https://doi.org/10.1890/0012-9615\(1998\)068\[0075:BACFIW\]2.0.CO;2](https://doi.org/https://doi.org/10.1890/0012-9615(1998)068[0075:BACFIW]2.0.CO;2)
- Shaw, A. N., & Cleveland, C. C. (2020). The effects of temperature on soil phosphorus availability and phosphatase enzyme activities: a cross-ecosystem study from the tropics to the Arctic. *Biogeochemistry*, 151(2), 113-125. <https://doi.org/10.1007/s10533-020-00710-6>
- Singleton, C. M., McCalley, C. K., Woodcroft, B. J., Boyd, J. A., Evans, P. N., Hodgkins, S. B., Chanton, J. P., Froelking, S., Crill, P. M., Saleska, S. R., Rich, V. I., & Tyson, G. W. (2018). Methanotrophy across a natural permafrost thaw environment. *The ISME Journal*, 12(10), 2544-2558. <https://doi.org/10.1038/s41396-018-0065-5>
- SIO, NOAA, Navy, U. S., NGA, & GEBCO. Eurasia. In.
- Skeeter, J., Christen, A., & Henry, G. H. R. (2022). Controls on carbon dioxide and methane fluxes from a low-center polygonal peatland in the Mackenzie River Delta, Northwest Territories. *Arctic Science*, 8(2), 471-497. <https://doi.org/10.1139/as-2021-0034>
- Skeeter, J., Christen, A., Laforce, A.-A., Humphreys, E., & Henry, G. (2020). Vegetation influence and environmental controls on greenhouse gas fluxes from a drained thermokarst lake in the Western Canadian Arctic. *Biogeosciences Discussions*, 17, 1-25. <https://doi.org/10.5194/bg-2019-477>
- Smirnov, N. (2017). *mikhail sumgin's subterranean museum of eternity*. Centre for Experimental Museology. Retrieved 16.02.2024 from [https://redmuseum.church/en/smironov\\_sumgin](https://redmuseum.church/en/smironov_sumgin)
- Souza, L. F. T., & Billings, S. A. (2022). Temperature and pH mediate stoichiometric constraints of organically derived soil nutrients. *Global Change Biology*, 28(4), 1630-1642. <https://doi.org/https://doi.org/10.1111/gcb.15985>
- St Pierre, K. A., Danielsen, B. K., Hermesdorf, L., D'Imperio, L., Iversen, L. L., & Elberling, B. (2019). Drivers of net methane uptake across Greenlandic dry heath tundra landscapes. *Soil Biology and Biochemistry*, 138, 107605-107605. <https://doi.org/https://doi.org/10.1016/j.soilbio.2019.107605>
- Stimmler, P., Goeckede, M., Elberling, B., Natali, S., Kuhry, P., Perron, N., Lacroix, F., Hugelius, G., Sonnentag, O., Strauss, J., Minions, C., Sommer, M., & Schaller, J. (2023). Pan-Arctic soil element bioavailability estimations. *Earth Syst. Sci. Data*, 15(3), 1059-1075. <https://doi.org/10.5194/essd-15-1059-2023>
- Strand, S. M., Christiansen, H. H., Johansson, M., Åkerman, J., & Humlum, O. (2021). Active layer thickening and controls on interannual variability in the Nordic Arctic compared to the
-

- circum-Arctic. *Permafrost and Periglacial Processes*, 32(1), 47-58. <https://doi.org/https://doi.org/10.1002/ppp.2088>
- Street, L. E., Mielke, N., & Woodin, S. J. (2018). Phosphorus Availability Determines the Response of Tundra Ecosystem Carbon Stocks to Nitrogen Enrichment. *Ecosystems*, 21(6), 1155-1167. <https://doi.org/10.1007/s10021-017-0209-x>
- Ström, L., Mastepanov, M., & Christensen, T. R. (2005). Species-specific effects of vascular plants on carbon turnover and methane emissions from wetlands. *Biogeochemistry*, 75(1), 65-82. <https://doi.org/10.1007/s10533-004-6124-1>
- Ström, L., Tagesson, T., Mastepanov, M., & Christensen, T. R. (2012). Presence of *Eriophorum scheuchzeri* enhances substrate availability and methane emission in an Arctic wetland. *Soil Biology and Biochemistry*, 45, 61-70. <https://doi.org/10.1016/j.soilbio.2011.09.005>
- Symons, G. E., & Buswell, A. M. (1933). The Methane Fermentation of Carbohydrates<sup>1,2</sup>. *Journal of the American Chemical Society*, 55(5), 2028-2036. <https://doi.org/10.1021/ja01332a039>
- Tagesson, T., Mölder, M., Mastepanov, M., Sigsgaard, C., Tamstorf, M. P., Lund, M., Falk, J. M., Lindroth, A., Christensen, T. R., & Ström, L. (2012). Land-atmosphere exchange of methane from soil thawing to soil freezing in a high-Arctic wet tundra ecosystem. *Global Change Biology*, 18(6), 1928-1940. <https://doi.org/https://doi.org/10.1111/j.1365-2486.2012.02647.x>
- Tolkien, J. R. R. (1954). *The Fellowship of the Ring*. Allen & Unwin.
- Treat, C. C., Natali, S. M., Ernakovich, J., Iversen, C. M., Lupascu, M., McGuire, A. D., Norby, R. J., Roy Chowdhury, T., Richter, A., Šantrůčková, H., Schädel, C., Schuur, E. A. G., Sloan, V. L., Turetsky, M. R., & Waldrop, M. P. (2015). A pan-Arctic synthesis of CH<sub>4</sub> and CO<sub>2</sub> production from anoxic soil incubations. *Global Change Biology*, 21(7), 2787-2803. <https://doi.org/10.1111/gcb.12875>
- Treat, C. C., Virkkala, A.-M., Burke, E., Bruhwiler, L., Chatterjee, A., Fisher, J. B., Hashemi, J., Parmentier, F.-J. W., Rogers, B. M., Westermann, S., Watts, J. D., Blanc-Betes, E., Fuchs, M., Kruse, S., Malhotra, A., Miner, K., Strauss, J., Armstrong, A., Epstein, H. E., . . . Hugelius, G. (2024). Permafrost Carbon: Progress on Understanding Stocks and Fluxes Across Northern Terrestrial Ecosystems. *Journal of Geophysical Research: Biogeosciences*, 129(3), e2023JG007638. <https://doi.org/https://doi.org/10.1029/2023JG007638>
- Treat, C. C., Wollheim, W. M., Varner, R. K., & Bowden, W. B. (2016). Longer thaw seasons increase nitrogen availability for leaching during fall in tundra soils. *Environmental Research Letters*, 11(6), 064013. <https://doi.org/10.1088/1748-9326/11/6/064013>
- Treat, C. C., Wollheim, W. M., Varner, R. K., Grandy, A. S., Talbot, J., & Frolking, S. (2014). Temperature and peat type control CO<sub>2</sub> and CH<sub>4</sub> production in Alaskan permafrost peats. *Global Change Biology*, 20(8), 2674-2686. <https://doi.org/https://doi.org/10.1111/gcb.12572>
- Turetsky, M. R., Abbott, B. W., Jones, M. C., Anthony, K. W., Olefeldt, D., Schuur, E. A. G., Grosse, G., Kuhry, P., Hugelius, G., Koven, C., Lawrence, D. M., Gibson, C., Sannel, A. B. K., & McGuire, A. D. (2020). Carbon release through abrupt permafrost thaw. *Nature Geoscience*, 13(2), 138-143. <https://doi.org/10.1038/s41561-019-0526-0>
- van Huissteden, J. (2020). *Thawing Permafrost: Permafrost Carbon in a Warming Arctic* (1 ed.). Springer Nature Switzerland AG. <https://doi.org/10.1007/978-3-030-31379-1>
-

- van Huissteden, J., Maximov, T. C., & Dolman, A. J. (2005). High methane flux from an arctic floodplain (Indigirka lowlands, eastern Siberia). *Journal of Geophysical Research: Biogeosciences*, 110(G2). <https://doi.org/https://doi.org/10.1029/2005JG000010>
- Vasiliev, A. A., Melnikov, V. P., Semenov, P. B., Oblogov, G. E., & Streletskaia, I. D. (2019). Methane concentration and emission in dominant landscapes of typical tundra of Western Yamal. *Doklady Earth Sciences*, 485(1), 284-287. <https://doi.org/10.1134/S1028334X19030085>
- Vaughn, L. J. S., Conrad, M. E., Bill, M., & Torn, M. S. (2016). Isotopic insights into methane production, oxidation, and emissions in Arctic polygon tundra. *Global Change Biology*, 22(10), 3487-3502. <https://doi.org/10.1111/gcb.13281>
- Virkkala, A.-M., Aalto, J., Rogers, B. M., Tagesson, T., Treat, C. C., Natali, S. M., Watts, J. D., Potter, S., Lehtonen, A., Mauritz, M., Schuur, E. A. G., Kochendorfer, J., Zona, D., Oechel, W., Kobayashi, H., Humphreys, E., Goeckede, M., Iwata, H., Lafleur, P. M., . . . Luoto, M. (2021). Statistical upscaling of ecosystem CO<sub>2</sub> fluxes across the terrestrial tundra and boreal domain: Regional patterns and uncertainties. *Global Change Biology*, 27(17), 4040-4059. <https://doi.org/https://doi.org/10.1111/gcb.15659>
- Virtanen, P., Gommers, R., Oliphant, T. E., Haberland, M., Reddy, T., Cournapeau, D., Burovski, E., Peterson, P., Weckesser, W., Bright, J., van der Walt, S. J., Brett, M., Wilson, J., Millman, K. J., Mayorov, N., Nelson, A. R. J., Jones, E., Kern, R., Larson, E., . . . SciPy, C. (2020). SciPy 1.0: fundamental algorithms for scientific computing in Python. *Nature Methods*, 17(3), 261-272. <https://doi.org/10.1038/s41592-019-0686-2>
- Vitousek, P. M., Porder, S., Houlton, B. Z., & Chadwick, O. A. (2010). Terrestrial phosphorus limitation: mechanisms, implications, and nitrogen–phosphorus interactions. *Ecological Applications*, 20(1), 5-15. <https://doi.org/https://doi.org/10.1890/08-0127.1>
- Voigt, C., Marushchak, M. E., Abbott, B. W., Biasi, C., Elberling, B., Siciliano, S. D., Sonnentag, O., Stewart, K. J., Yang, Y., & Martikainen, P. J. (2020). Nitrous oxide emissions from permafrost-affected soils. *Nature Reviews Earth & Environment*, 1(8), 420-434. <https://doi.org/10.1038/s43017-020-0063-9>
- Voigt, C., Virkkala, A. M., Hould Gosselin, G., Bennett, K. A., Black, T. A., Detto, M., Chevrier-Dion, C., Guggenberger, G., Hashmi, W., Kohl, L., Kou, D., Marquis, C., Marsh, P., Marushchak, M. E., Nesic, Z., Nykanen, H., Saarela, T., Sauheitl, L., Walker, B., . . . Sonnentag, O. (2023). Arctic soil methane sink increases with drier conditions and higher ecosystem respiration. *Nat Clim Chang*, 13(10), 1095-1104. <https://doi.org/10.1038/s41558-023-01785-3>
- Vonk, J. E., Tank, S. E., Bowden, W. B., Laurion, I., Vincent, W. F., Alekseychik, P., Amyot, M., Billet, M. F., Canário, J., Cory, R. M., Deshpande, B. N., Helbig, M., Jammet, M., Karlsson, J., Larouche, J., MacMillan, G., Rautio, M., Walter Anthony, K. M., & Wickland, K. P. (2015). Reviews and syntheses: Effects of permafrost thaw on Arctic aquatic ecosystems. *Biogeosciences*, 12(23), 7129-7167. <https://doi.org/10.5194/bg-12-7129-2015>
- Wagner, D., Kobabe, S., Pfeiffer, E. M., & Hubberten, H. W. (2003). Microbial controls on methane fluxes from a polygonal tundra of the Lena Delta, Siberia. *Permafrost and Periglacial Processes*, 14(2), 173-185. <https://doi.org/10.1002/ppp.443>
- Wagner, I., Hung, J. K. Y., Neil, A., & Scott, N. A. (2019). Net greenhouse gas fluxes from three High Arctic plant communities along a moisture gradient. *Arctic Science*, 5(June), 185-201.
-

- Walz, J., Knoblauch, C., Böhme, L., & Pfeiffer, E.-M. (2017). Regulation of soil organic matter decomposition in permafrost-affected Siberian tundra soils - Impact of oxygen availability, freezing and thawing, temperature, and labile organic matter. *Soil Biology and Biochemistry*, 110, 34-43. <https://doi.org/10.1016/j.soilbio.2017.03.001>
- Wang, Y.-P., Houlton, B. Z., & Field, C. B. (2007). A model of biogeochemical cycles of carbon, nitrogen, and phosphorus including symbiotic nitrogen fixation and phosphatase production. *Global Biogeochemical Cycles*, 21(1). <https://doi.org/10.1029/2006GB002797>
- Wania, R., Ross, I., & Prentice, I. C. (2010). Implementation and evaluation of a new methane model within a dynamic global vegetation model: LPJ-WHyMe v1.3.1. *Geoscientific Model Development*, 3(2), 565-584. <https://doi.org/10.5194/gmd-3-565-2010>
- Wegner, R., Fiencke, C., Knoblauch, C., Sauerland, L., & Beer, C. (2022). Rapid Permafrost Thaw Removes Nitrogen Limitation and Rises the Potential for N<sub>2</sub>O Emissions. *Nitrogen*, 3(4), 608-627. <https://doi.org/10.3390/nitrogen3040040>
- Weintraub, M. N. (2011). Biological Phosphorus Cycling in Arctic and Alpine Soils. In E. Bünemann, A. Oberson, & E. Frossard (Eds.), *Phosphorus in Action: Biological Processes in Soil Phosphorus Cycling* (pp. 295-316). Springer Berlin Heidelberg. [https://doi.org/10.1007/978-3-642-15271-9\\_12](https://doi.org/10.1007/978-3-642-15271-9_12)
- Westermann, P., Ahring, B. K., & Mah, R. A. (1989). Temperature Compensation in *Methanosarcina barkeri* by Modulation of Hydrogen and Acetate Affinity. *Applied and Environmental Microbiology*, 55(5), 1262-1266. <https://doi.org/10.1128/aem.55.5.1262-1266.1989>
- Whalen, S. C. (2005). Natural wetlands and the atmosphere. *Environmental Engineering Science*, 22(1), 73-94. <https://doi.org/10.1089/ees.2005.22.73>
- Wickland, K. P., Jorgenson, M. T., Koch, J. C., Kanevskiy, M., & Striegl, R. G. (2020). Carbon dioxide and methane flux in a dynamic arctic tundra landscape: decadal-scale impacts of ice wedge degradation and stabilization. *Geophysical Research Letters*, 47(22), e2020GL089894-e082020GL089894. <https://doi.org/10.1029/2020GL089894>
- Wickland, K. P., Striegl, R. G., Neff, J. C., & Sachs, T. (2006). Effects of permafrost melting on CO<sub>2</sub> and CH<sub>4</sub> exchange of a poorly drained black spruce lowland. *Journal of Geophysical Research: Biogeosciences*, 111(G2). <https://doi.org/10.1029/2005JG000099>
- Wieder, W. R., Cleveland, C. C., Smith, W. K., & Todd-Brown, K. (2015a). Future productivity and carbon storage limited by terrestrial nutrient availability. *Nature Geoscience*, 8(6), 441-444. <https://doi.org/10.1038/ngeo2413>
- Wieder, W. R., Cleveland, C. C., Smith, W. K., & Todd-Brown, K. (2015b). Reply to 'Land unlikely to become large carbon source'. *Nature Geoscience*, 8(12), 893-894. <https://doi.org/10.1038/ngeo2606>
- Wilber, A. C., Kratz, D. P., & Gupta, S. K. (1999). *Surface Emissivity Maps for Use in Satellite Retrievals of Longwave Radiation*.
- Wrage-Mönnig, N., Horn, M. A., Well, R., Müller, C., Velthof, G., & Oenema, O. (2018). The role of nitrifier denitrification in the production of nitrous oxide revisited. *Soil Biology and Biochemistry*, 123, A3-A16. <https://doi.org/10.1016/j.soilbio.2018.03.020>
-

- Wrage, N., Velthof, G. L., van Beusichem, M. L., & Oenema, O. (2001). Role of nitrifier denitrification in the production of nitrous oxide. *Soil Biology and Biochemistry*, 33(12), 1723-1732. [https://doi.org/https://doi.org/10.1016/S0038-0717\(01\)00096-7](https://doi.org/https://doi.org/10.1016/S0038-0717(01)00096-7)
- WRB, I. W. G. (2015). *World reference base for soil resources 2014: International soil classification system for naming soils and creating legends for soil maps*.
- Yang, G., Peng, Y., Abbott, B. W., Biasi, C., Wei, B., Zhang, D., Wang, J., Yu, J., Li, F., Wang, G., Kou, D., Liu, F., & Yang, Y. (2021). Phosphorus rather than nitrogen regulates ecosystem carbon dynamics after permafrost thaw. *Glob Chang Biol*, 27(22), 5818-5830. <https://doi.org/10.1111/gcb.15845>
- Yang, X., Thornton, P. E., Ricciuto, D. M., & Post, W. M. (2014). The role of phosphorus dynamics in tropical forests – a modeling study using CLM-CNP. *Biogeosciences*, 11(6), 1667-1681. <https://doi.org/10.5194/bg-11-1667-2014>
- Yershov, E. D. (1998). *General Geocryology*. Cambridge University Press. <https://doi.org/10.1017/CBO9780511564505>
- Yuan, K., Li, F., McNicol, G., Chen, M., Hoyt, A., Knox, S., Riley, W. J., Jackson, R., & Zhu, Q. (2024). Boreal–Arctic wetland methane emissions modulated by warming and vegetation activity. *Nature Climate Change*. <https://doi.org/10.1038/s41558-024-01933-3>
- Yvon-Durocher, G., Allen, A. P., Bastviken, D., Conrad, R., Gudas, C., St-Pierre, A., Thanh-Duc, N., & del Giorgio, P. A. (2014). Methane fluxes show consistent temperature dependence across microbial to ecosystem scales. *Nature*, 507(7493), 488-491. <https://doi.org/10.1038/nature13164>
- Zeikus, J. G., & Winfrey, M. R. (1976). Temperature limitation of methanogenesis in aquatic sediments. *Applied and Environmental Microbiology*, 31(1), 99-107. <https://doi.org/doi:10.1128/aem.31.1.99-107.1976>
- Zhang, D., Wang, L., Qin, S., Kou, D., Wang, S., Zheng, Z., Peñuelas, J., & Yang, Y. (2023). Microbial nitrogen and phosphorus co-limitation across permafrost region. *Global Change Biology*, 29(14), 3910-3923. <https://doi.org/https://doi.org/10.1111/gcb.16743>
- Zheng, J., RoyChowdhury, T., Yang, Z., Gu, B., Wullschleger, S. D., & Graham, D. E. (2018). Impacts of temperature and soil characteristics on methane production and oxidation in Arctic tundra. *Biogeosciences*, 15(21), 6621-6635. <https://doi.org/10.5194/bg-15-6621-2018>
- Zheng, X., Wang, S., Xu, X., Deng, B., Liu, X., Hu, X., Deng, W., Zhang, W., Jiang, J., & Zhang, L. (2022). Soil N<sub>2</sub>O emissions increased by litter removal but decreased by phosphorus additions. *Nutrient Cycling in Agroecosystems*, 123(1), 49-59. <https://doi.org/10.1007/s10705-021-10125-w>
- Zhu, Q., Riley, W. J., Tang, J., Collier, N., Hoffman, F. M., Yang, X., & Bisht, G. (2019). Representing Nitrogen, Phosphorus, and Carbon Interactions in the E3SM Land Model: Development and Global Benchmarking. *Journal of Advances in Modeling Earth Systems*, 11(7), 2238-2258. <https://doi.org/https://doi.org/10.1029/2018MS001571>
- Zhu, R., Chen, Q., Ding, W., & Xu, H. (2012). Impact of seabird activity on nitrous oxide and methane fluxes from High Arctic tundra in Svalbard, Norway. *Journal of Geophysical Research: Biogeosciences*, 117(G4). <https://doi.org/https://doi.org/10.1029/2012JG002130>
-

- Zinder, S. H., Anguish, T., & Cardwell, S. C. (1984). Effects of Temperature on Methanogenesis in a Thermophilic (58°C) Anaerobic Digestor. *Applied and Environmental Microbiology*, 47(4), 808-813. <https://doi.org/doi:10.1128/aem.47.4.808-813.1984>
- Zubrzycki, S., Kutzbach, L., Grosse, G., Desyatkin, A., & Pfeiffer, E. M. (2013). Organic carbon and total nitrogen stocks in soils of the Lena River Delta. *Biogeosciences*, 10(6), 3507-3524. <https://doi.org/10.5194/bg-10-3507-2013>
-